ANALYSIS OF ICE AND METOCEAN MEASUREMENTS, CHUKCHI SEA, 2009-2010

Prepared for:

ConocoPhillips Alaska Inc.
Anchorage, Alaska
Attn: John Cologgi

By:
T.D. Mudge, D.B. Fissel, N. Kulan, D. Sadowy, K. Borg, J. Lawrence, J.R. Marko, D. Billenness, T. Hung, A. Kanwar, and A. Bard

ASL Environmental Sciences Inc.
#1 - 6703 Rajpur Place,
Victoria, B.C.
Canada V8M 1Z5

ASL File: PR-702
2011
Final Version

The correct citation for this report is:

T.D. Mudge, D.B. Fissel, N. Kulan, D. Sadowy, K. Borg, J. Lawrence, J.R. Marko, D. Billenness, T. Hung, A. Kanwar, and A. Bard, 2011. Analysis of Ice and Metocean Measurements, Chukchi Sea, 2009-2010. Report for ConocoPhillips Alaska Inc., Anchorage, Alaska by ASL Environmental Sciences Inc., Victoria, B.C. Canada. x + 118 p.

EXECUTIVE SUMMARY

A program of ice keel depth and ice velocity measurements was carried out off northwestern Alaska in support of oil and gas exploration by ConocoPhillips Alaska Inc. (CPAI) in the Chukchi Sea from August 2009 to July 2010. The data collection program involved the deployment and operation of two underwater, internally recording instruments at two sites (Site 1 and Site 2) in 37-46 m depth for nearly a year. The 2009 to 2010 data sets represent the second year of a multiyear measurement program planned for the two offshore sites in the Chukchi Sea, offshore of Wainright, Alaska.

Key results of the 2009 to 2010 measurement program included:

Ocean Wave measurements

In October 2009, there were six storms when the significant wave heights approached or exceeded 4 m. The largest wave heights (October 21 to 25) at Site 1 reached a maximum significant wave height value of 5.4 m (10.6 m maximum individual wave height) with a corresponding peak period of 10 s. At Site 2, during this same event, the largest significant wave height was 4.6 m. During this event, wind speeds at Point Lay exceeded 19 knots for several hours. For all non-ice measurement times, the average significant wave heights were 1.3 m at Site 1 and 1.1 m at Site 2.

Large Ice Keels

Very deep ice keels were observed at both Sites 1 and 2 with 19 keels at Site 1 and 24 keels at Site 2 measuring over 20 m ice draft. The deepest keels at Sites 1 and 2 were 26.7 m and 30.0 m respectively.

Keels exceeding 12 m ice draft were measured in all months from January 2010 to May 2010 at both sites and in December 2009 at Site 2. The total number of ice keels having ice drafts exceeding 5, 8 and 11 m were 6723, 2010 and 612 respectively for Site 1 and 7828, 2318 and 701 for Site 2. The average widths for the individual ice draft thresholds of 5, 8 and 11 m were 28.8, 34.3 and 39.8 m for Site 1 and 28.4, 35.0 and 42.8 m for Site 2, respectively.

By comparison to the first year of measurements, 2008-2009, there was a notable reduction at Site 1 for the total number of keels and the total distance of ice measured (in 2008-2009, the number of keels > 5 m ice draft were 14,484). The 2008-2009 maximum keel ice draft at Site 1 was 26.4 m, very similar to the maximum ice draft of 26.7 m at this site in 2009-2010.

There were occurrences of ice keels with very large horizontal dimensions of up to a few hundred meters. The widest keels, using a threshold of 5 m, were 490 m for Site 1 and 328 m for Site 2. The average keel width, at 5 m ice draft threshold, was 30 m.

Ice Velocities

The region had a very dynamic ice regime with ice movement occurring 98% to 95% of the time at Sites 1 and 2 respectively from August 2009 to July 2010. The greatest percentage of no-motion events for a month in this measurement period was 17% at Site 2 in February 2010.

Over ten occurrences of large ice velocities were measured throughout the year with peak ice velocities of 76 cm/s at Site 1 and 115 cm/s at Site 2. The episodes of large ice velocities were associated with strong wind events having peak speeds of 6 to 12 m/s (12 to 24 knots). At both sites, the median ice drift was generally highest in June (19-38 cm/s) and lower (5-20 cm/s) from November to April.

Ocean Currents

The ocean currents at Site 1 were weaker than those observed at Site 2 with events rarely exceeding 30 cm/s near the surface. From September to late December, current speeds were typically large and associated with strong wind events that were at times greater than 8 m/s as measured at Wainwright, AK. During January, the currents were typically lower except for a large event late in the month. Currents then generally stayed weak for the rest of the ice season, except for about ten high speed events.

The surface currents at Site 1 were variable but predominantly directed to the ENE, whereas the surface current direction at Site 2 aligned along an E-W axis. Mid-depth and near-bottom current directions were less variable than the surface currents and were predominately towards the ENE and ESE for Site 1 and Site 2, respectively.

Inertial oscillations are present in the ocean current data during the times of reduced or zero ice concentrations. These twice-daily ocean current variations produced a peak to trough current variation of up to 25 cm/s, and they appeared to be more prevalent at Site 1 than at Site 2.

ACKNOWLEDGEMENTS

Many persons and organizations contribute to making a project of this scope possible, including:

Our Client, ConocoPhillips Alaska Inc. (CPAI):

Jim Darnall, Project Manager, CPAI

The Captain and Crew of the vessels MV Norseman (deployment) and MV Norseman II (recovery)

Logistical support and vessel for recovery provided by:

Jeff Hastings, Project Manager, Olgoonik Fairweather LLC

Sheyna Wisdom and Tom Ainsworth of Olgoonik Fairweather LLC

Dave Aldrich and Daniel Doolittle of Aldrich Marine

Technical Support from:

Dave English, Jeremy Lawrence and Rick Birch of ASL Environmental Sciences Inc.

IPS-5 construction:

Paul Johnson and Kelvin Nelson of ASL Environmental Sciences Inc.

Program Management Support from:

Bernadette Fissel and Des Buermans of ASL Environmental Sciences Inc.

TABLE OF CONTENTS

LIST OF FIGURES

LIST OF TABLES

1 INTRODUCTION

1.1 STUDY OBJECTIVES

The ConocoPhillips Alaska Inc. (CPAI) team is examining geotechnical and environmental forcing issues related to offshore production systems for the Chukchi Sea exploration lease areas off northwestern Alaska. As part of the study, ASL Environmental Sciences (ASL) was contracted to collect and analyze data on ice drafts and ice velocities in the lease areas. Additionally, ocean current profiles, non-directional waves, salinity and temperature of seawater were also measured and analyzed.

Measurements of ice drafts and velocities were obtained with upward looking sonar instrumentation in taut-line moorings at two sites in Chukchi Sea (Figure 1-1). 2009-2010 measurement program began in late August 2009. It is part of an ongoing program conducted by ASL for CPAI that started in September 2008 in Chukchi Sea. This report presents the results of the measurements obtained in the second year of the Chukchi Sea measurement program from August 2009 to July 2010.

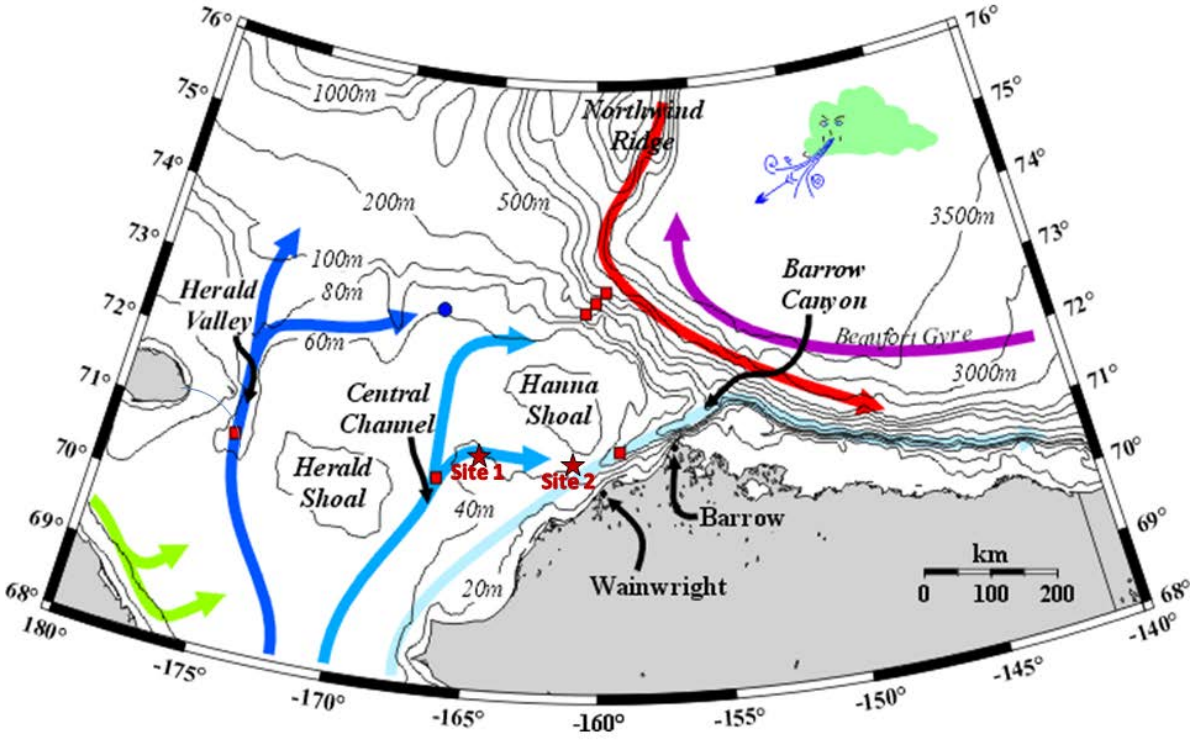

Figure 1-1. The location of the two measurement sites (dark red stars), Site 1 and Site 2, are plotted on a map by University of Alaska Institute of Marine Science (Weingartner et al., 2009) of the Chukchi and Beaufort Seas. Also plotted are the main currents and the depth contours from 20 to 3500 m. Pacific waters (3 shades of blue), Siberian Coastal Current (green), Atlantic Water on the continental slope (red) and the anticyclonic circulation of the Beaufort Gyre surface waters (purple). The red squares represent the locations of previous oceanographic moorings operated by the U. of Alaska.

The field portion of the project was conducted for CPAI via Olgoonik Fairweather LLC (Fairweather) of Anchorage, Alaska. Fairweather provided logistical support to the ASL field personnel in the recovery and redeployment of Site 1 and Site 2 equipments in August 2009. ASL provided assistance in deployment and recovery of the equipment, in addition to processing and analyzing the collected data sets.

1.2 OVERVIEW OF THE STUDY AREA AND SEASONAL ICE CONDITIONS

The Chukchi Sea is a shelf sea with water depths of less than 200 m and it is part of the western Arctic Ocean. However, it is closely linked to the Pacific Ocean both atmospherically (through Aleutian Low) and oceanographically (through Bering Strait). The water masses in the study area are dominated by the inflow of Pacific waters that enter the Arctic Ocean through Bering Strait (Figure 1-1). The three branches of Pacific waters are color-coded with dark blue being the most nutrient-rich waters and light blue being the least nutrient-rich (Weingartner et al., 2009).

The Site 1 measurement site lies in a 37 m deep region southwest of Hanna Shoal where the central channel flow has split into a predominately easterly flow. Site 2 is located to the south of Hanna Shoal in the same branch of the bifurcated central channel flow at about 46 m isodepth. On average, the flow direction in the vicinity of both Sites 1 and 2 is eastward. While the average current speed of the central channel flow is approximately 8 cm/s (Weingartner et al., 2009), short-term wind forced currents can dominate with larger observed currents of 50 cm/s.

The sea ice in the region is characterized by three major categories: the offshore, mobile polar pack ice of the Arctic Ocean, a narrow region of landfast ice adjacent to the coast, and a poorly studied area of highly mobile coastal zone ice (Norton and Gaylord 2004, Figure 1-2). Landfast ice zone is typically on the order of 10 km wide, however, the ice is frozen to the seafloor only over the shallowest part (< 2m) part of the inner shelf and floats in the outer part. Between the landfast ice zone nearshore and the pack ice zone offshore, there is a transitional zone, also known as *stamukhi* zone, where most intense ridging occurs, roughly between 15 to 40 m isobaths.

Sea-ice is for the most part consolidated in the region over winter. By March, the on-average, anti-cyclonic (clockwise) pattern of movement known as Beaufort Gyre, which moves the polar pack ice with it, produces a semi-permanent polynya (Chukchi flaw zone) within about 100 km of the coast. Site 2, 50 km northwest of Wainwright, is within the flaw zone while Site 1, about 190 km west-northwest of Wainwright, is most likely dominated by coherent pack ice.

New ice formation in the Chukchi Sea begins in nearshore areas in early October while the outer edge of the offshore ice pack edge can be several hundred kilometers north of the coastline. Growth is characterized by outward extension and thickening of the nearshore ice cover. Simultaneously, new growth also appears in the offshore pack, primarily in areas of open water and thin ice.

Breakup of landfast ice near Barrow since 2000 has occurred in a period from mid June to early July. The 2010 breakup of sea ice in the CPAI lease area began in early May with the formation of a large flaw lead. Occasional ice floes continued to pass through the region until well into July. Compared to the previous year, eastern Chukchi Sea was ice-free three

to five weeks earlier, although the ice conditions in the northern and western Chukchi Sea were comparable between 2009 and 2010.

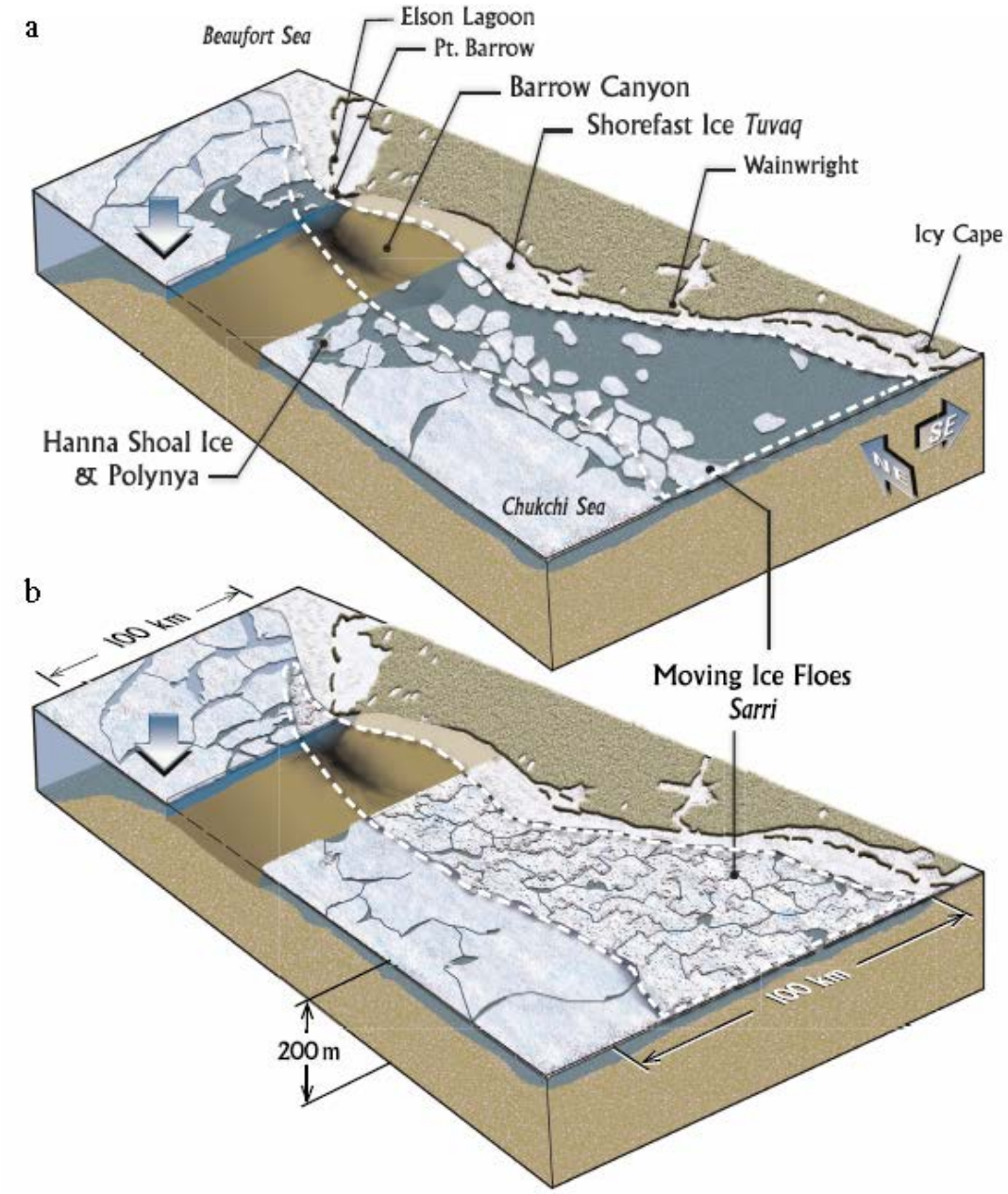

Figure 1-2. Ice dynamics in the Chukchi Sea (Norton and Gaylord, 2004). The dashed white line indicates Alaska's northern Chukchi Sea flaw zone from Icy Cape to the western edge of the Beaufort Sea. a) Ice moving to the southwest and b) ice moving to the northeast.

The coastal ice zone (sometimes referred to as the *stamukhi* or transition zone), is located between the near-shore landfast ice and the offshore polar pack zone, is characterized by very dynamic ice conditions. This zone is characterized by interactions involving incursions of the the polar pack-ice along with the mobile locally grown sea ice with the outer edge of the landfast ice which results in the formation of ridges, leads, and polynyas. The large ridge fragments, either as mobile or grounded ice features, are referred to as *stamukhi* ice. A system of leads or long narrow bands of open water, also occur intermittently along the edge of the landfast ice. Under offshore movements of the mobile ice, large areas of open water can also occur as polynyas or large-scale flaw leads offshore of the coastline and its adjoining landfast ice.

In the adjoining Beaufort Sea where *stamukhi* have been studied since the 1970's, they are known to establish the seaward boundary of the immobile landfast ice through contact between their keels and sea floor. Ice movements in the *stamukhi* region are usually not detectable, but do occur on some occasions on scales of meters and, anecdotally, with magnitudes extending beyond a few tens of meters. Movement of ice in the landfast zone, called ice shove or *ivu* by the Inupiaq, may occur any time but is more common during freeze-up and break-up. In the landfast ice zone, ice movements ranging from 5 to 395 m near Point Barrow have been reported by Huntington et al. (2001), Mahoney et al. (2004).

A floeberg is another ice feature that is commonly observed in the Beaufort Sea but not in Chukchi Sea, except for a large region of grounded ice on Hanna Shoal identified as Katie's Floeberg (Barrett and Stringer, 1978) and observed only in some years. A floeberg is a massive hummock sea ice or a group of hummock sea ice frozen together. Hummock sea ice is formed when individual ice floes impinge upon each other or push against weaker ice resulting in the "haphazard accumulation of ice blocks of a most irregular and formidable appearance" (Kovacs and Mellor, 1974). In the Alaskan Beaufort Sea floebergs have been observed to extend over distances of many kilometres parallel to the coastline with sail heights of 5 to 25 m.

The presence of a semi-permanent flaw zone in northern Chukchi Sea due to an abrupt change in landmass distribution resisting the westward movement of polar pack ice past Point Barrow is the reason for coastal ice regimes to differ between the Beaufort and Chukchi Seas. Individual ice floes in the Chukchi Sea flaw zone move differently than the polar pack ice. The dominant direction of motion for ice floes in the northern Chukchi Sea flaw zone is East-Northeast, while polar pack ice moves westward on-average. The maximum speed attained by individual ice floes in the flaw zone can be much larger than the polar pack ice, according to a study by Norton and Gaylord (2004) based on analysis of satellite imagery. They also found that fastest ice floes were moving to the West-Southwest, opposite to the dominant ice floe motion. Medium to large size floes can reach speeds as large as 140 cm/s (Norton and Gaylord, 2004).

1.3 ORGANIZATION OF THE REPORT

This report is organized into several sections reflecting the various phases of the study.

- Section 2 presents a summary of the data collection program, including the field operations (Deployment and Recovery) and the instrumentation and methodology used for data collection.
- Section 3 presents summaries of the data processing results for each type of data collected.
- Section 4 presents the results of an analysis of the ice draft data set involving detailed statistical summaries, and the width of very large observed ice features. Analysis results are also presented for ice velocities and ocean waves.
- Finally, a summary of the study and analyses of the largest observed ice keels are presented in Section 5, followed by literature and report citations in Section 6.

More detailed information, key study data sets and results derived from the data processing tasks of this study are provided in a Data Archive on an FTP site or upon request on DVD.

2 DATA COLLECTION

2.1 INSTRUMENTATION

The primary instruments utilized in this study were the Ice Profiling Sonar (IPS-5), manufactured by ASL Environmental Sciences Inc (ASL), which allows measurements of ice keel depths, and the Teledyne RDI Acoustic Doppler Current Profiler (ADCP), which measures ice and ocean current velocities.

The IPS and ADCP instruments were deployed using separate near-bottom taut line moorings at Site 1 and 2 (Figure 2-1). The two moorings were located within 200 metres of each other and their configurations were as shown in Figure 2-2. To provide additional speed of sound information, a self-contained conductivity/temperature sensor, a SeaBird model SBE37, was attached to the IPS-5 mooring frame at both sites (Figure 2-3). Recovery was carried out through use of acoustic release devices, which are activated by sonar signals transmitted from a command unit operated from the deck of the deployment/recovery vessel. Mooring details, including their location, depth, and deployment and recovery times are shown in Table 2-1.

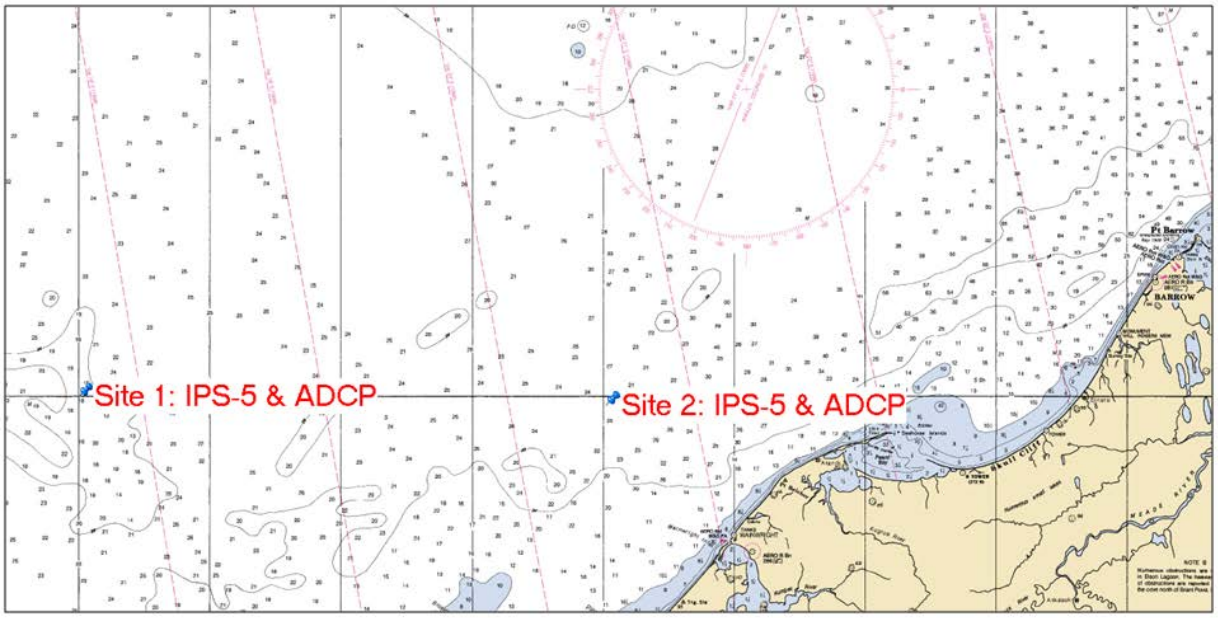

Figure 2-1. Map of mooring locations for IPS-5 and ADCP instruments at Site 1 (71˚N and 165˚W) and Site 2 (71˚N and 161˚W), 2009-2010 field program.

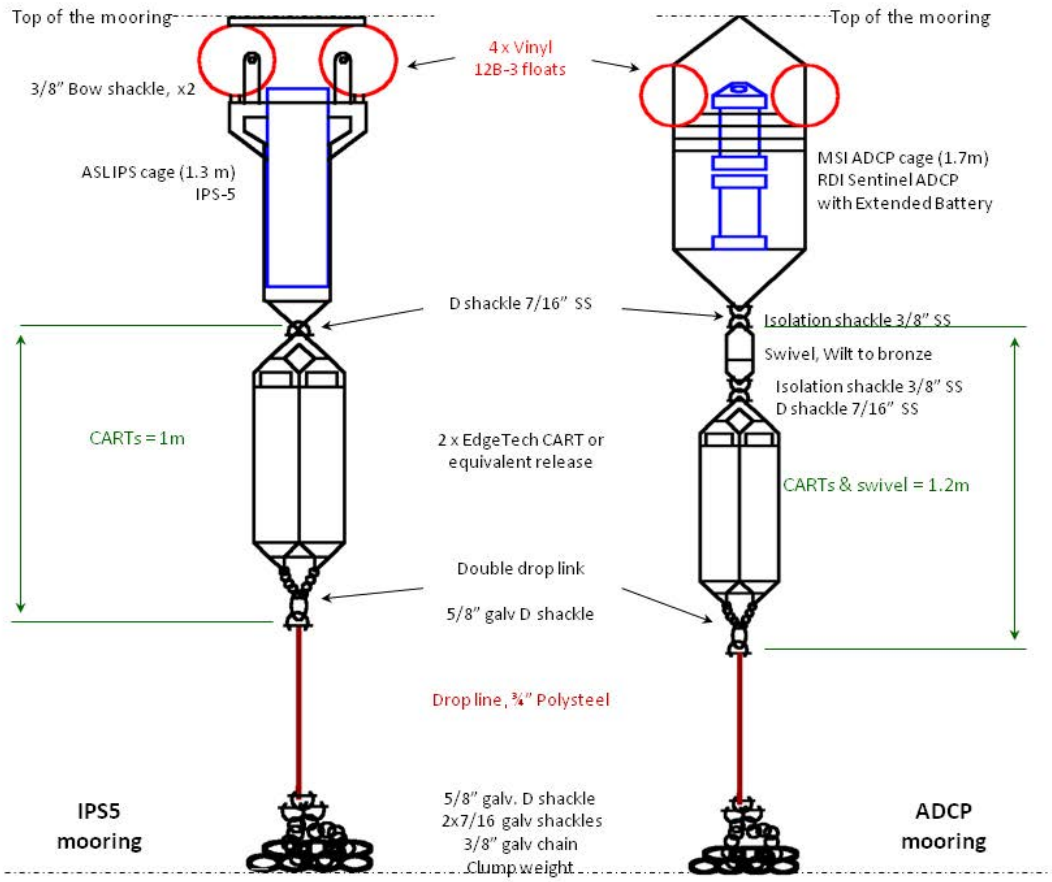

Figure 2-2. A schematic diagram of the taut line moorings used for deployment of the IPS and ADCP instruments. Each instrument is at the upper end of the mooring supported by four plastic Vinyl floats. Two acoustic releases (EdgeTech CART units) are located below.

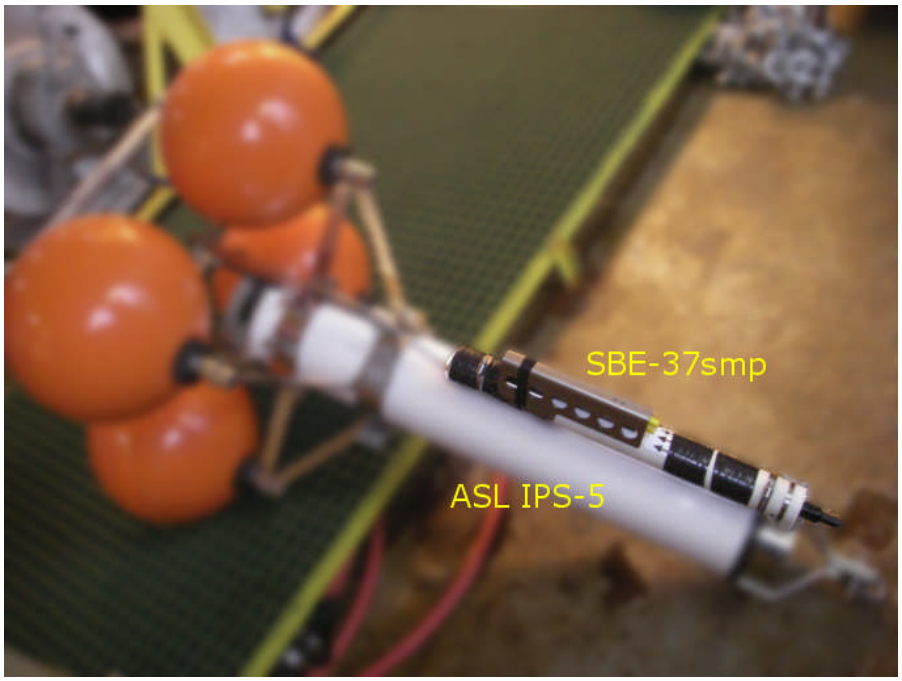

Figure 2-3. SBE 37-SMP mounted on IPS-5 frame. All of the image but the SBE 37 has been intentionally blurred.

The ASL IPS-5 provides a continuous over-winter record of ice draft at sampling rates of once every 1 or 2 seconds. In combination with ADCPs, used to measure ice velocities, ice draft time series acquired with IPS instruments can be converted to a distance series equivalent. The IPS-5 also provided 2 Hz wave bursts during the ice-free season.

The instrumentation used in this study has been widely used in other parts of the world, including the greater Arctic Ocean region, where sea ice is present for nearly the entire year (Melling et al., 1995), and in marginal seasonal ice zones (Fissel et al., 2008).

Table 2-1. Instrumentation, locations, and deployment and recovery times for the moorings operated in the Chukchi Sea from October 2009 to July 2010. Further details are available in the Cruise Report (Borg et al., 2010).

Site	Instr. Type	Latitude	Longitude	Water Depth (m)	Deployment Date	Recovery Date
Site 1	IPS-5	70°59.9510' N	165°0.1340' W	36	August 28, 2009	July 26, 2010
	ADCP	70°59.9130' N	165°0.0720' W	38	August 28, 2009	July 26, 2010
Site 2	IPS-5	70°58.7001' N	160°58.4029' W	46	August 29, 2009	July 28, 2010
	ADCP	70°58.7320' N	160°58.2330' W	47	August 29, 2009	July 28, 2010

The use of two separate moorings at each monitoring site was dictated by a need to keep the instruments as close to the seabed as possible, whereas, in deeper waters, the IPS instrument is often located above the ADCP instrument on a single taut line mooring. It was expected that the largest sea-ice keels could have keels nearly as deep as the water depth at the measurement locations, raising concerns that collisions with sea-ice could lead to loss of the instruments as well as of the collected data sets.

2.1.1 ICE PROFILING SONAR (IPS)

The IPS instrument is an upward-looking ice profiling sonar, which provides the high-quality ice thickness, or more correctly ice draft, data required. Originally, this instrument was designed by the Institute of Ocean Sciences, Sidney, BC, Canada, and has been further developed and subsequently manufactured by ASL Environmental Sciences Inc. of Victoria, BC, Canada. The ice keel depth is determined from the return travel time of an acoustic pulse (420 kHz; 1.8° beam at -3 dB) reflected off the underside of the sea ice. The return time is converted to an acoustic range value through use of the speed of sound in seawater.

The IPS-5 units were setup to run through various configurations (phases) to acquire the best data based on climatological conditions. Site 1 and Site 2 IPS-5 samplings were done in six phases. The phases one, five and six had 2048 seconds of 2 Hz wave bursts repeated every hour for phase one (August 28, 2009 - October 14, 2009), and every hour and 20 minutes for phases five and six (August 1, 2010 - recovery date) for wave sampling. No wave sampling was done in the remainder of phases (phases 2, 3 and 4) as there is no or very little open water exists during this period (October 15 to July 31). Ice profiling was done during all six phases with the range data being sampled at 10, 1, 2, 1, 10 and 10 second intervals for phases one through six, respectively. The same IPS-5 settings were used at both Site 1 and Site 2.

A pressure sensor (Paroscientific Digiquartz), installed on each IPS unit, was used to measure water level changes due to tidal and wind forcing, as well as apparent water level changes arising from depression/tilt of the mooring. The measured acoustic range, after correction for instrument tilt, is subtracted from the water level in order to get an accurate computation of ice keel drafts. The IPS contains pitch/roll sensors, to permit additional data compensation for instrument tilt and also collects near-bottom ocean temperature measurements.

The newer generation of IPS instruments can take compact-flash cards (8 GB as deployed and a max. 16 GB as of writing). This increased data storage allows for the recording of up to 5 targets per individual ping and a subset of the raw acoustic backscatter profiles. The IPS-5 also has a wave mode, allowing bursts of wave data to be collected at up to 2 Hz. The 122 Alkaline D-cell batteries provided the necessary power to collect over 32 million pings over a 1 year period.

Instrument specification sheets for the IPS-5 instruments used in this project are included in the Data Archive.

2.1.2 ACOUSTIC DOPPLER CURRENT PROFILER (ADCP)

The Acoustic Doppler Current Profiler (ADCP), Sentinel Workhorse series, manufactured by Teledyne RD Instruments of Poway, California, USA was used at Sites 1 and 2. The ADCP technology is widely used for oceanic environmental monitoring applications. Mounted near the sea bottom, the ADCP unit provides precise measurements of ocean currents (both the horizontal and vertical components) at levels within the water column, from near surface to near-bottom. In addition, the ADCP provides time series measurements of the velocity of the pack ice moving on the ocean's surface, as well as near-bottom ocean temperature data.

The ADCP instruments measure velocity by detecting the Doppler shift in acoustic frequency, arising from water current (or ice) movements, of the backscattered returns of upward (20° from vertical) transmitted acoustic pulses. The Doppler shift of the 300 kHz acoustic signals is used to determine water velocities at a vertical spacing of 2 m at Sites 1 and 2. The Sentinel ADCPs were modified by RDI in 1996 to use the Doppler shift from the ice bottom surface to measure ice velocity as well [this is now a standard option]. The sampling scheme involved 5-minute ensembles composed of water-column pings, interleaved with 5 bottom-track pings.

The data measurements are stored internally on a PCMCIA recorder card(s). Because of the extended 12-month deployment, the internal alkaline battery packs were supplemented with external battery packs (doubles).

Instrument specification sheets for the ADCP instruments used in this project are included in the Data Archive.

2.1.3 CT SENSOR

An SBE-37SMP internal recording conductivity and temperature (CT) sensor was mounted on the IPS-5 frames at both Sites 1 and 2. This CT provided continuous measurements of salinity and temperature for use in adjusting the speed of sound to provide more accurate acoustic ranges (Section 3.1).

Refer to the Data Archive for further specifications on the CT sensors.

2.2 DEPLOYMENT AND RECOVERY

Originally, the deployment of the ADCP and IPS-5 moorings at Site 1 and 2 to start the 2009-2010 measurement program was planned to be done from the M/V *Westward Wind*. At short notice, arrangements had been made to do the work from the R/V *Norseman*, which introduced some logistical issues. However, due to the efforts of all the parties involved, the deployment program was still carried out successfully. Dave Aldrich of Aldrich Marine and Fairweather's efforts to locate and replace misplaced instruments were particularly appreciated.

Recovery of the data collected by the moored instruments was carried out in July 2010 from R/V *Norseman II* (Figure 2-4), the sister ship of R/V *Norseman*. The ORE Coastal Acoustic Release Transponders (CARTs) were used to bring the IPS-5 and ADCP moorings to the surface. With a release load of 500 kg, a maximum depth rating of 1000 m and battery lifetime of 1.5 years, they are ideal for the deployments in the Chukchi Sea.

Figure 2-4. MV Norseman II in Nome.

The recovery operations started at Site 1 on the morning of July 26, 2010. The ADCP was released and reached the surface around 14:17 (UTC) and the IPS-5 was released and reached the surface around 14:30 (UTC). A preliminary examination of the data indicated that the IPS recorded a full data record. The ADCP, on the other hand, stopped recording

data on June 21, 2010 due to corrosion of the external power cable. The recovery operations started at Site 2 on the evening of July 27, local time. The ADCP was released and reached the surface around 05:08 UTC and the IPS-5 was released and reached the surface around 05:13 UTC. The IPS-5 and ADCP recorded full data record at Site 2.

2.2.1 PRE-DEPLOYMENT INSTRUMENTATION CHECKOUT

All the instrumentation had undergone extensive testing at ASL facilities in Canada prior to shipment to the Arctic. The orientations of the ADCP-measured currents were determined at each instrument by using an internal magnetic flux-gate compass. Because of the close proximity of the measurement locations to the north magnetic pole in the Canadian Arctic Islands, and the consequent weakness of the earth's horizontal magnetic field component, regional calibrations of the instrument compass must be carried out. These calibrations were carried out at a beach in Nome, Alaska, away from metallic objects. Calibrations were completed on August 24, 2009.

2.2.2 ON-SITE DATA DOWNLOADING

All 2009-2010 data sets were downloaded from the retrieved instruments onboard the vessel (MV Norseman II), with timing checks made on the instrument clocks to measure the clock drift over the period of the deployment. A preliminary examination of the data indicated that the IPS-5 and ADCP instruments recorded full datasets at Site 2. The IPS-5 at Site 1 recorded a full dataset, while the ADCP stopped recording data prematurely on June 21, 2010 due to a corroded pin of the external power cable.

All data downloaded during the July 2010 cruise were initially inspected, and found to be of uniformly high quality.

3 DATA PROCESSING

3.1 ICE DRAFT

3.1.1 INTRODUCTION

The processing of the Ice Profiling Sonar (IPS) data involves the conversion of the time-of-travel measurement recorded internally by the IPS unit into a calibrated time-series of ice draft in units of meters at 1 or 2 second intervals. The ice draft time-series is then converted to a spatial (or distance) data series, i.e. the time coordinate is transformed to distance using the measured ice velocities (section 3.1.2.3). The general approach to the data processing follows that of Melling et al. (1995). The implementation of the procedures, along with many further refinements, have been developed and carried out by ASL personnel over the past 12 years.

The raw data recorded by the IPS instrument consists of two measured parameters: the time-of-travel to the selected target echo and the amplitude and persistence (duration above a threshold amplitude level) of the target echo. The basic operation of the IPS instrument is outlined briefly below (more details are provided in the *IPS-5 Users Manual*). Essentially, the IPS operates in a pulsed mode with its acoustic beam directed toward zenith. A multi-faceted algorithm (Melling et al., 1995) identifies the echo, which is intended to be that of the bottom of the sea-ice, if present, or in the absence of sea-ice, from the ocean-atmosphere interface. The following describes the target selection algorithm:

- Select those echoes that are returned from beyond a minimum range but within a maximum range whose amplitudes and durations (persistence) exceed chosen minimum values (i.e. the echo start amplitude and the minimum persistence).
- From this initial selection, the echoes of longest duration are chosen (up to 5 targets). Choice of the control parameters must be carried out with a view to minimizing the likelihood that the algorithm will select echoes from sources within the water-column as opposed to the ice under-surface.

The time of travel value was converted to a one-way range by applying a first estimate of the speed of sound of seawater, c, in m s^{-1}. For this study the initial value of c was chosen to be 1438 ms^{-1}.

The IPS units when recovered had range data sets of approximately eleven months duration. Given the sampling intervals at Site 1 and Site 2, the total data record for an IPS unit over this time has over 19,000,000 logical records of acoustic range and amplitude data. The IPS units also provided measurements of near-bottom pressure, two-components (x and y) of instrument tilt, and the near-bottom ocean temperature.

As expected, the raw IPS data contain “drop-outs” for pings in which an acoustic target exceeding the threshold amplitude was not found. The number of occurrences of such

dropouts was very small. The Ice Profiler model IPS-5 instruments have a feature where the range to the maximum amplitude value (index target) is also recorded. When drop-outs occur, the index target range value is then used.

Less frequently, other types of erroneous values occurred in the form of 'spikes', i.e. one or a few data points that were markedly inconsistent with the measured neighbouring values. These were removed through automated programs that detected and replaced the erroneous values using linear interpolation. In the IPS datasets, some segments of consecutive "drop-outs" were found. These segments contained more points than the threshold for allowing automatic interpolation during automated despiking. A method for removing most of these segments was developed (see following section) and a small number of segments that could not be edited automatically were reviewed manually.

3.1.2 PROCESSING IPS DATA

Steps in the IPS data processing, as developed from processing many dozens of IPS data sets, consisted of:

1. Converting raw IPS data from binary form in instrument units to nominal engineering units.
2. Preparing time-series plots of the raw range measurements. Sample plots are shown in Figure 3-1 and Figure 3-2. Note that the plots show 'raw' data presented exactly as measured without any corrections or changes. In addition to the 'spikes' evident in the raw data, the data have not been corrected for variations in water levels due to tides and other effects, nor for changes in the speed of sound in the water column or the effects of instrument tilt.
3. Manual examination of the time-series plots of range to determine where editing is required. Segments of the data set characterized by level ice errors, recurrent spikes to a specific range, and 'missing' ice echoes were noted. The portion of the data sets where the instrument was not in measurement position (i.e. before and during deployment and following release of instrument from bottom mooring) were also noted and checked against log sheets. A first order assessment of occurrences of open water conditions was also made during this first examination and review of the data.
4. Editing IPS range data using automated data editing algorithms.
5. The times in the data file are corrected for the effects of instrument clock time drift (as derived from comparison of instrument start and stop times with times recorded on start-up and shut-down of the instrument). Clock drifts are typically small – 0 to 10 minutes over deployments of several months.
6. Remove unwanted data at the beginning or end of each data record (obtained during deployment and recovery operations).
7. Identify, and set to flag values (-9999), data segments where false subsurface acoustic targets, likely bubbles associated with strong winds and large waves, were detected rather than the underside of the sea ice or the water surface. Occasionally, the

amplitude values were useful as a guide in detecting these scattering events, as the onset of such events were characterized by reduced amplitudes. More commonly, the detection of these events was based on large variations in successive range measurements, which clearly were inconsistent with surface wave effects.

8. Automated removal of erroneous values that occur with the following attributes:
   - range values < 0.01 m to remove range dropouts
   - range values that exceed a reasonable value computed as: high tide = instrument depth + 8.0 m
9. The erroneous values, identified in the steps immediately above, are replaced through linear interpolation. On completion of the automated editing, longer sequences of consecutive data values (10 points or more) that were removed were examined manually to ensure that the error detection algorithm had functioned as expected.
10. The boundary points of segments of consecutive null range records were compared. If the range values of these points differed by less than 10 cm then the range values of these records were calculated by linear interpolation of the boundary points. The remaining segments were investigated and edited manually.
11. Replot the edited data set and review for any additional spikes or suspect values. Manually replace any further spikes (usually occurrences over 5 to 10 consecutive data values) using linear interpolation; occasionally, longer segments of suspect data are replaced with 'flag' values at this stage.

The numbers of erroneous data values detected and removed using the procedures described above are summarized in Table 3-1 and Table 3-2.

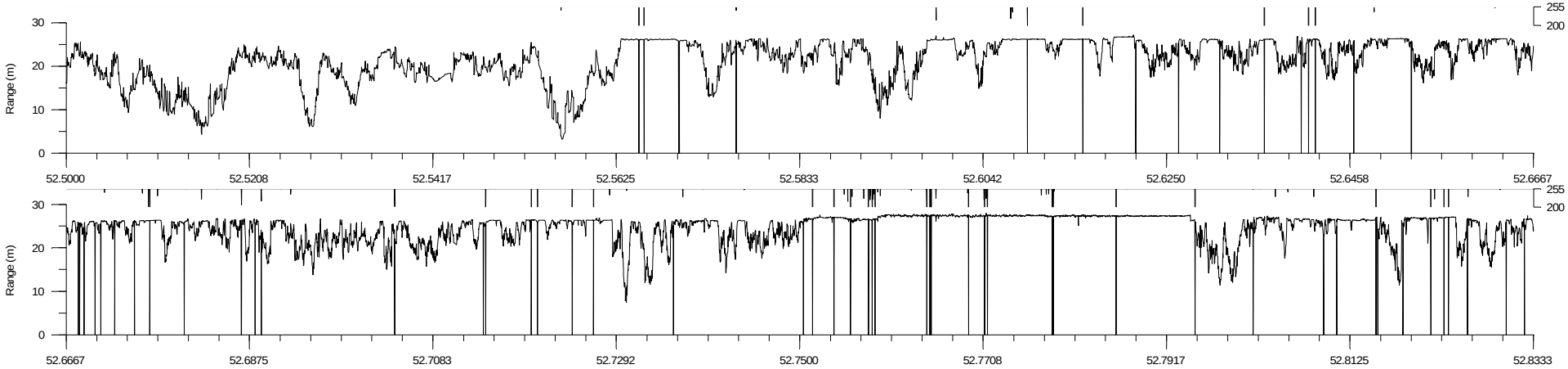

Figure 3-1. An example of the unedited range and amplitude data measured by an IPS showing a period characterized by sea-ice floes and some range "drop-outs".

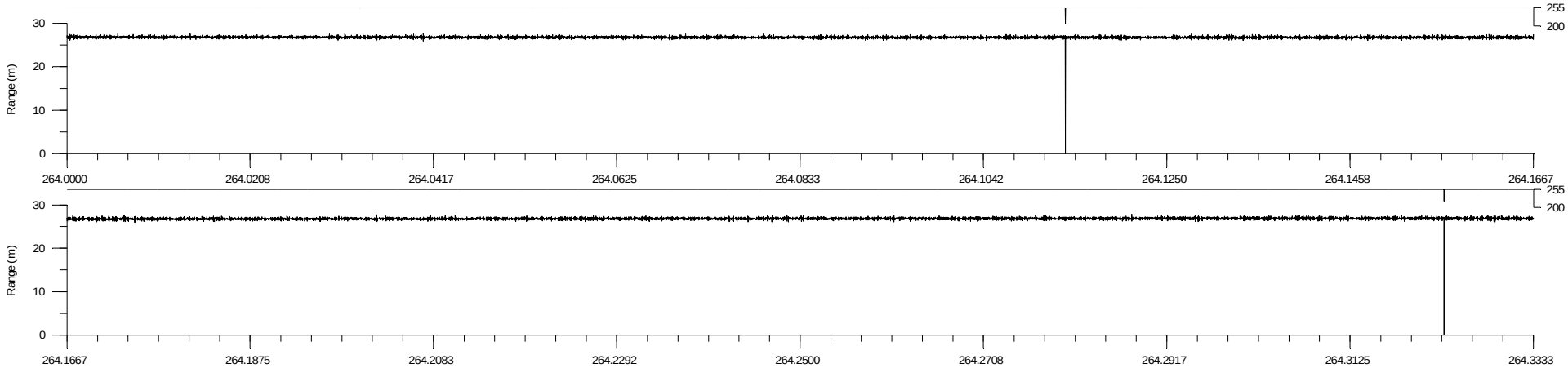

Figure 3-2. An example of the unedited range and amplitude data measured by an IPS showing a period following the main part of the ice season. This is an example of 'rough open water' in which the returns obtained from targets below mean sea level are believed to result from the troughs of ocean waves and from bubbles located beneath the surface

Table 3-1. Summary of the two main stages of ice draft data processing for Site 1, giving number of data records having errors that were detected and replaced or flagged. Where applicable, the number of segments of edited data and/or the percentage of the total number of points is provided in parentheses.

	Site 1				
	Phase	**1**	**2**	**3**	**4**
	Start date/time	28-Aug-2009 01:00:00	15-Oct-2009 00:01:06	01-Dec-2009 00:02:10	01-Apr-2010 00:04:56
	Stop date/time	15-Oct-2009 00:00:58	01-Dec-2009 00:02:10	01-Apr-2010 00:04:54	26-Jul-2010 17:46:39
	Sample interval	9.9991260	0.9999996	1.9999991	0.9999999
Range data	**# records as lower out-of-bound**	0	0	0	0
	# records as upper out-of-bound	0	0	0	0
	# records as single negative spikes	510	1,322	480	2,672
	# records as single positive spikes	666	108	588	1,708
	# records as double negative spikes	8	10	50	138
	# records as double positive spikes	10	46	32	166
	# records as triple spikes	0	0	9	15
	# records as quadruple spikes	4	0	8	4
	# records replaced by manual editing	0	0	0	0
Ice draft data	**# records flagged as bad**	0	0	0	0
	# records replaced manually	0	1	11	104
	# records flagged as open water/thin ice	413,061 (99.97%)	3,327,780 (81.95%)	8,870 (0.17%)	5,606,875 (55.65%)
	Total # of records	413,168	4,060,842	5,227,200	10,074,366
	Final # of replaced data records (excluding open water/thin ice)	1,198 (0.290%)	1,487 (0.037%)	1,178 (0.023%)	4,807 (0.048%)

Table 3-2. Summary of the two main stages of ice draft data processing for Site 2, giving number of data records having errors that were detected and replaced or flagged. Where applicable, the number of segments of edited data and/or the percentage of the total number of points is provided in parentheses.

	Site 2				
	Phase	**1**	**2**	**3**	**4**
	Start date/time	29-Aug-2009 15:00:00	15-Oct-2009 00:01:35	01-Dec-2009 00:03:11	01-Apr-2010 00:07:20
	Stop date/time	15-Oct-2009 00:01:26	01-Dec-2009 00:03:10	01-Apr-2010 00:07:19	29-Jul-2010 00:25:21
	Sample interval	10.0002158	1.0000218	2.0000436	1.0000218
Range data	**# records as lower out-of-bound**	0	0	0	0
	# records as upper out-of-bound	0	0	0	0
	# records as single negative spikes	0	16	623	1058
	# records as single positive spikes	0	11	760	1343
	# records as double negative spikes	0	0	64	110
	# records as double positive spikes	0	0	34	96
	# records as triple spikes	0	0	15	24
	# records as quadruple spikes	0	0	0	0
	# records replaced by manual editing	0	4	8	31
Ice draft data	**# records flagged as bad**	0	33	0	70
	# records replaced manually	0	70	16	147
	# records flagged as open water/thin ice	398,911 (100.0%)	2,553,425 (62.88%)	15,936 (0.30%)	6,679,264 (65.41%)
	Total # of records	398,911	4,060,808	5,227,211	10,212,021
	Final # of replaced data records (excluding open water/thin ice)	0 (0.000%)	134 (0.003%)	1,520 (0.029%)	2,879 (0.028%)

3.1.2.1 COMPUTATION OF ICE DRAFT

The next stage of data processing deals with converting the measured ranges into ice drafts. The ice draft, *d*, is derived from the edited ice ranges, *r*, and the water level, η. η is computed from the measured ocean bottom pressure, P_{btm}, and atmospheric pressure, P_{atm}, as follows:

$$\eta = \frac{(P_{btm} - P_{atm})}{\rho \cdot g} \qquad (1)$$

where g is the calculated local acceleration due to gravity and ρ is the density of sea water. Table 3-3 lists the values of these parameters for the IPS measurement sites. Measurements of P_{atm} were obtained from Wainwright, Alaska. The ice draft, *d*, is then computed from the edited range data as:

$$d = \eta - \beta \cdot r - \Delta D \qquad (2)$$

where β is a calibration factor for the actual mean speed of sound in sea-water, *c*, relative to the initially assumed value of 1438 ms^{-1} and ΔD is the distance of the pressure sensor below the acoustic transducer as shown in Table 3-3. Note that the sign convention for ice draft is positive downwards, i.e. a draft of +5 m represents an ice keel, which extends 5 m below sea level.

Table 3-3. Values used in the calculation of water level for Site 1 and Site 2.

Site	ρ (kg m^{-3})	g (m s^{-2})	ΔD (m)
Site 1	1026.20	9.826658	0.1940
Site 2	1026.03	9.826642	0.1758

The density values were derived from historical temperature-salinity-density data sets available for the Chukchi Sea and from the measured density values, as derived from the Conductivity-Temperature (CT) instrument data available at both Site 1 and Site 2 (section 3.5). The CT derived densities represent an upper bound of the actual water column density values due to density stratification of the water column, especially during summer and fall.

Corrections were also made for the effect of instrument tilt on the measured ranges. Generally, if not corrected for, this source of uncertainty would result in errors of a few centimetres or less on the ice drafts.

3.1.2.2 RANGE CORRECTION FACTOR

The factor, β, applied to the measured range in equation (2) represents the ratio of the actual sound speed to the nominal value of 1438 ms^{-1}. To determine β, open water segments in the range data set were selected (i.e. *d = 0* in equation 2 above) and β was empirically computed. The empirical values of β seem to follow reasonably well the variation

in the local speed of sound as computed from the measured near-bottom temperatures obtained from the IPS values at the measurement locations.

A fit was made to determine the time varying β values over the full duration of the time-series data based on:

- the empirical computations of β realized from periods of open water;
- the computed effect of near-bottom temperatures on c (using a fixed salinity and the speed of sound algorithm of Urick, 1983).

Plots of the time varying $\Delta\beta$ values are shown in Figure 3-3 and Figure 3-4 where:

$$\Delta\beta = (\beta - 1) \times 1000 \qquad (3)$$

The empirically derived values of β were applied through equation 2 to the edited range data to compute ice drafts.

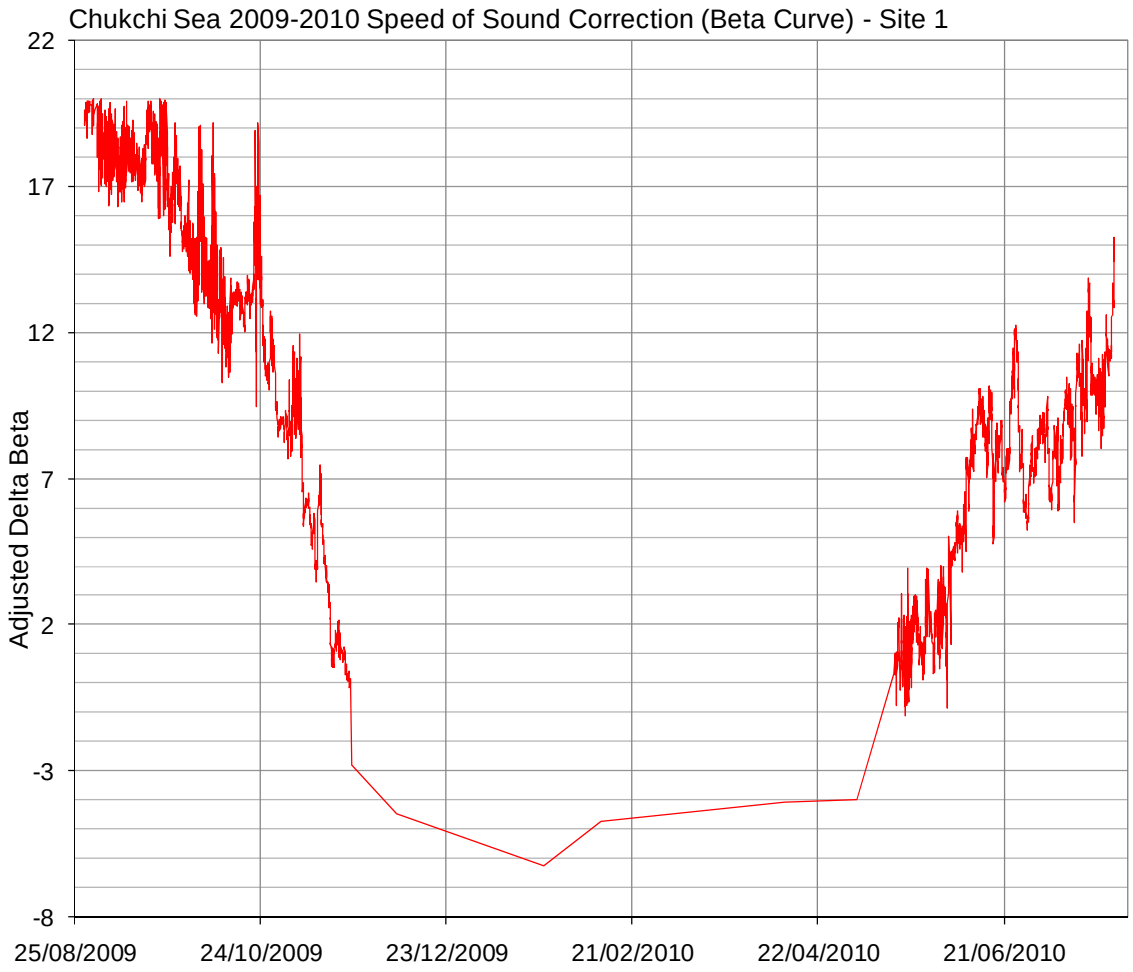

Figure 3-3. Plot of the time varying $\Delta\beta$ values for Site 1.

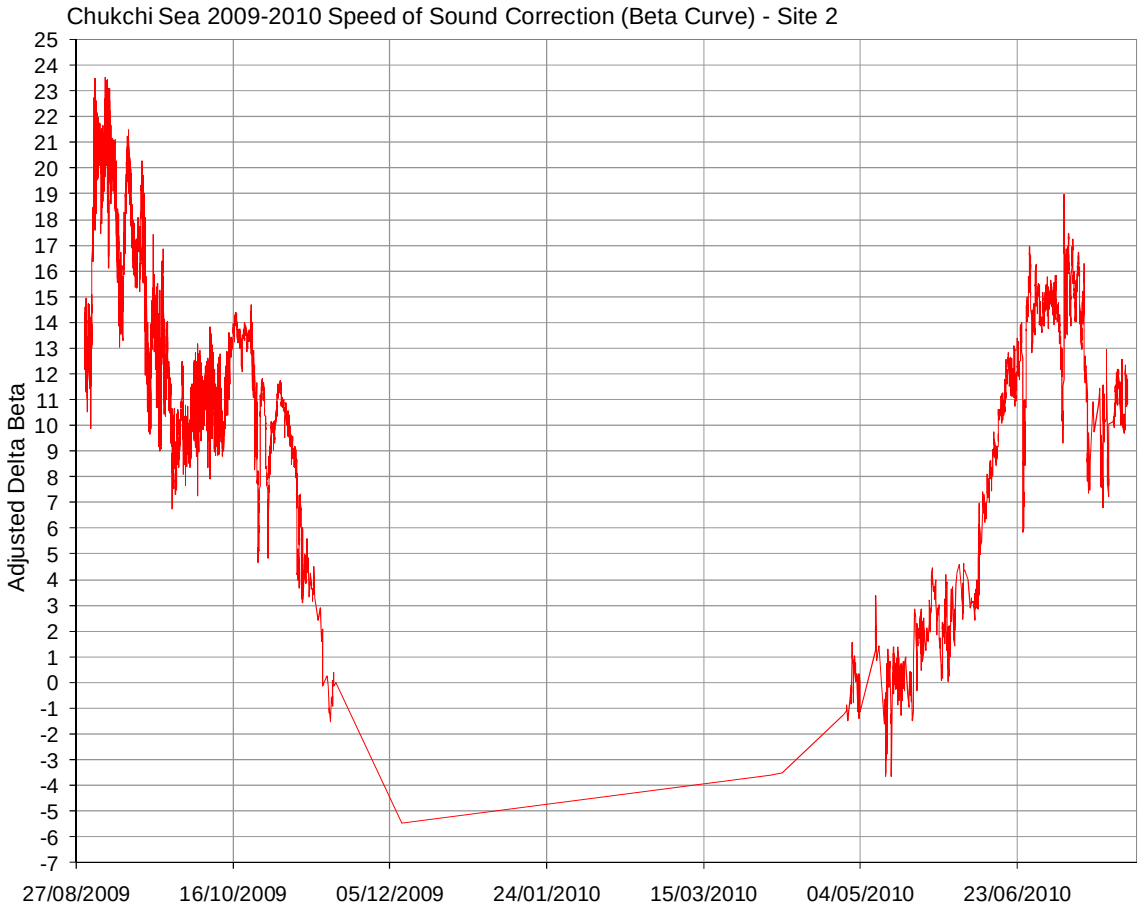

Figure 3-4. Plot of the time varying $\Delta\beta$ values for Site 2.

3.1.2.3 Conversion of Time-Series to Distance-Series for Ice Draft Data Sets

The ice draft time-series data sets were converted to a distance (or spatial) series using the processed ADCP ice velocities (Section 3.3). The resulting spatial data file contained east and north displacements and ice drafts beginning at zero east and north displacement incrementing until the end of the file. The cumulative ice path length, or distance, was then calculated using the east and north displacements for each sample.

The ice draft was sampled at regular time intervals, but due to the irregular motion of the ice the resulting distance-series was unevenly spaced in distance. The distance-series was interpolated to regular increments using a double-weighted double-quadratic interpolation scheme. As shown in Figure 3-5, the value Y_1 represents the value obtained from a quadratic interpolation using two points to the left and one to the right of x_i {($y(u_{i-1})$, $y(u_i)$ and $y(u_{i+1})$} and Y_2 represents the interpolated value using two points to the right and one to the left of x_i {($y(u_i)$, $y(u_{i+1})$ and $y(u_{i+2})$}. In the figure, the desired regularly spaced interpolation point is x_i, and the measurement locations are given by u_{i-1}, u_i, u_{i+1} and u_{i+2}. The two

interpolated values were then averaged using a weight based on the distance between points and on the change in draft between points. The double weighting scheme, as shown in equation 4, was adopted to avoid overshoots in areas of sudden draft changes.

In order to represent the ice drafts at low ice velocities, the draft data file was interpolated to 0.10 m distances then block averaged to 1.0 m distances. The 1.0 m spacing represents a distance slightly less than the width of the IPS sonar footprint at an average 30 m water depth and the smallest resolvable distance.

As part of reviewing the data for open water occurrences, a manual review was conducted to identify data segments, which contain both thin ice and waves (denoted as "waves in ice"). The flagging of long sections of open water occurred at times when air temperatures rose above 0 degrees, and low concentrations of sea-ice with only occasional large keel occurrences were detected.

The final step in reviewing the spatial series was to search for unrealistic features. These features were generally located where the uncertainty in the ice velocities was largest. Modifications were made to the ice velocities, and the spatial series were recalculated.

$$y(x_i) = \frac{Y_1\left[y(u_{i+2}) - y(u_{i+1})\right]\left[x_i - x(u_{i+1})\right] + Y_2\left[y(u_i) - y(u_{i-1})\right]\left[x_i - x(u_i)\right]}{\left[y(u_{i+2}) - y(u_{i+1})\right]\left[x_i - x(u_{i+1})\right] + \left[y(u_i) - y(u_{i-1})\right]\left[x_i - x(u_i)\right]} \qquad (4)$$

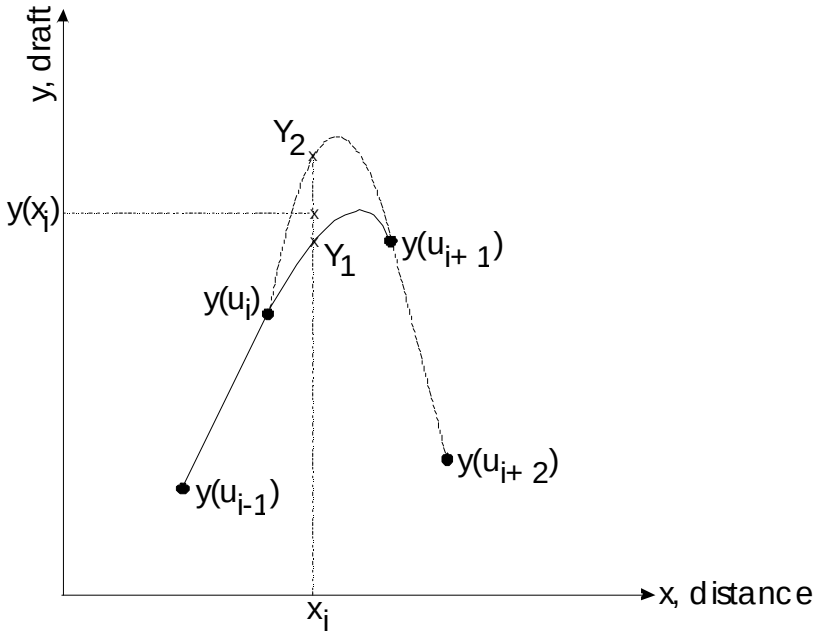

Figure 3-5. The double quadratic interpolation method used to convert the ice draft time series into a spatial series.

3.1.3 SUMMARY OF ICE DRAFT

The measured acoustic range, pressure, and tilt data channels recorded by the IPS-5 instrument, combined with sea level pressure measurements were processed and analyzed to compute time- and distance-series of ice keel drafts. Following a careful and thorough review of the ice drafts, final edited versions of ice draft time- and distance-series were created and plotted. The duration of the ice draft records with time and distance at the measurement sites are shown in Table 3-4 and Table 3-5. Sea ice was first detected on November 22 at Site 1 and November 6 at Site 2. The ice had mostly disappeared after June 2 and after May 16 at Site 1 and Site 2 respectively, but ice was present on an intermittent basis until June 5 at Site 1 and July 22 at Site 2. The clearing dates for sea ice in summer are 4 to 5 weeks earlier than median value of break-up dates, derived from ice charts for the years of 1971 to 2000. The earlier clearing dates are consistent with the general trend of reduced ice concentrations in the summer over the past decade.

The distance-series of ice drafts have interruptions in May, June and July 2010 due to reduced ice concentrations, which makes ice velocity measurements unreliable.

Table 3-4. Final time-series and distance-series segments of valid data for Site 1.

Site 1		
Time-Series		
Phase	**Start Date / Time**	**Stop Date / Time**
1	28-Aug-2009 01:00:00	15-Oct-2009 00:00:58
2	15-Oct-2009 00:01:06	01-Dec-2009 00:02:10
3	01-Dec-2009 00:02:10	01-Apr-2010 00:04:54
4	01-Apr-2010 00:04:56	26-Jul-2010 17:46:39
Distance-Series		
Segment	**Start Date/Time**	**Stop Date/Time**
1	22-Nov-2009 14:11:22	21-May-2010 08:12:11
2	30-May-2010 22:42:32	02-Jun-2010 11:57:24

Table 3-5. Final time-series and distance-series segments of valid data for Site 2.

Site 2		
Time-Series		
Phase	**Start Date / Time**	**Stop Date / Time**
1	29-Aug-2009 15:00:00	15-Oct-2009 00:01:26
2	15-Oct-2009 00:01:35	01-Dec-2009 00:03:10
3	01-Dec-2009 00:03:11	01-Apr-2010 00:07:19
4	01-Apr-2010 00:07:20	29-Jul-2010 00:25:21
Distance-Series		
Segment	**Start Date/Time**	**Stop Date/Time**
1	06-Nov-2009 19:55:18	7-Nov-2009 17:25:08
2	11-Nov-2009 11:54:59	11-Nov-2009 18:54:49
3	13-Nov-2009 08:39:52	08-May-2010 21:12:40
4	10-May-2010 03:12:43	16-May-2010 17:57:09
5	29-May-2010 07:27:13	01-Jun-2010 19:56:04
6	15-Jul-2010 10:53:14	16-Jul-2010 04:53:01

The final versions of the ice draft data series (Data Archive) are considered to be generally accurate to within 0.3 m for the largest keel features and to somewhat better accuracies, to as good as 0.05 to 0.1 m, for thinner ice, based on the estimated uncertainties in the various stages of data processing. These accuracy estimates are consistent with inspections of the final edited data sets for data segments consisting of open water intervals when the ice draft, after allowing for any ocean wave effects, should be identically zero.

The processed ice draft data files are provided as part of the Data Archive, both as time-series data and as distance-series data. Plots of the distance-series ice drafts are also provided in the Data Archive for each of the segments of continuous good ice velocities. In the ice draft plots, segments containing waves in ice were flagged to -500 and segments containing open water were flagged to -200 but were plotted as values slightly above the abscissa. Segments of bad data were flagged to -9999.

3.2 OCEAN WAVE DATA DERIVED FROM ICE PROFILER

The range data from ASL Ice Profiler was used to derive information on ocean waves when sea ice was not present.

The processing of the IPS-5 data sets involved the conversion of the time-of-travel measurement recorded internally by the instrument, to an edited time series of wave heights.

Wave autospectra were computed using the Fast Fourier Transform (FFT) technique. Two quantities, or non-directional wave parameters, were then computed from the autospectra: the significant wave height (H_s), calculated as four times the square root of the area under the autospectral curve; and the peak period (T_p), calculated as the corresponding period at which the autospectra reaches its maximum. At Site 1, the maximum wave height (H_{max}) was computed from the largest crest to trough distance in the segment.

The data was collected in four phases consisting of different sampling intervals:

- Phase 1 (Aug 28/09 to Oct 14/09) – the wave heights and tilts were were collected in wave burst mode at 2 Hz (4096 points every hour). Each burst of data consists of 34 minutes of data collection. The significant wave height (H_s) and the peak period (T_p) were computed from the autospectra using cutoffs of 20 seconds (0.05 Hz) to 1 second (1 Hz) and 4096 points.
- Phase 2 (Oct 15/09 to Nov 30/09) – the wave heights were measured continuously at 1-second intervals, and instrument tilts were measured at 40-second intervals. The significant wave height (H_s) and the peak period (T_p) were computed from the autospectra using cutoffs of 20 seconds (0.05 Hz) to 2 sec (0.5 Hz) and 3600 points.
- Phase 3 (Dec 01/09 to Mar 31/10) – contained no wave data.
- Phase 4 (Apr 01/10 to Jul26/10) – same as Phase 2.

For both data sets, the acoustic travel time was converted to a one-way range (distance from the IPS-5 to the air/water interface) by applying an estimate of the speed of sound in seawater of 1438 m/sec. Steps in the data processing consisted of:

1. Automated removal by linear interpolation of erroneous values that occur with the following attributes:
   - Out-of-range values
   - Null values
   - Statistical outliers
2. Trimming the start and end dates corresponding to the start and end of good data.
3. Applying a tilt correction using the recorded tilt values. For phase 1, the range and tilt were measured at 0.5s intervals and each range was corrected using the corresponding tilt value. In Phases 2 and 4, the tilt values were recorded at a 40

second interval and were smoothed using a 31 point running average and then interpolated to the 1-second range sampling interval.

4. Preparing time series plots of the edited wave data showing 12 hours of data per page.
5. Manual examination of the time series plots for remaining spikes that are replaced by linear interpolation and bubble clouds (erroneous data) that are replaced with 'flag' values (-9999). Ice data was also flagged.
6. Computing and plotting the autospectra. If more than 50% of the data in a burst was flagged, the H_s and T_p values are set to –9999. The peak period was flagged if the significant wave height was less than 0.1 m.
7. Manually reviewing each autospectral curve and the computed values for H_s and T_p.

Detailed processed results for each of the study sites are presented in Section 4.5 and are also included in the Data Archive.

3.3 ICE VELOCITY

3.3.1 INTRODUCTION

Ice velocity measurements were made with an Acoustic Doppler Current Profiler (ADCP) operated from the seabed (section 2.1.2), using the "Bottom-Track Upgrade" feature of the RD Instruments Sentinel Workhorse. The ADCP's at Site 1 and Site 2 recorded ice velocities at 5 minute sample intervals. Each measurement was derived using the observed Doppler shifts as realized from the four individual acoustic beams (each beam was oriented at a 20 degree angle from the vertical). Each 5 minute water velocity sample is an ensemble average of multiple acoustic water column pings. Each 5 minute ice velocity sample is an ensemble average of special "bottom tracking" pings which are used only for ice tracking and not for water column ocean current profiles. The details of the number of ADCP pings for each measurement ensemble are given in Table 3-6.

Table 3-6. Summary of ADCP configurations.

	Site 1	Site 2
	2009-2010	
Water Pings	25	24
Bottom Pings	5	5
Cell Size (m)	2	2
Processing Bandwidth	Wide Band	Narrow Band

According to the manufacturer, the accuracy of the "bottom track" velocity measurements is:

0.7 cm s^{-1}/(no. of pings per ensemble)$^{1/2}$. The accuracy of ice velocity measurements may be degraded because of the weak scattering coefficient from sea ice (Garrison et al., 1991); scattering energy from the seabed, which the manufacturers' specification is based on, is expected to be generally larger than that from sea-ice. However, the ADCP instruments have been demonstrated to effectively track ice velocities under at least some ice conditions (Belliveau et al., 1990; Melling et al., 1995).

Use of the ADCP for ice velocity measurements presents some special problems not encountered when used for bottom tracking (Melling et al., 1995):

Open water conditions: poorer accuracies for measurements of ice velocities under largely open-water conditions; under these conditions, the ADCP measurements are too noisy to be meaningful due to the rapid movement of the new targets (air bubbles and very short, capillary waves on the ocean surface) in response to the energetic motion of ocean waves. Due to the separation of the four acoustic beams, the wave-dominated velocities are unlikely to be equal within each beam. The assumption of uniform velocities among the four beams is fundamental to the operation of the ADCP instrument. As a result, the derived velocity is very noisy and has little information content. Such occurrences of noisy velocities associated with open water conditions are generally indicated by marked increases in the values of the vertical and error velocity components (the error velocity component is indicative of the degree of divergence in the Doppler velocities from each of the four acoustic beams).

Smooth ice: the occurrence of very weak echoes from smooth first year ice providing poor signal-to-noise ratio for velocities, so that the precision of the ice velocities is degraded. Uncertainties from smooth ice were not found to be a problem in the present ice velocity data set. However, episodes of open water or very low ice concentrations were often apparent in the ice velocity data set.

3.3.2 PROCESSING ICE VELOCITIES

The procedures for processing the ice velocity data (using the oceanographic direction convention of motion towards rather than the wind direction convention) involved the following sequence of tasks:

1. The ice velocities were screened for Correlation < 64, Amplitude < 50 and Verror > 5 cm/s and then averaged from 5 minute to 15 minute sampling intervals.
2. Prepare plots of raw east, north, vertical and error velocity channels.
3. Identify periods of probable open water for each data record using the plots from step (1) and other available information, including ice profiling sonar records supplemented by ice charts, and satellite imagery. For these periods, set the values of the horizontal velocity components to flag values of –9999. The first part of the time series records, when sea ice had not yet entered the area, or was of very low concentration, is also flagged.

4. Identify horizontal velocity values exceeding the out-of-bound threshold in absolute value (150 cms^{-1}).
5. Identify horizontal velocity values associated with error velocities exceeding 10 cm/s in absolute value.
6. Identify single point 'spikes' in each component of the horizontal velocities. A single point spike is where two successive first difference values exceed a single point threshold and are opposite in sign.
7. Identify 'double spikes' exceeding a double spike threshold in each component of the horizontal velocities. A double spike consists of two consecutive points, both of which are either larger or smaller than the preceding and following points by more than the double spike threshold.
8. Identify 'triple spikes' exceeding a triple spike threshold in each component of the horizontal velocities. A triple spike consists of three consecutive points which are smaller than the preceding and following points by more than triple spike threshold, but whose middle points may not change by more than one third of the triple spike threshold from their respective leading neighbours.
9. Identify 'quadruple spikes' exceeding a quadruple spike threshold in each component of the horizontal velocities. A quadruple spike consists of four consecutive points which are smaller than the preceding and following points by more than quadruple spike threshold, but whose middle points may not change by more than one third of the quadruple spike threshold from their respective leading neighbours.
10. For all suspect values found as above in items 3 to 8, the values are replaced by linear interpolation, over all individual segments with durations of less than three hours (one eighth the duration of the tidal signal which is predominantly diurnal). For longer segments of erroneous or suspect data, the values are replaced with flag values (-9999) and reviewed again in step 10.
11. Plots of the edited data sets (following step 9) are prepared and manually reviewed. Any remaining suspect values are manually edited using the ASL_EDIT display/editing software package. These suspect values are generally determined as being anomalous from adjoining values at nearby times and at nearby velocity bins containing data consistent with measurements on either side of the values in question.
12. Identify data segments where low ice concentrations increase the uncertainties in the ice velocities to unacceptable levels by further examination of the now-edited ice velocity times series, ice profiling sonar range plots and ice charts.
13. Reconstruct these sections, if possible, using nearby ice velocities or upper level ocean current measurements from the same site. If the ice velocities cannot be reconstructed, then flag the values as unreliable using –9999.
14. Plot the fully edited ice velocity data file to evaluate and continue editing, as required.

15. The final step before starting the analysis of the data was to convert the ice velocities from magnetic coordinates to geographic coordinates.

At Site 1 and Site 2, open water was encountered until the ice finally set in November. Afterwards, open water was not encountered again until the early summer break-up. A summary by site of the start and end times of the periods of valid ice velocity measurements is given in Table 3-7.

Time series plots of the ice velocities are presented in Figure 3-6 and Figure 3-7. The plots show the major and minor components at Site 1 and Site 2, respectively. Segments of bad data are denoted by vertical lines. The direction of the major ice drift component, including the positive major component, is tabulated in Table 3-8. At Site 1, the ice motion was oriented from 66.5° to 246.5° (66.5º positive) and at Site 2 the motion was oriented from 81° to 261° (81º positive). This rotation is optimized to maximize the variance in the major current component. The minor current component is perpendicular to the major current component.

Table 3-7. Summary of segments of the ice velocity data sets that were judged to be reliable or unreliable. Unreliable data includes open water.

Site 1			
Valid Date Start	**Valid Data End**	**Bad Data Start**	**Bad Data End**
		28-Aug-2009 04:55	22-Nov-2009 13:56
22-Nov-2009 14:11	21-May-2010 07:57	21-May-2010 08:12	24-May-2010 14:57
24-May-2010 15:12	24-May-2010 23:57	25-May-2010 00:12	25-May-2010 11:12
25-May-2010 11:27	25-May-2010 23:27	25-May-2010 23:42	26-May-2010 04:12
26-May-2010 04:27	26-May-2010 10:12	26-May-2010 10:27	28-May-2010 09:27
28-May-2010 09:42	30-May-2010 11:57	30-May-2010 12:12	30-May-2010 22:27
30-May-2010 22:42	02-Jun-2010 11:42	02-Jun-2010 11:57	07-Jun-2010 11:27
07-Jun-2010 11:42	08-Jun-2010 03:57	08-Jun-2010 04:12	21-Jun-2010 12:12
10664 bad data points out of 28542 total for entire record (37.4%)			
1090 bad data points out of 18968 total from first ice to last ice (5.7%)			
Site 2			
Valid Date Start	**Valid Data End**	**Bad Data Start**	**Bad Data End**
		29-Aug-2009 18:44	06-Nov-2009 19:40
06-Nov-2009 19:55	07-Nov-2009 17:10	07-Nov-2009 17:25	11-Nov-2009 11:39
11-Nov-2009 11:54	11-Nov-2009 18:39	11-Nov-2009 18:54	13-Nov-2009 08:24
13-Nov-2009 08:39	08-May-2010 20:57	08-May-2010 21:12	10-May-2010 02:57
10-May-2010 03:12	16-May-2010 17:42	16-May-2010 17:57	29-May-2010 07:11
29-May-2010 07:26	01-Jun-2010 19:41	01-Jun-2010 19:56	10-Jun-2010 15:10
10-Jun-2010 15:25	10-Jun-2010 17:55	10-Jun-2010 18:10	15-Jul-2010 10:38
15-Jul-2010 10:53	16-Jul-2010 04:38	16-Jul-2010 04:53	28-Jul-2010 04:37
13797 bad data points out of 31914 total for entire record (43.2%)			
6016 bad data points out of 24133 total from first ice to last ice (24.9%)			

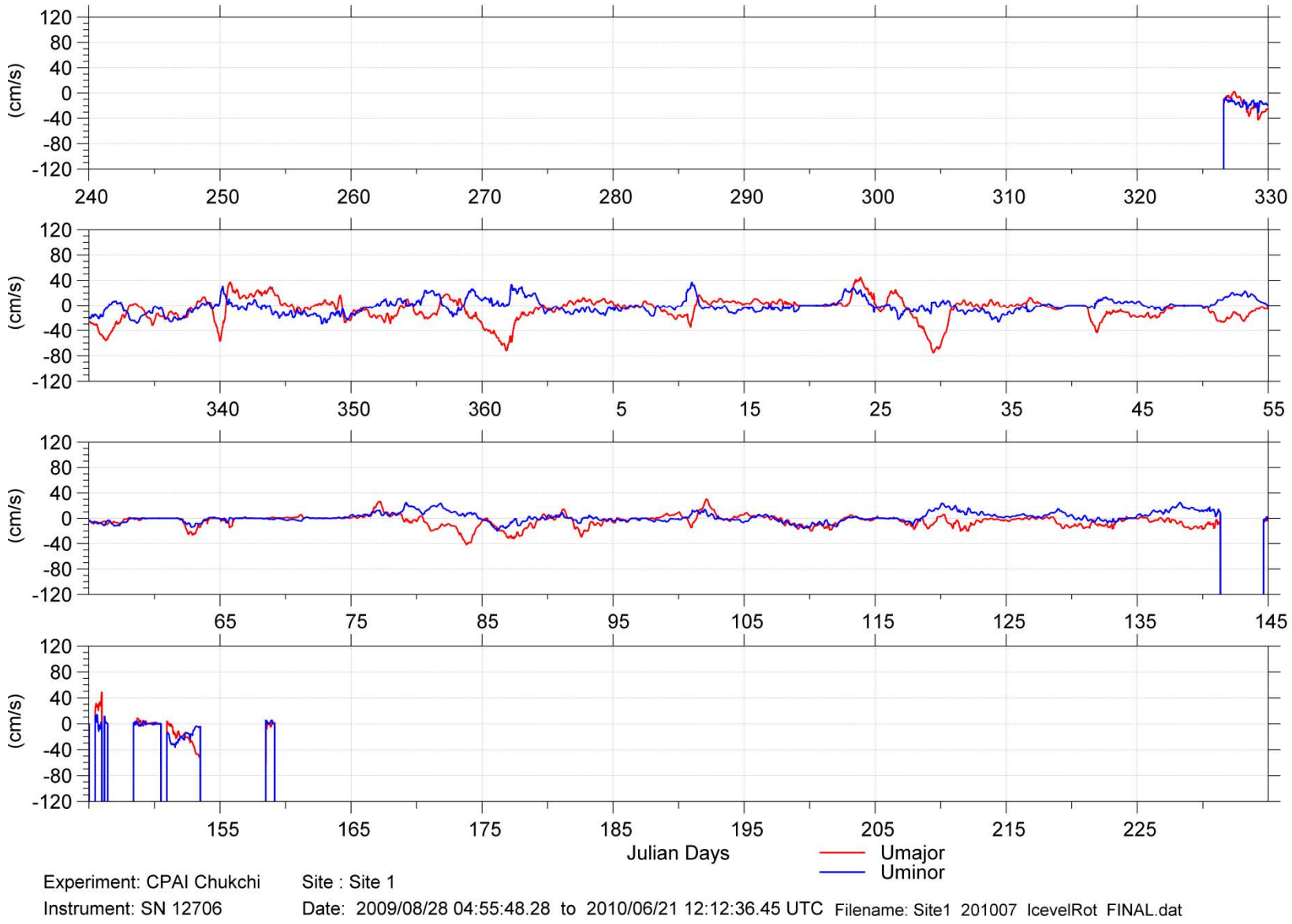

Figure 3-6. Plot of the edited ice velocity for Site 1 as a time series of the major and minor components of the ice velocity. Segments of bad data are denoted by vertical lines.

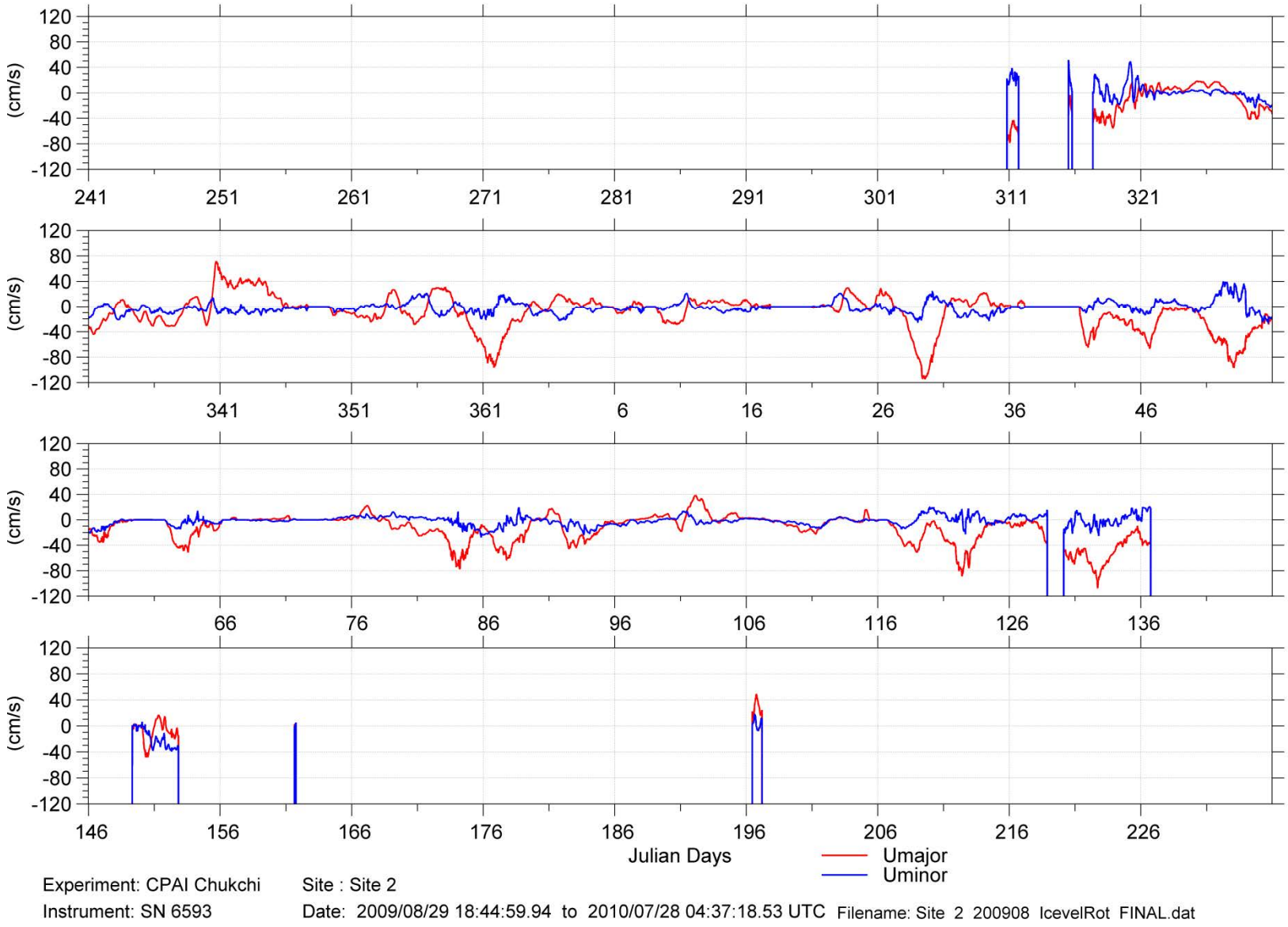

Figure 3-7. Plot of the edited ice velocity for Site 2 as a time series of the major and minor components of the ice velocity. Segments of bad data are denoted by vertical lines.

Table 3-8. Summary of the major current direction for the ice velocities at each site.

Site	Current Direction (°)	Heading of Positive Umajor (°)
1	66.5 - 246.5	66.5
2	81 - 261	81

Table 3-9. Summary of the number of ice velocity points that were edited.

	Site 1		Site 2	
	East/ West	North/ South	East/ West	North/ South
Out of Range	1	1	184	77
Single Spike	141	154	135	151
Double Spike	73	54	58	87
Triple Spike	1	0	4	4
Quad. Spike	0	1	1	3
Manual Edit	2609	2362	2259	2185
% Edit	9.1%	8.3%	7.1%	6.8%
# Flags in Raw Data (%)	6598 (23.1%)		10038 (31.5%)	
# Flags Final (%)	10664 (37.4%)		13797 (43.2%)	
Total Pts	28542		31914	

3.3.3 SUMMARY OF ICE VELOCITY

Reliable ice velocity measurements were obtained at both measurement sites starting from November 2009, when new sea-ice formation began. At Site 1, the ADCP was recovered on the morning of July 26, 2010, but was not pinging at recovery. The last recorded data record was on June 21, 2010 and an examination of the y-cable determined that there was a power pin which was pitted by corrosion. At Site 2, there were no issues with the ADCP and the instrument collected a full data record.

The ice velocities at the measurement sites exhibited coherent variations, as can be seen by the many similarities between the time series plots (Figure 3-6 and Figure 3-7). During the fall season the ice is constantly moving while ice is forming and high winds are prevalent, compared with the winter and spring where periods of no-motion events are observed. The number of no-motion points in each month is summarized in Table 3-10. The proportion of no-motion observations reaches a maximum of 16.8% in February at Site 2. For the same month, there was no-motion at Site 1 for 8.1% of the time.

Monthly statistics are given in Table 3-11 and Table 3-12 for Site 1 and Site 2 respectively. The number of valid points *versus* the total number of points for each month shows which months have smaller numbers of valid ice velocity samples, and thus less reliability. The

largest ice speeds were measured at Site 2, where the maximum speed reached 114.8 cm/s. At Site 1, the maximum ice speed reached was 75.8 cm/s. The mean speeds of the entire deployment were 13.8 and 19.8 cm/s at Site 1 and Site 2 respectively.

The ice velocities are further illustrated through compass plots, which show the speed and direction joint frequency distribution. The color of each segment denotes its speed interval. The radial length of each segment denotes the proportion of measurements within the illustrated speed and direction interval. The maximum and mean are illustrated through the second radial scale as the red and green lines respectively for clear viewing. The speed and direction distributions are shown for the full deployment in Figure 3-10 while the monthly compass plots of ice velocity are shown in Figure 3-11 and Figure 3-12.

The full set of joint frequency tabulations of Ice Speed vs. Ice Direction for each site (full record plus each individual month) are provided as part of the Data Archive on ASL's FTP site.

Table 3-10. Summary of the number of no-motion points encountered at each site from August 2009 to July 2010. Note that the ice velocity data ended in late June at Site 1.

	Site 1			Site 2		
Month	**# points**	**# zero points**	**% zero points**	**# points**	**# zero points**	**% zero points**
Aug-09	365	0	0.0%	214	0	0.0%
Sept-09	2880	0	0.0%	2880	0	0.0%
Oct-09	2976	0	0.0%	2976	0	0.0%
Nov-09	2880	0	0.0%	2880	0	0.0%
Dec-09	2976	0	0.0%	2976	164	5.5%
Jan-10	2976	99	3.3%	2976	468	15.7%
Feb-10	2688	219	8.1%	2688	451	16.8%
Mar-10	2976	137	4.6%	2976	442	14.9%
Apr-10	2880	30	1.0%	2881	82	2.8%
May-10	2976	0	0.0%	2976	0	0.0%
Jun-10	1969	0	0.0%	2880	0	0.0%
Jul-10	-	-	-	2611	0	0.0%

Table 3-11. Statistical summary of measured ice velocities by month at Site 1.

Site 1	chan	min	1%	5%	25%	50%	mean	75%	95%	99%	std	max	# valid	total #
Time	cm/s													
28-Aug-2009	Umajor	0.0	0.0	0.0	0.0	0.0	0.0	0.0	0.0	0.0	0.0	0.0		
-	Uminor	0.0	0.0	0.0	0.0	0.0	0.0	0.0	0.0	0.0	0.0	0.0		
31-Aug-2009	Speed	0.0	0.0	0.0	0.0	0.0	0.0	0.0	0.0	0.0	0.0	0.0	0	365
01-Sep-2009	Umajor	0.0	0.0	0.0	0.0	0.0	0.0	0.0	0.0	0.0	0.0	0.0		
-	Uminor	0.0	0.0	0.0	0.0	0.0	0.0	0.0	0.0	0.0	0.0	0.0		
30-Sep-2009	Speed	0.0	0.0	0.0	0.0	0.0	0.0	0.0	0.0	0.0	0.0	0.0	0	2880
01-Oct-2009	Umajor	0.0	0.0	0.0	0.0	0.0	0.0	0.0	0.0	0.0	0.0	0.0		
-	Uminor	0.0	0.0	0.0	0.0	0.0	0.0	0.0	0.0	0.0	0.0	0.0		
31-Oct-2009	Speed	0.0	0.0	0.0	0.0	0.0	0.0	0.0	0.0	0.0	0.0	0.0	0	2976
01-Nov-2009	Umajor	-56.3	-55.1	-49.7	-30.9	-22.6	-21.6	-7.0	1.6	2.7	15.6	3.3		
-	Uminor	-31.4	-28.8	-25.5	-18.6	-15.0	-13.5	-9.8	4.5	6.9	8.6	7.6		
30-Nov-2009	Speed	9.0	11.3	13.4	19.6	27.3	28.9	35.0	52.1	55.4	11.3	56.5	808	2880
01-Dec-2009	Umajor	-72.3	-62.5	-46.0	-18.3	-7.5	-8.3	3.5	21.7	29.4	19.3	37.8		
-	Uminor	-30.1	-26.1	-21.2	-11.7	-1.8	-1.5	6.1	22.9	27.5	13.0	34.3		
31-Dec-2009	Speed	0.4	2.3	5.9	13.2	18.6	21.3	26.9	47.3	63.8	12.5	72.3	2976	2976
01-Jan-2010	Umajor	-75.7	-69.3	-43.5	-3.3	2.2	-1.4	6.5	20.8	39.8	18.5	44.8		
-	Uminor	-22.7	-17.4	-13.4	-7.9	-3.7	-2.1	0.0	22.2	28.5	9.5	37.3		
31-Jan-2010	Speed	0.0	0.0	0.1	5.7	10.2	14.8	17.5	47.1	69.4	14.8	75.8	2976	2976
01-Feb-2010	Umajor	-43.9	-36.2	-25.2	-12.0	-4.5	-6.8	0.0	4.4	9.5	9.3	12.7		
-	Uminor	-26.8	-22.2	-13.5	-5.8	-0.2	-0.6	3.7	16.5	20.2	8.6	23.3		
28-Feb-2010	Speed	0.0	0.0	0.0	3.3	10.0	11.1	17.4	27.5	36.5	9.1	44.6	2688	2688
01-Mar-2010	Umajor	-41.9	-38.4	-27.8	-10.9	-0.1	-4.9	0.7	6.8	22.7	11.2	26.9		
-	Uminor	-20.6	-16.4	-11.8	-1.8	0.0	1.6	5.2	18.0	22.1	7.7	25.0		
31-Mar-2010	Speed	0.0	0.0	0.0	1.0	5.5	10.0	17.1	29.7	39.1	10.5	42.2	2976	2976
01-Apr-2010	Umajor	-29.8	-22.1	-16.4	-8.3	-1.1	-2.5	2.0	10.2	23.6	8.4	30.6		
-	Uminor	-16.4	-14.5	-11.1	-4.0	-1.3	-0.7	1.2	13.4	19.7	6.7	23.9		
30-Apr-2010	Speed	0.0	0.0	0.2	2.8	6.0	8.5	14.5	21.0	28.2	7.1	32.1	2880	2880
01-May-2010	Umajor	-23.0	-19.6	-16.1	-10.7	-3.5	-4.9	-0.2	2.1	28.8	8.0	49.1		
-	Uminor	-37.2	-31.3	-6.8	-0.1	4.0	3.9	10.0	16.6	20.9	9.1	25.1		
31-May-2010	Speed	0.0	0.2	0.5	4.1	9.8	10.9	16.0	26.8	35.5	8.3	49.1	2365	2976
01-Jun-2010	Umajor	-53.2	-52.7	-49.5	-33.6	-21.1	-21.5	-4.4	1.4	2.3	16.8	2.9		
-	Uminor	-25.8	-25.5	-23.2	-16.0	-6.4	-8.7	0.2	4.2	5.9	9.1	6.4		
21-Jun-2010	Speed	0.3	0.3	0.5	5.8	28.7	25.1	35.7	49.6	52.7	16.5	53.4	209	1969
Entire	Umajor	-75.7	-56.3	-31.0	-12.4	-2.2	-5.7	1.3	13.5	28.0	14.4	49.1		
-	Uminor	-37.2	-25.1	-17.2	-6.0	-0.5	-0.7	4.1	17.7	25.0	9.9	37.3		
Record	Speed	0.0	0.0	0.1	4.3	11.3	13.8	19.7	36.5	57.0	12.2	75.8	17878	28542

Table 3-12. Statistical summary of measured ice velocities by month at Site 2.

Site 2	chan	min	1%	5%	25%	50%	mean	75%	95%	99%	std	max	# valid	total #
Time	cm/s													
29-Aug-2009	Umajor	0.0	0.0	0.0	0.0	0.0	0.0	0.0	0.0	0.0	0.0	0.0		
-	Uminor	0.0	0.0	0.0	0.0	0.0	0.0	0.0	0.0	0.0	0.0	0.0		
31-Aug-2009	Speed	0.0	0.0	0.0	0.0	0.0	0.0	0.0	0.0	0.0	0.0	0.0	0	213
01-Sep-2009	Umajor	0.0	0.0	0.0	0.0	0.0	0.0	0.0	0.0	0.0	0.0	0.0		
-	Uminor	0.0	0.0	0.0	0.0	0.0	0.0	0.0	0.0	0.0	0.0	0.0		
30-Sep-2009	Speed	0.0	0.0	0.0	0.0	0.0	0.0	0.0	0.0	0.0	0.0	0.0	0	2880
01-Oct-2009	Umajor	0.0	0.0	0.0	0.0	0.0	0.0	0.0	0.0	0.0	0.0	0.0		
-	Uminor	0.0	0.0	0.0	0.0	0.0	0.0	0.0	0.0	0.0	0.0	0.0		
31-Oct-2009	Speed	0.0	0.0	0.0	0.0	0.0	0.0	0.0	0.0	0.0	0.0	0.0	0	2976
01-Nov-2009	Umajor	-78.4	-69.0	-49.5	-28.4	-6.7	-11.6	7.1	16.5	17.9	21.7	18.8		
-	Uminor	-23.7	-21.4	-18.2	-6.9	-0.1	0.1	3.5	24.6	41.9	12.3	51.5		
30-Nov-2009	Speed	0.1	0.7	2.6	9.1	18.1	22.2	33.1	53.3	70.8	16.3	81.4	1808	2880
01-Dec-2009	Umajor	-96.5	-86.7	-55.5	-18.6	-5.7	-4.0	14.3	40.7	58.2	28.8	71.9		
-	Uminor	-21.5	-16.2	-12.8	-7.3	-2.8	-2.1	1.1	14.4	19.5	7.5	21.6		
31-Dec-2009	Speed	0.0	0.0	0.0	10.0	18.9	23.4	32.3	63.1	87.1	18.9	96.7	2976	2976
01-Jan-2010	Umajor	-114.7	-109.7	-62.8	-3.2	0.4	-4.2	6.9	18.7	27.4	24.3	30.1		
-	Uminor	-25.8	-20.8	-14.5	-5.4	-1.4	-1.6	0.0	14.7	20.4	7.6	25.2		
31-Jan-2010	Speed	0.0	0.0	0.0	2.5	8.3	14.9	18.9	64.5	109.8	21.2	114.8	2976	2976
01-Feb-2010	Umajor	-97.0	-86.8	-64.8	-32.9	-7.2	-17.2	0.0	10.2	20.8	24.0	22.6		
-	Uminor	-26.6	-20.9	-17.6	-8.0	-0.2	-1.0	2.6	21.5	36.2	11.2	40.3		
28-Feb-2010	Speed	0.0	0.0	0.0	3.2	16.7	22.2	34.8	69.8	91.3	22.4	100.1	2688	2688
01-Mar-2010	Umajor	-77.5	-65.3	-51.3	-20.1	-0.9	-11.9	0.2	5.3	19.0	18.7	22.8		
-	Uminor	-27.7	-22.5	-15.9	-2.5	0.0	-1.2	2.4	6.6	10.9	6.5	19.8		
31-Mar-2010	Speed	0.0	0.0	0.0	1.1	7.7	15.1	23.8	52.1	65.5	17.4	77.7	2976	2976
01-Apr-2010	Umajor	-51.2	-46.0	-37.4	-13.5	-1.6	-5.4	2.6	16.7	33.4	15.7	38.3		
-	Uminor	-23.6	-19.0	-13.0	-6.3	-2.2	-2.4	0.7	11.6	17.4	6.8	20.5		
30-Apr-2010	Speed	0.0	0.0	0.4	3.4	8.8	13.2	19.5	38.6	46.0	12.4	51.2	2881	2881
01-May-2010	Umajor	-107.7	-91.4	-77.5	-49.8	-30.6	-30.9	-6.1	1.4	13.3	26.6	16.7		
-	Uminor	-38.3	-34.7	-23.1	-6.2	-0.1	-1.4	5.9	14.4	19.1	10.9	21.3		
31-May-2010	Speed	0.0	0.3	2.4	10.7	34.1	34.3	50.7	78.1	91.8	24.6	108.7	1650	2976
01-Jun-2010	Umajor	-20.3	-20.3	-18.7	-14.4	-11.2	-10.4	-8.3	2.1	2.7	5.9	3.4		
-	Uminor	-39.4	-39.4	-36.8	-36.0	-34.3	-29.9	-30.4	0.1	2.7	11.6	5.2		
30-Jun-2010	Speed	0.8	0.8	2.2	33.2	37.5	32.3	38.2	38.7	39.7	11.5	40.1	90	2880
01-Jul-2010	Umajor	11.1	11.1	12.3	17.9	27.4	28.3	38.3	46.5	48.6	11.4	48.7		
-	Uminor	-7.5	-7.5	-7.1	-3.6	3.1	3.6	9.9	17.0	17.8	7.9	18.2		
28-Jul-2010	Speed	11.7	11.7	13.3	19.2	28.6	29.7	40.1	46.6	48.6	11.3	48.7	72	2611
Entire	Umajor	-114.7	-86.1	-58.2	-22.4	-3.0	-10.6	2.4	20.8	40.4	24.4	71.9		
-	Uminor	-39.4	-23.7	-16.6	-6.2	-0.9	-1.6	1.9	14.0	25.3	9.1	51.5		
Record	Speed	0.0	0.0	0.0	4.3	14.0	19.8	29.4	61.3	88.4	20.1	114.8	18117	31914

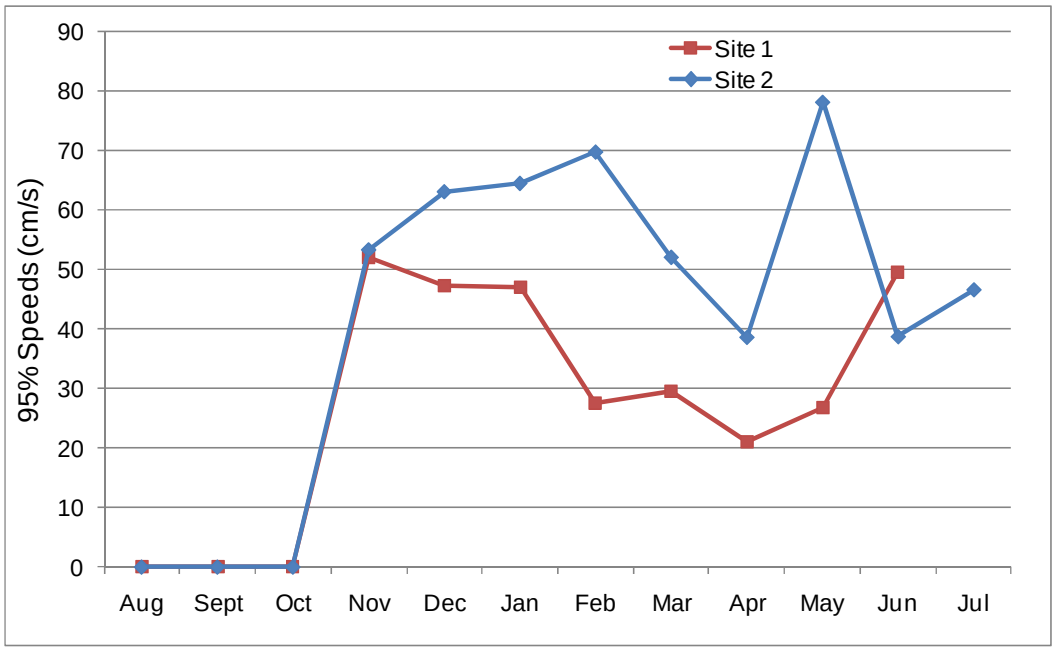

Figure 3-8. The 95 percentile speeds (cm/s) by month at Site 1 and Site 2.

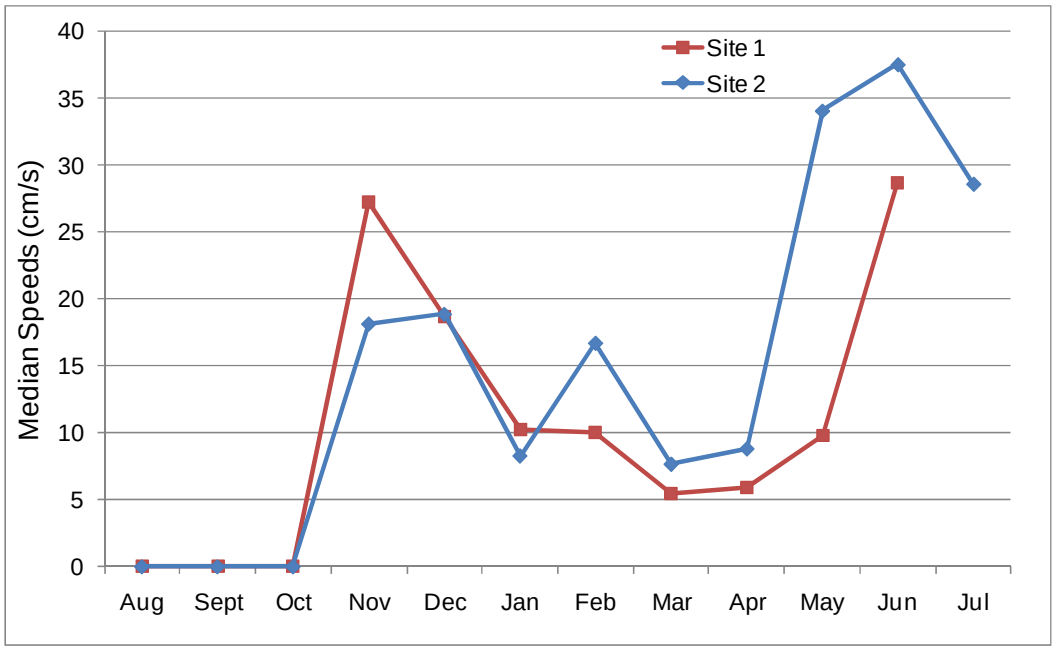

Figure 3-9. The median speeds (cm/s) by month at Site 1 and Site 2.

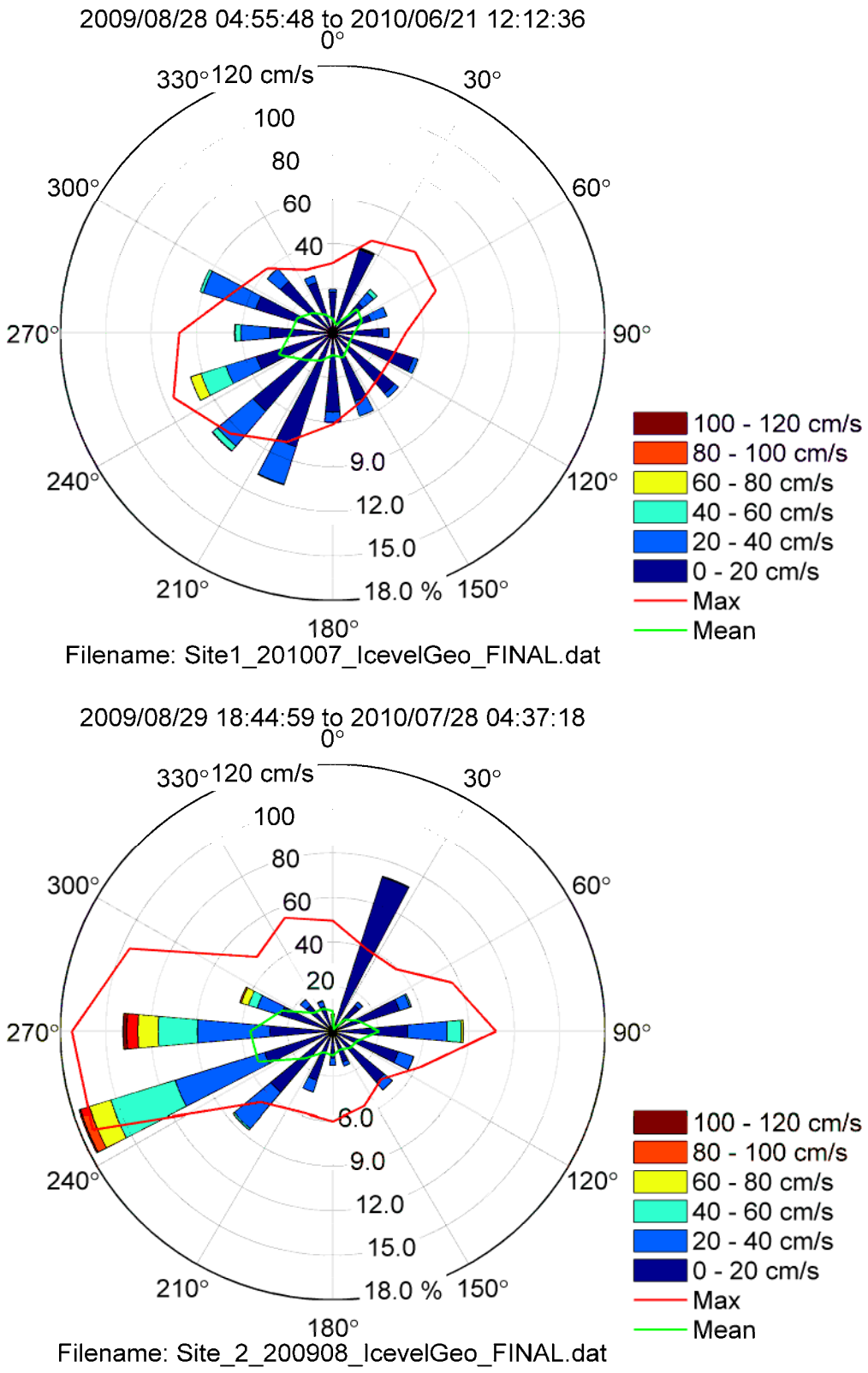

Figure 3-10. Compass plots of the directional (towards) distribution of the observed ice velocity over the full deployment for Site 1 (top) and Site 2 (bottom). The next pages contain the monthly compass plots for each site.

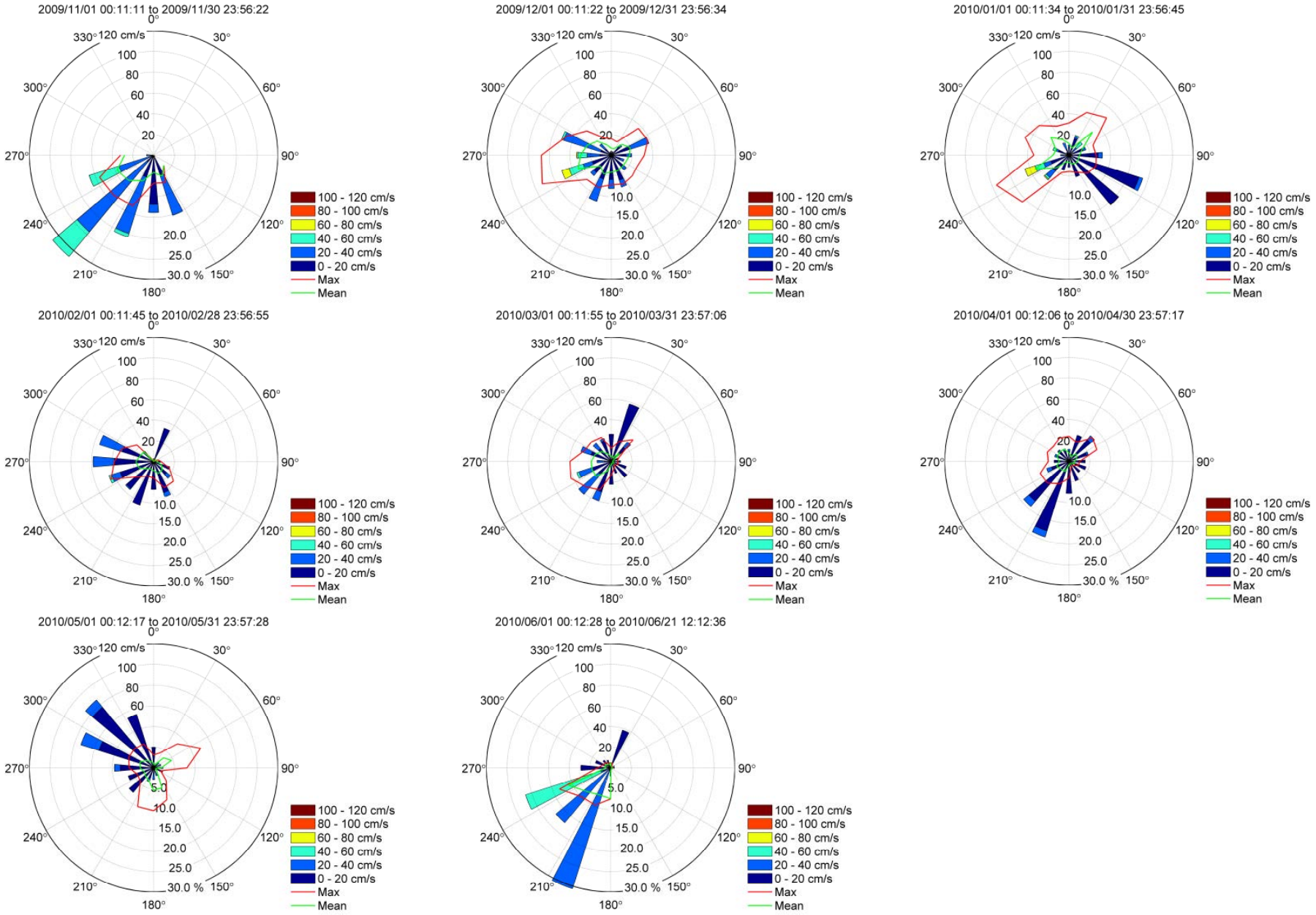

Figure 3-11. Monthly compass plots of the directional (towards) distribution of ice velocities at Site 1 from November 2009 to June 2010.

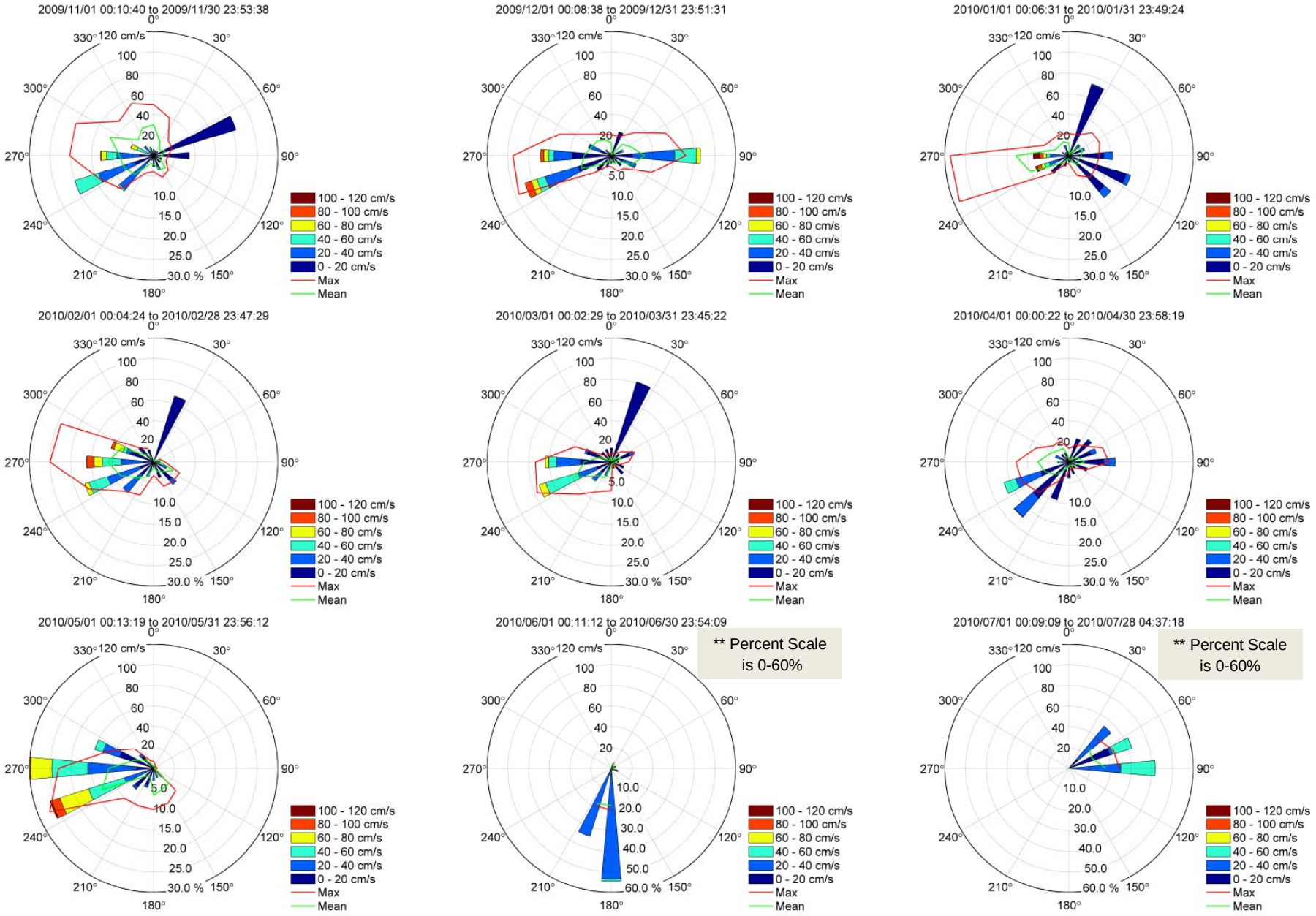

Figure 3-12. Monthly compass plots of the directional (towards) distribution of ice velocities at Site 2 from November 2009 to July 2010.

3.4 OCEAN CURRENT DATA

3.4.1 PROCESSING CURRENT PROFILER DATA

The Acoustic Doppler Current Profiler (ADCP) instrument, operating in the conventional water column data acquisition mode, provided time series measurements of three dimensional ocean currents, at 5 minute sampling intervals and with a vertical resolution of 2 m at Site 1 and Site 2. The near-bottom ADCP measurements correspond to measurements about 4 m above the instrument due to the blanking distance associated with the instrument. Table 3-13 tabulates several of the measurement parameters associated with the water column measurements as well as the acoustic bins which yielded useful data.

The data from the instrument at Site 1 ended on June 21, 2010 due to the corrosion of a pin on the external power cable. A time check showed the ADCP at this site to be 2 minutes 1 second slow. At Site 2, the ADCP collected a full data record from August 29, 2009 to July 28, 2010 and was found to be 2 minutes 6 seconds slow.

Horizontal velocities were analyzed from three levels, near surface, mid-depth and near bottom. The mid and near bottom levels currents were derived from single ADCP bins. However, the ADCP currents in bins near the water-air interface are at times contaminated by waves. Similarly, the currents in the upper-most bins near the ice-water interface are at times contaminated by the presence of ice keels. A semi-automated methodology was developed to identify the first uncontaminated bin nearest the air-water interface for open water conditions or nearest the ice-water interface for ice covered conditions. This involved the use of the ADCP's pressure and bottom track channels in the following way:

1. The data was viewed in WinADCP, and for large wave events, the nearest surface bin that contained acceptable data was chosen.
2. The pressure record and the pressure standard deviation record were extracted from the ADCP.
3. The depth of water in each beam at which the bottom track was located was extracted from the ADCP (i.e. the vertical component of the bottom track range in each beam).
4. Due to the possibility of acceptable three beam solutions of the ice velocity, an assumption was made that if ice was present in one of the beams, but not the other three, the built-in data rejection algorithms of the ADCP would discard the data in the blocked beam, and generate an acceptable solution. Therefore, the second deepest depth by beam was extracted.
5. The pressure was converted to approximate depth by multiplying by a density of 1.025 and the time series was plotted.
6. The second deepest bottom track depth time series was overlaid on the same plot.
7. An approximation of the significant wave height was found (4 * pressure standard deviation).

8. The factor by which the pressure standard deviation was multiplied was increased until the bin chosen visually in step one was picked by this algorithm for large wave events.
9. A sidelobe correction factor of 0.87333 was applied.
10. The mean pressure was found and subtracted from the series.
11. The series was low-pass filtered using the parameters b=[1/6, 1/6, 1/6, 1/6, 1/6, 1/6] and a=1.
12. The series was flipped along the x axis and filtered again using the same parameters.
13. The mean pressure was added back into the series.
14. The deeper of the modified pressure channel and the bt range * 0.87333 was chosen, and the bin corresponding to this was used.
15. The chosen bin was averaged with the two below it, to give a near-surface current.
16. During large wave events, smoothing was applied manually as necessary.

The ADCP's *false target rejection* algorithm calculates a three-beam solution if the intensity from a single beam differs by a significant amount from the other beams. However, if more than one beam's intensity was significantly different from the other values or too small, no measured value was recorded. Time series plots of the depths chosen for the near surface bins at Site 1 and Site 2 are shown in Figure 3-13 and Figure 3-14.

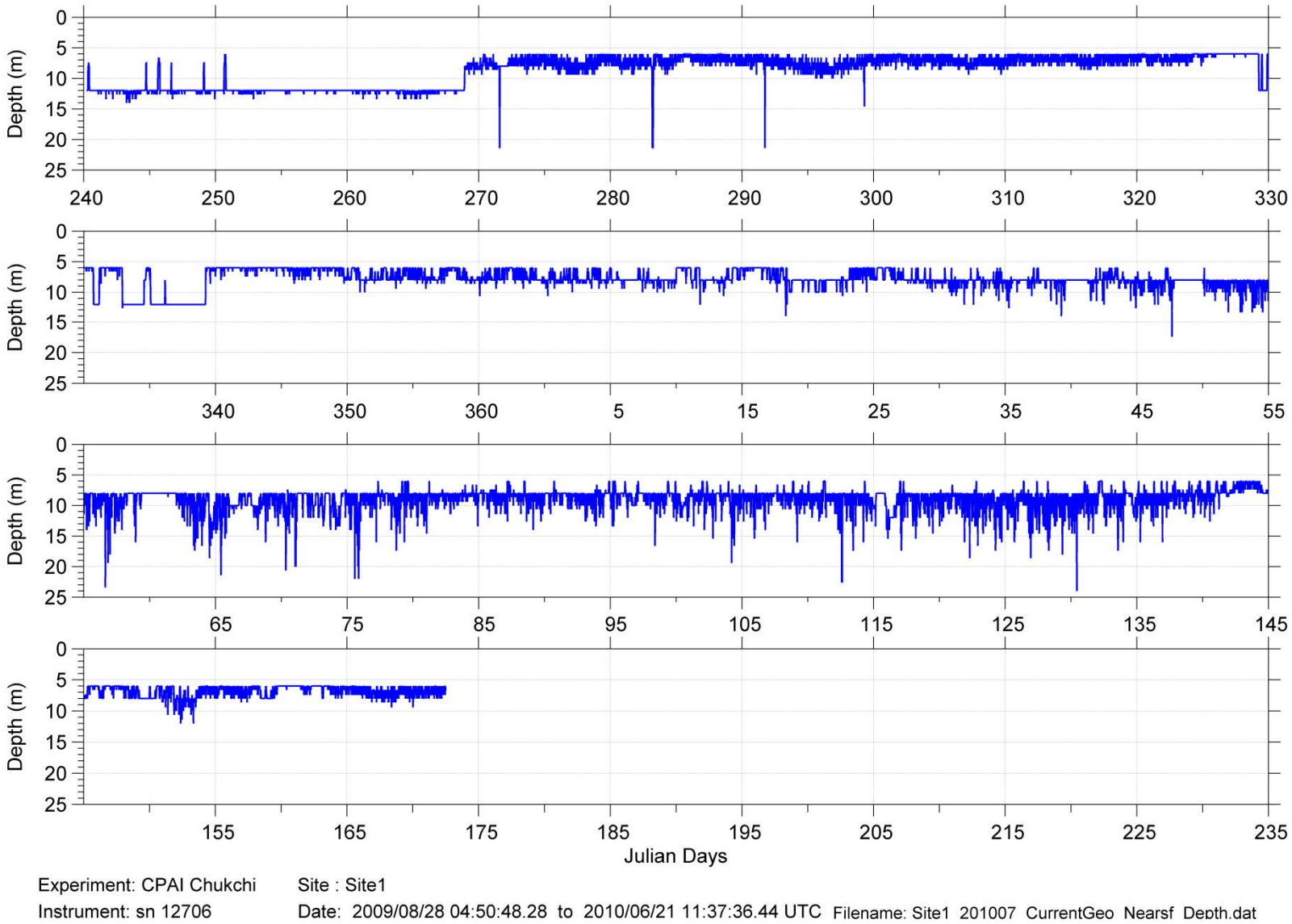

Figure 3-13. Time series plot of the depth chosen for the near surface bin at Site 1.

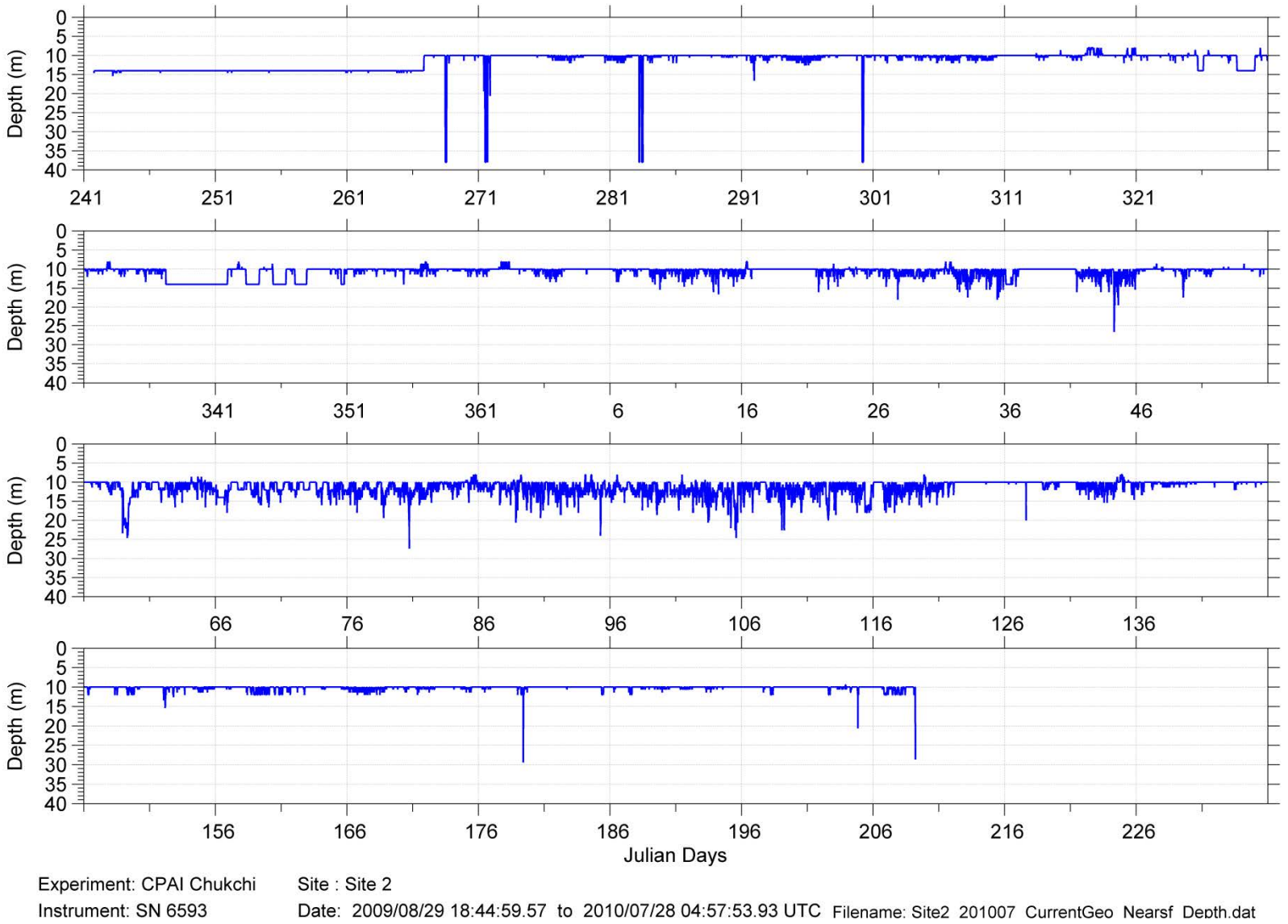

Figure 3-14. Time series plot of the depth chosen for the near surface bin at Site 2.

Table 3-13. Summary of current measurement parameters.

	Site 1	Site 2
Latitude	N 70° 59.913'	N 70° 58.732'
Longitude	W 165° 0.072'	W 160° 58.233'
Instrument Depth (m)	32	43
Bin Size (m)	2	2
Sample Interval (min)	5	5
Number of Data Values	28542	31914
Instrument Bin Number	Measurement Depth (m)	
1	28	39
2	26	37
3	24	35
4	22	33
5	20	31
6	18	29
7	16	27
8	14	25
9	12	23
10	10	21
11	8	19
12	6	17
13	4	15
14	2	13
15	0	11
16	-	9
17	-	7
18	-	5
19	-	3
20	-	1

Each time series data set was subjected to quality control procedures. The steps in the error detection and removal procedures were applied as follows:

1. The currents were screened for Correlation < 64, Amplitude < 50 and Verror > 5 cm/s and then averaged from 5 minute to 15 minute sampling intervals.
2. Plots of all the raw data sets were prepared and reviewed, including the ADCP vertical and error velocities.
3. Values of measured horizontal components of current that had absolute values exceeding the out-of-bound threshold were selected.
4. Values of measured horizontal components of current with accompanying error velocities that exceeded 10 cm s^{-1} were selected.
5. Single point 'spikes' in each component of the horizontal velocities were identified. A single point spike consisted of two successive first difference values exceeding a single spike threshold and opposite in sign.

6. 'Double spikes' exceeding a double spike threshold in each component of the horizontal velocities were identified. A double spike consisted of two consecutive points, both of which were either larger or smaller than the preceding and following points by more than the double spike threshold.
7. 'Triple spikes' exceeding a triple spike threshold in each component of the horizontal velocities were identified. A triple spike consisted of three consecutive points which were smaller than the preceding and following points by more than the triple spike threshold, but whose middle points could not change by more than one third of the triple spike threshold from their respective leading neighbours.
8. 'Quadruple spikes' exceeding a quadruple spike threshold in each component of the horizontal velocities were identified. A quadruple spike consisted of four consecutive points which were smaller than the preceding and following points by more than the quadruple spike threshold, but whose middle points could not change by more than one third of the quadruple spike threshold from their respective leading neighbours.
9. For all suspect values found as above in items 2 to 7, the values were replaced by linear interpolation, over all individual segments with durations of less than two and a half hours (approximately one eighth of the tidal signal which was predominantly diurnal). For longer segments of erroneous or suspect data, the values were replaced with flag values (-9999) and reviewed again in step 9.
10. Plots of the edited data sets (following step 8) were prepared and manually reviewed. Any remaining suspect values were manually edited. These suspect values were generally determined as being anomalous from adjoining values at nearby times or at adjacent bins above and below.
11. In cases where there were flags (from step 8), velocity data from neighbouring bins were used to reconstruct the segments.

The number of data points which were identified as suspect in accordance with the above methodology is summarized in Table 3-14. The final step before starting the analysis of the data was to convert the currents from magnetic coordinates to geographic coordinates. This step included the application of the compass calibration information measured prior to the deployment of the ADCP's.

Table 3-14. Summary of the number of points modified at Site 1 and Site 2 for selected bins.

	Veast			Vnorth		
	Near Surface	**16m**	**26m**	**Near Surface**	**16m**	**26m**
	Site 1					
Out of Range	24	0	0	2	0	0
Single Spike	319	292	127	229	233	77
Double Spike	69	36	6	41	36	16
Triple Spike	4	2	2	1	4	0
Quad. Spike	1	1	0	1	0	0
Manual Edit	762	1098	686	471	1201	493
Total # Edited (%)	1179 (4.13%)	1429 (5.01%)	821 (2.88%)	745 (2.61%)	1474 (5.16%)	586 (2.05%)
# Flagged	0	0	0	2	0	0
Total Pts	28541			28541		
	Veast			**Vnorth**		
	Near Surface	**23m**	**39m**	**Near Surface**	**23m**	**39m**
	Site 2					
Out of Range	0	0	0	0	0	0
Single Spike	572	189	128	389	156	91
Double Spike	88	25	12	61	9	14
Triple Spike	6	0	0	1	2	5
Quad. Spike	0	0	1	0	0	1
Manual Edit	3793	394	307	2292	242	241
Total # Edited (%)	4459 (13.97%)	608 (1.91%)	448 (1.40%)	2743 (8.59%)	409 (1.28%)	352 (1.10%)
# Flagged	0	0	0	0	0	0
Total Pts	31914			31914		

3.4.2 PLOTS AND STATISTICAL SUMMARIES FOR NEAR-SURFACE, MID-DEPTH AND NEAR-BOTTOM MEASUREMENT LEVELS

A major/minor coordinate system (u-major and u-minor) was used, similar to the one already presented for the ice velocities in the previous section. Table 3-15 tabulates the direction axis that the currents at each depth were oriented along, and specifies the direction of positive u-major.

Table 3-15. Summary of the rotation applied at the near-surface, mid-depth, and near-bottom bins of each site to obtain the major/minor velocity components.

Site 1	Current Direction (°)	Heading of Positive Umajor (°)
Bin 2	77 - 257	77
Bin 7	78 - 258	78
Near Surface	79 - 259	79
Site 2	**Current Direction (°)**	**Heading of Positive Umajor (°)**
Bin 1	88 - 268	88
Bin 9	98 - 278	98
Near Surface	98 - 278	98

The final versions of the edited current meter data sets for the two sites are presented for the near-surface, mid-depth, and near-bottom as time series plots (Figure 3-15 through Figure 3-20).

Statistical summaries of the near-surface, mid-depth and near-bottom current speeds are given for the full deployment period in Table 3-16 and quarterly statistical tables are given in Table 3-17 through Table 3-22. The current speeds are further illustrated through compass plots (Figure 3-21), which show the speed and direction joint frequency distribution for the entire deployment. The color of each segment denotes its speed interval. The radial length of each segment denotes the proportion of measurements within the illustrated speed and direction interval. The maximum and mean are illustrated through the second radial scale as the red and green lines respectively.

The full set of joint frequency tabulations of current speed vs. current direction for each depth at each site (full record plus each individual month) are provided in the Data Archive to this report which can be downloaded from the ASL FTP site.

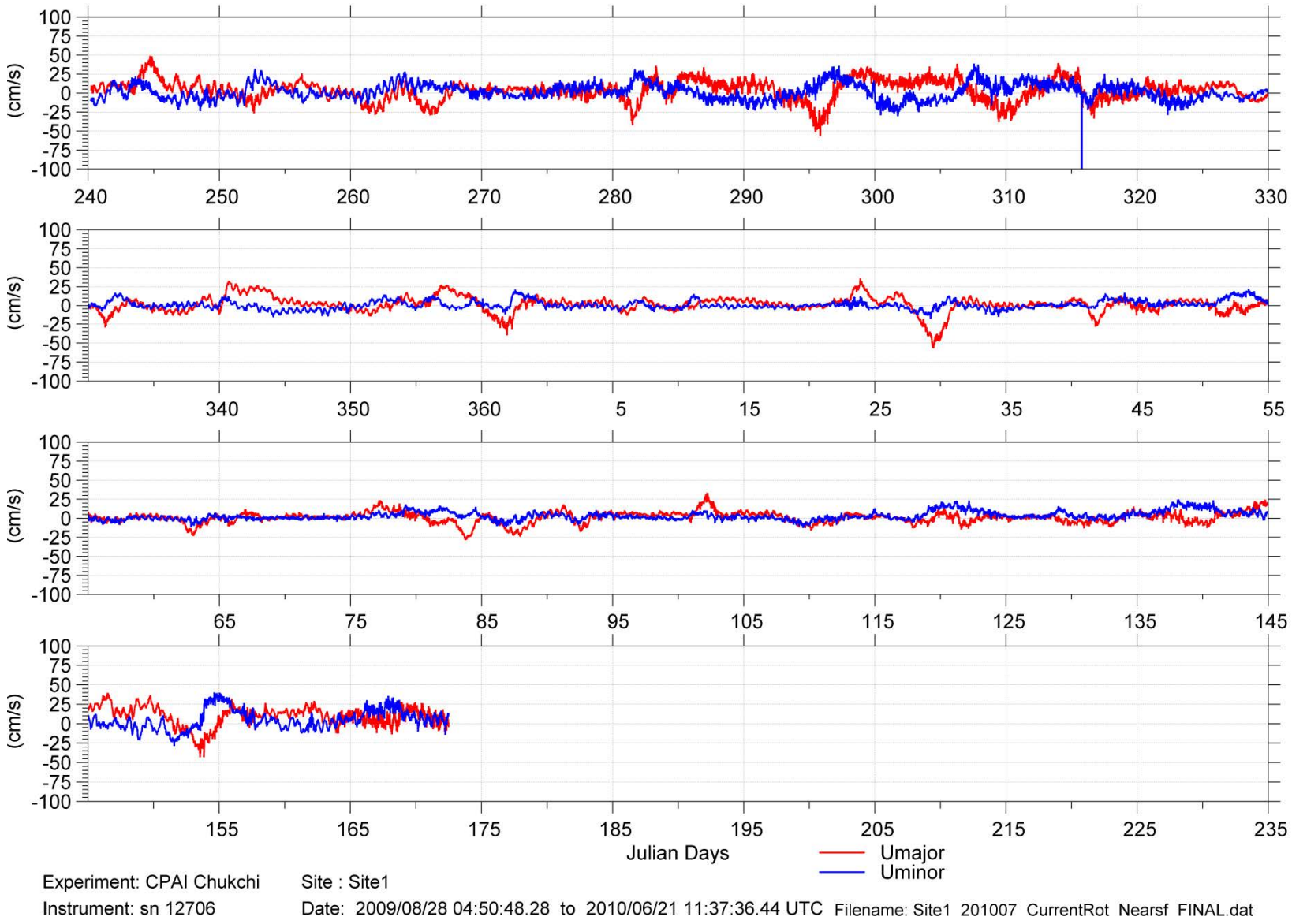

Figure 3-15. Plot of the variable near surface current measurements at Site 1.

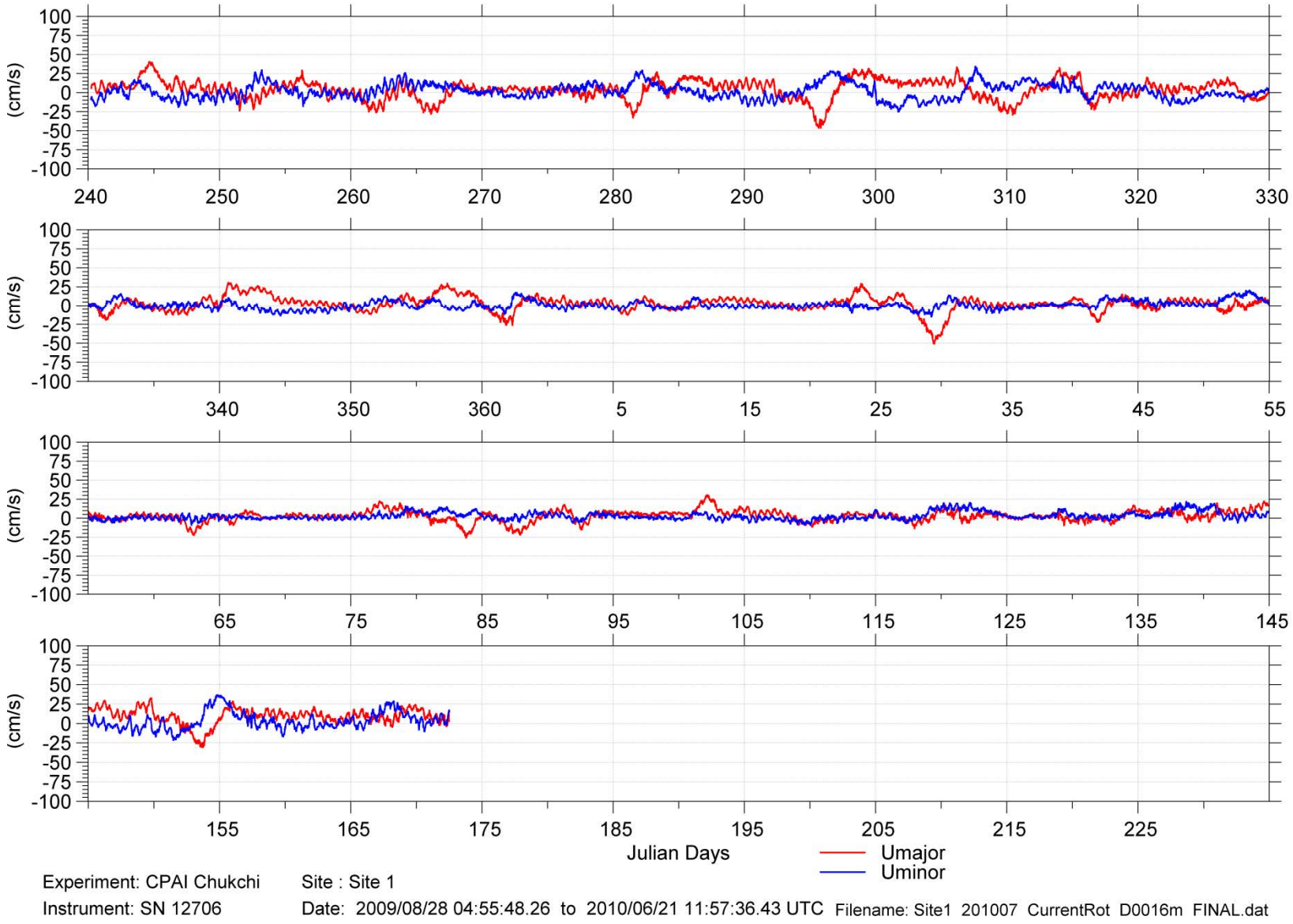

Figure 3-16. Plot of the mid-depth (16m) current measurements at Site 1.

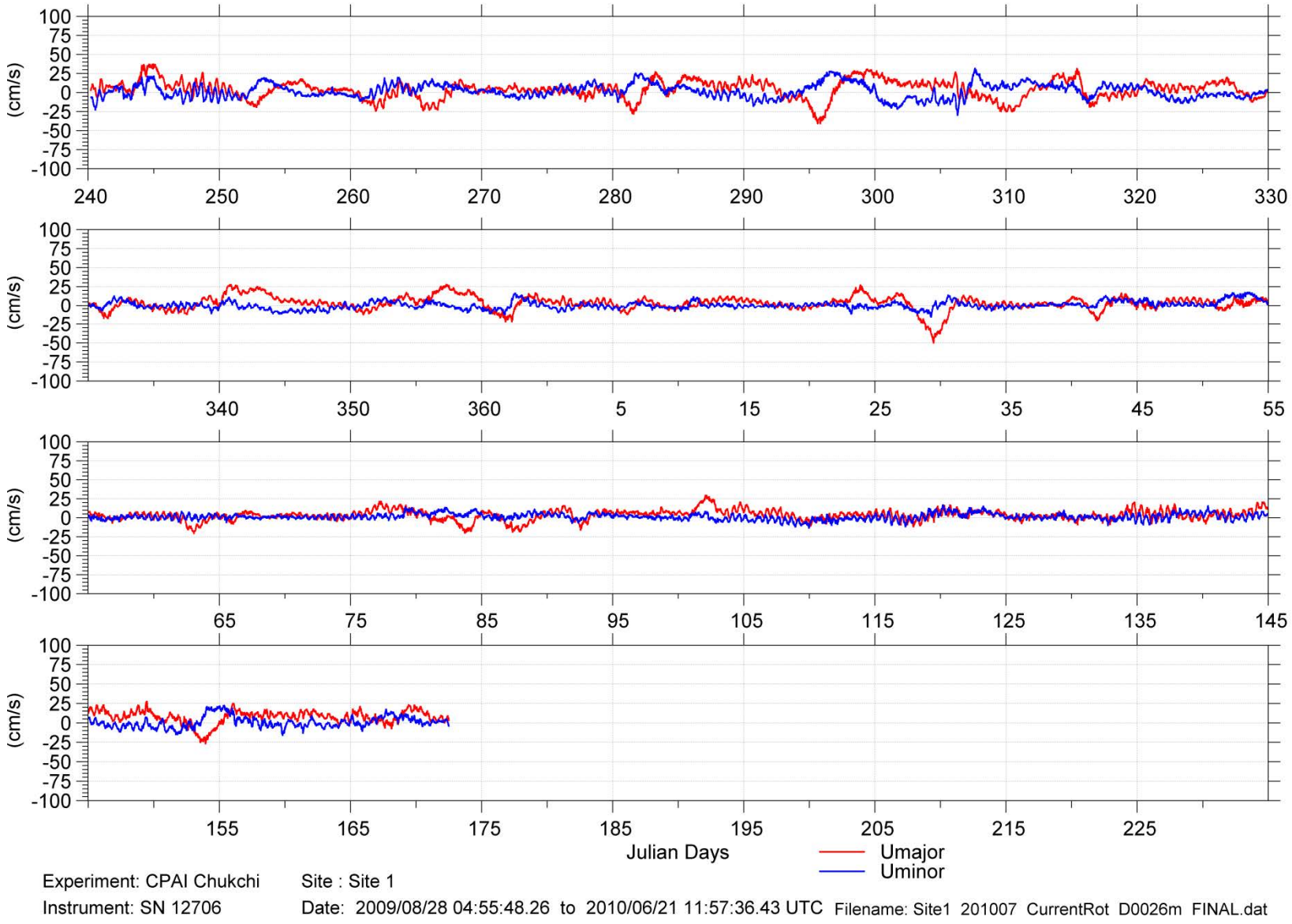

Figure 3-17. Plot of the near bottom (26m) current measurements at Site 1.

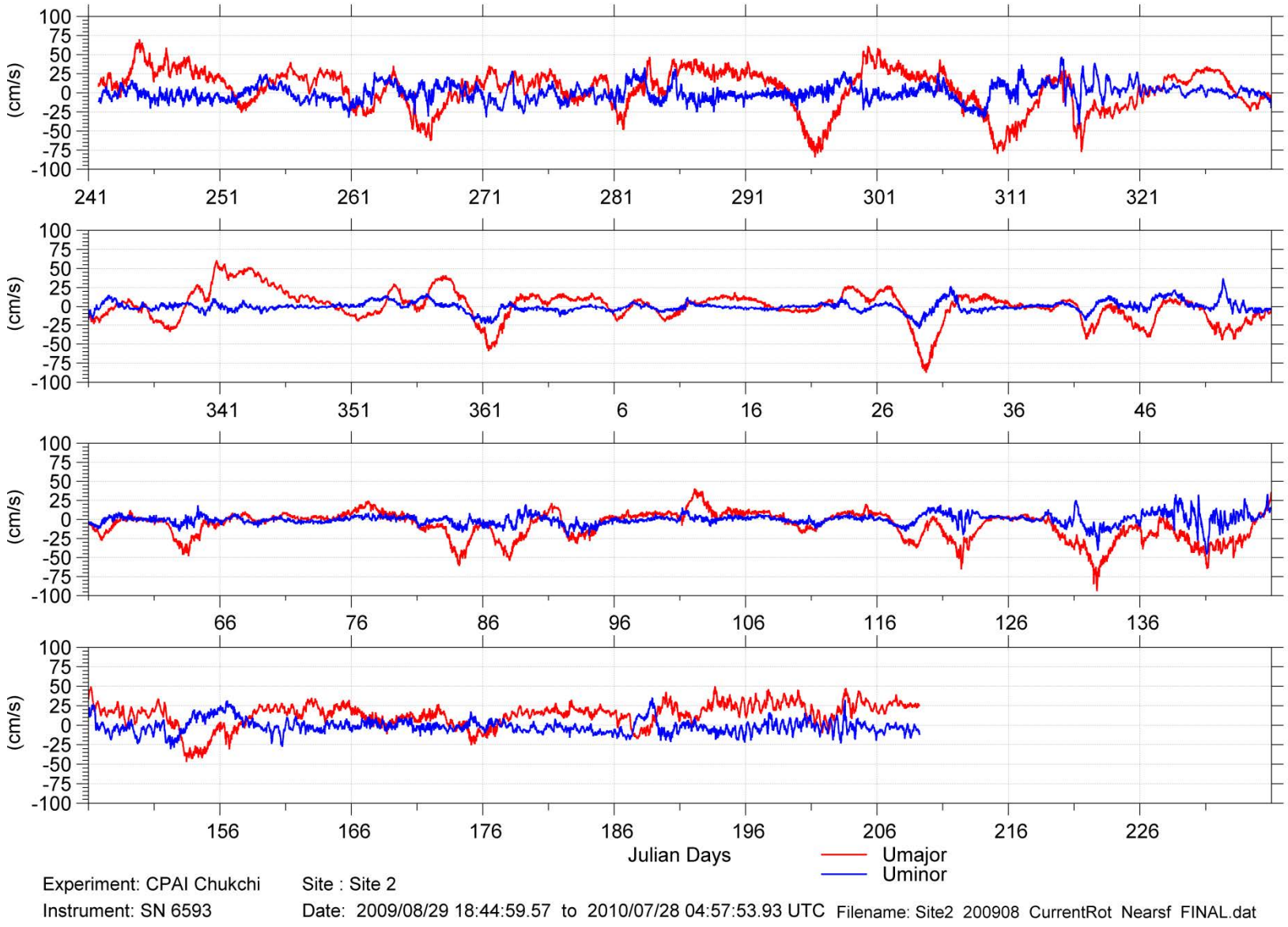

Figure 3-18: Plot of the variable near surface current measurements at Site 2.

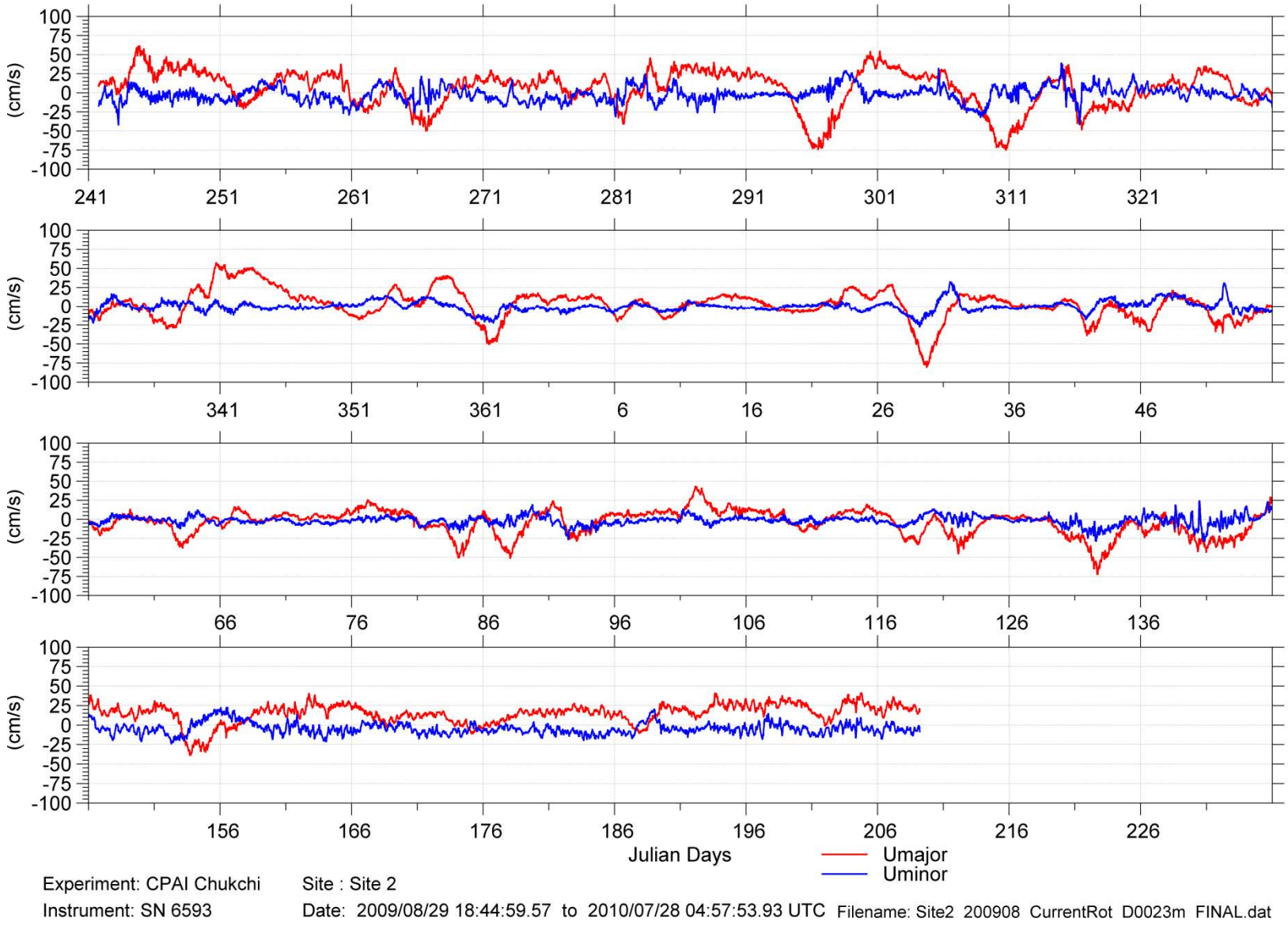

Figure 3-19: Plot of the mid-depth (23m) current measurements at Site 2.

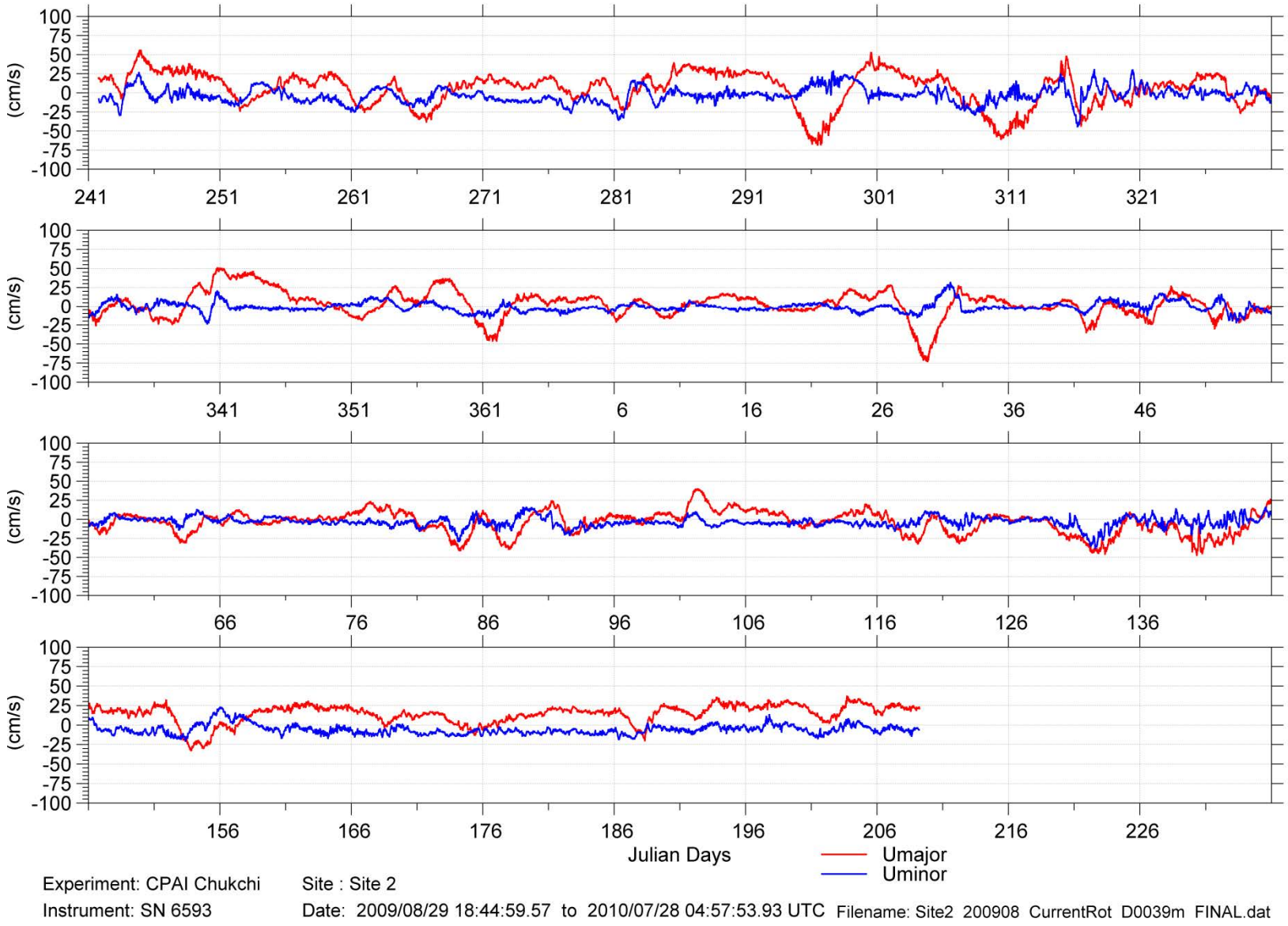

Figure 3-20. Plot of the near bottom (39m) current measurements at Site 2.

Table 3-16. Statistical summary of current components and speeds at Site 1 and Site 2 for the entire deployment.

			Annual Statistics (cm/s)												
Site	Depth (m)	chan	min	1%	5%	25%	50%	mean	75%	95%	99%	std	max	# valid	total #
1	Near Surface	Umajor	-56.8	-29.7	-16.8	-3.1	2.9	2.6	8.5	21.3	29.8	11.3	48.8		
		Uminor	-30.4	-17.3	-10.2	-2.6	1.4	2.3	6.6	17.1	27.0	8.3	40.2		
		Speed	0.1	0.9	2.1	5.6	9.8	11.8	16.5	27.8	37.0	8.3	57.1	2853	2854
	16	Umajor	-51.0	-26.7	-14.9	-1.4	4.2	3.6	9.3	20.3	27.4	10.5	41.0		
		Uminor	-25.8	-15.5	-9.7	-2.5	1.1	1.9	5.8	15.5	25.3	7.7	37.6		
		Speed	0.0	1.0	2.2	5.6	9.6	11.3	15.4	25.8	34.9	7.6	51.1	2854	2854
	26	Umajor	-50.4	-24.3	-13.3	-0.9	4.3	3.8	9.2	19.2	26.4	9.7	37.9		
		Uminor	-30.4	-14.1	-9.1	-2.8	0.7	1.2	4.7	12.9	20.2	6.7	32.4		
		Speed	0.0	0.9	2.1	5.3	8.9	10.3	13.7	23.7	32.5	6.9	50.4	2854	2854
2	Near Surface	Umajor	-94.2	-63.4	-39.2	-10.2	4.3	1.7	16.3	33.4	47.0	22.2	70.2		
		Uminor	-46.0	-22.3	-14.1	-5.1	-0.7	-0.4	3.7	14.6	23.9	8.6	47.2		
		Speed	0.1	1.3	3.2	8.9	16.8	19.5	26.7	46.0	66.1	13.8	98.4	3191	3191
	23	Umajor	-81.2	-60.1	-32.9	-7.0	6.4	3.7	16.9	32.2	45.6	20.3	62.0		
		Uminor	-42.4	-21.9	-14.8	-6.3	-1.9	-1.9	2.3	11.7	18.9	7.9	39.6		
		Speed	0.1	1.6	3.7	9.3	16.2	18.5	25.0	41.7	62.1	12.3	81.7	3191	3191
	39	Umajor	-73.5	-50.9	-30.0	-6.2	5.8	3.8	16.8	30.0	40.9	18.6	56.3		
		Uminor	-45.1	-24.3	-14.7	-7.7	-3.5	-3.1	1.0	10.7	19.1	7.9	32.3		
		Speed	0.2	1.7	3.6	9.4	16.2	17.7	23.6	37.8	53.8	10.9	73.5	3191	3191

Table 3-17. Summary of ocean current quarterly statistics for Site 1 at the near-surface.

Site 1: Near Surface	chan	min	1%	5%	25%	50%	mean	75%	95%	99%	std	max	# valid	total #
Time	cm/s													
28-Aug-2009	Umajor	-29.3	-25.5	-19.6	-2.9	4.2	3.1	9.5	21.7	38.0	12.0	48.8		
-	Uminor	-23.8	-16.7	-11.5	-4.8	0.9	1.7	7.4	17.5	24.2	9.0	32.3		
30-Sep-2009	Speed	0.3	1.4	3.3	7.2	11.6	13.2	17.8	27.9	39.3	8.0	49.1	3245	3245
01-Oct-2009	Umajor	-56.7	-32.1	-19.9	-4.9	3.6	3.3	12.2	23.7	29.7	13.1	39.5		
-	Uminor	-30.4	-20.0	-13.4	-4.9	0.5	1.4	7.5	18.3	26.1	9.6	38.9		
31-Dec-2009	Speed	0.2	1.4	3.4	8.0	13.0	14.4	19.9	29.6	37.3	8.3	56.9	8830	8832
01-Jan-2010	Umajor	-56.8	-39.0	-17.7	-3.1	1.4	0.0	5.2	11.2	21.6	9.5	36.1		
-	Uminor	-18.3	-10.5	-6.3	-1.9	0.6	1.3	3.7	11.4	16.1	5.2	21.7		
31-Mar-2010	Speed	0.1	0.7	1.5	3.7	6.5	8.4	10.6	21.4	40.0	7.0	57.1	8640	8640
01-Apr-2010	Umajor	-43.0	-22.3	-9.8	-1.5	4.0	4.6	9.8	22.1	31.1	10.0	39.5		
-	Uminor	-28.6	-18.1	-7.8	-0.3	3.1	4.6	8.5	20.3	32.2	8.7	40.2		
21-Jun-2010	Speed	0.2	0.9	2.3	5.7	10.2	12.2	17.2	29.2	35.8	8.3	44.9	7823	7823

Table 3-18. Summary of ocean current quarterly statistics for Site 1 at mid-depth (16 m).

Site 1: 16 m	chan	min	1%	5%	25%	50%	mean	75%	95%	99%	std	max	# valid	total #
Time	cm/s													
28-Aug-2009	Umajor	-28.8	-24.5	-18.9	-2.0	4.3	3.2	9.5	20.8	35.8	11.5	41.0		
-	Uminor	-19.8	-15.9	-11.6	-4.8	0.5	1.3	6.8	16.2	23.5	8.6	30.4		
30-Sep-2009	Speed	0.3	1.2	3.0	7.1	11.4	12.7	16.9	27.2	36.1	7.5	41.7	3245	3245
01-Oct-2009	Umajor	-47.3	-31.3	-17.4	-3.4	4.9	4.2	12.8	23.1	28.2	12.3	34.0		
-	Uminor	-25.8	-17.8	-12.8	-4.8	0.3	1.3	7.0	17.1	26.1	9.0	34.7		
31-Dec-2009	Speed	0.1	1.7	3.6	7.9	12.5	13.9	18.8	27.6	35.5	7.7	49.5	8832	8832
01-Jan-2010	Umajor	-51.0	-35.4	-15.9	-2.1	2.3	1.1	6.1	12.2	20.5	9.0	29.9		
-	Uminor	-15.9	-9.2	-5.2	-1.5	0.9	1.6	3.8	11.2	15.9	4.9	21.4		
31-Mar-2010	Speed	0.0	0.8	1.6	4.0	6.6	8.2	10.6	19.8	36.8	6.4	51.1	8640	8640
01-Apr-2010	Umajor	-31.3	-20.0	-6.9	1.3	5.8	6.0	10.5	20.4	26.7	8.4	33.2		
-	Uminor	-22.1	-14.6	-7.3	-1.1	2.1	3.4	6.7	18.1	29.4	7.9	37.6		
21-Jun-2010	Speed	0.2	0.9	2.2	5.7	9.7	11.3	15.4	26.0	33.6	7.3	37.6	7824	7824

Table 3-19. Summary of ocean current quarterly statistics for Site 1 at near-bottom (26 m).

Site 1: 26 m	chan	min	1%	5%	25%	50%	mean	75%	95%	99%	std	max	# valid	total #
Time	cm/s													
28-Aug-2009	Umajor	-25.0	-21.8	-16.2	-1.8	4.0	3.4	9.1	21.4	35.1	10.9	37.9		
-	Uminor	-23.7	-14.1	-9.5	-4.0	0.6	1.6	6.9	15.4	19.7	7.6	22.3		
30-Sep-2009	Speed	0.3	1.3	2.9	6.2	10.5	11.7	14.9	24.7	39.6	7.4	43.3	3245	3245
01-Oct-2009	Umajor	-41.5	-28.7	-16.0	-2.7	5.3	4.5	12.3	22.8	27.2	11.6	32.0		
-	Uminor	-30.4	-17.1	-12.0	-5.0	0.1	0.9	6.5	16.1	24.8	8.6	32.4		
31-Dec-2009	Speed	0.1	1.6	3.5	7.8	11.9	13.3	17.8	27.3	33.1	7.4	43.2	8832	8832
01-Jan-2010	Umajor	-50.4	-32.3	-13.7	-1.5	2.7	1.6	6.5	12.2	18.1	8.4	27.8		
-	Uminor	-16.5	-8.5	-4.8	-1.3	1.0	1.5	3.7	10.0	14.6	4.4	18.3		
31-Mar-2010	Speed	0.0	0.7	1.5	3.9	6.4	7.8	10.2	17.8	32.8	5.8	50.4	8640	8640
01-Apr-2010	Umajor	-27.3	-16.7	-5.8	1.4	5.4	5.5	9.8	17.5	23.2	7.3	30.2		
-	Uminor	-16.6	-11.4	-7.7	-2.6	0.5	0.9	4.0	10.5	18.3	5.6	23.0		
21-Jun-2010	Speed	0.2	0.8	2.0	5.1	8.3	9.3	12.3	20.2	25.5	5.5	31.1	7824	7824

Table 3-20. Summary of ocean current quarterly statistics for Site 2 at the near-surface.

Site 2: Near Surface	chan	min	1%	5%	25%	50%	mean	75%	95%	99%	std	max	# valid	total #
Time	cm/s													
29-Aug-2009	Umajor	-63.1	-52.0	-34.1	-4.1	13.6	9.3	24.0	40.5	60.1	22.9	70.2		
-	Uminor	-32.5	-23.2	-17.6	-8.7	-2.6	-1.4	5.8	17.0	21.8	10.4	28.8		
30-Sep-2009	Speed	0.3	4.3	8.6	16.1	22.6	24.1	29.3	48.1	60.6	11.7	70.2	3093	3093
01-Oct-2009	Umajor	-84.7	-70.1	-48.8	-12.4	6.8	3.5	22.5	40.6	50.8	26.3	61.5		
-	Uminor	-42.2	-23.9	-15.6	-4.4	0.0	0.4	5.0	16.8	27.6	9.6	47.2		
31-Dec-2009	Speed	0.3	2.4	5.1	12.8	21.1	23.8	31.1	53.7	71.1	15.0	84.8	8831	8831
01-Jan-2010	Umajor	-87.4	-62.1	-39.0	-11.4	-0.7	-4.7	7.0	15.4	24.2	17.4	27.9		
-	Uminor	-29.8	-16.9	-9.6	-4.0	-0.6	-0.5	2.5	10.7	18.6	6.4	37.1		
31-Mar-2010	Speed	0.1	0.9	2.1	5.5	10.0	14.1	17.7	40.5	65.3	12.9	88.1	8640	8640
01-Apr-2010	Umajor	-94.2	-58.0	-38.5	-14.9	2.8	-2.0	11.7	24.4	33.3	20.0	49.9		
-	Uminor	-46.0	-23.6	-13.7	-4.6	-0.1	-0.1	4.0	14.6	24.2	8.6	33.3		
30-Jun-2010	Speed	0.1	1.2	2.9	8.0	15.3	17.7	24.4	40.7	60.7	12.8	98.4	8736	8736
01-Jul-2010	Umajor	-17.3	-13.9	-5.1	13.1	21.0	19.7	28.0	37.5	43.8	12.1	50.1		
-	Uminor	-23.2	-19.0	-15.0	-8.6	-4.3	-3.3	0.5	11.2	25.2	8.3	35.6		
28-Jul-2010	Speed	0.2	4.7	9.2	16.8	22.9	23.1	29.0	38.3	45.1	8.9	55.5	2612	2612

Table 3-21. Summary of ocean current quarterly statistics for Site 2 at mid-depth (23 m).

Site 2: 23 m	chan	min	1%	5%	25%	50%	mean	75%	95%	99%	std	max	# valid	total #
Time	cm/s													
29-Aug-2009	Umajor	-50.6	-41.0	-29.3	-0.7	14.0	10.5	23.8	38.4	54.6	20.0	62.0		
-	Uminor	-42.4	-24.2	-17.8	-9.9	-4.0	-3.5	2.8	12.9	17.0	9.3	22.3		
30-Sep-2009	Speed	2.2	5.6	9.4	15.1	21.0	22.5	27.7	41.4	54.8	10.1	62.4	3093	3093
01-Oct-2009	Umajor	-75.6	-68.9	-45.1	-9.6	7.9	4.7	22.6	40.1	49.8	25.1	58.0		
-	Uminor	-42.3	-24.8	-16.7	-5.4	-0.9	-0.9	4.1	13.2	22.5	8.9	39.6		
31-Dec-2009	Speed	0.2	2.6	5.1	12.3	20.4	23.0	30.1	50.2	69.1	14.2	75.9	8831	8831
01-Jan-2010	Umajor	-81.2	-59.8	-33.0	-9.0	0.8	-2.3	8.8	16.5	24.6	16.1	29.7		
-	Uminor	-28.2	-16.1	-9.2	-4.1	-0.9	-0.5	2.4	11.5	19.5	6.5	32.7		
31-Mar-2010	Speed	0.1	1.1	2.7	6.1	10.3	13.4	16.6	34.5	61.3	11.2	81.7	8640	8640
01-Apr-2010	Umajor	-72.9	-48.2	-30.7	-9.2	4.9	1.3	13.8	25.0	34.7	17.8	43.8		
-	Uminor	-30.0	-20.9	-15.0	-7.3	-2.5	-2.8	1.3	9.4	17.1	7.3	24.9		
30-Jun-2010	Speed	0.2	1.3	3.3	8.6	14.6	16.5	22.7	34.5	50.5	10.4	75.9	8736	8736
01-Jul-2010	Umajor	-11.2	-7.6	0.0	14.8	20.9	19.9	26.6	32.9	37.7	9.5	41.8		
-	Uminor	-20.2	-17.6	-14.7	-9.5	-5.7	-5.2	-1.9	6.1	16.3	6.5	21.0		
28-Jul-2010	Speed	3.2	5.7	9.5	17.5	22.8	22.4	27.6	33.6	38.0	7.1	42.7	2612	2612

Table 3-22. Summary of ocean current quarterly statistics for Site 2 at the near-bottom (39 m).

Site 2: 39 m	chan	min	1%	5%	25%	50%	mean	75%	95%	99%	std	max	# valid	total #
Time	cm/s													
29-Aug-2009	Umajor	-39.0	-32.8	-24.3	-3.4	12.2	9.0	21.2	34.2	48.4	18.1	56.3		
-	Uminor	-30.5	-24.0	-17.3	-10.5	-5.7	-4.4	1.6	11.4	18.4	8.9	27.1		
30-Sep-2009	Speed	1.1	3.9	7.4	14.5	19.8	20.6	25.3	35.9	52.4	9.1	60.5	3093	3093
01-Oct-2009	Umajor	-69.0	-58.0	-39.8	-8.1	7.7	4.9	21.1	36.9	45.5	22.6	53.3		
-	Uminor	-45.1	-29.3	-18.9	-6.7	-2.2	-2.0	3.2	14.1	21.3	9.5	31.1		
31-Dec-2009	Speed	0.2	2.5	5.2	12.3	19.7	21.8	29.0	45.0	59.2	12.5	72.4	8831	8831
01-Jan-2010	Umajor	-73.5	-53.9	-30.2	-7.6	0.5	-1.6	8.3	16.9	23.1	14.7	28.7		
-	Uminor	-29.8	-17.0	-10.9	-4.9	-1.9	-1.3	1.7	10.6	18.9	6.6	32.3		
31-Mar-2010	Speed	0.2	1.4	2.6	5.9	10.0	12.6	16.2	31.7	54.6	10.1	73.5	8640	8640
01-Apr-2010	Umajor	-48.0	-40.1	-28.3	-8.0	3.4	1.5	14.2	24.0	30.6	16.5	40.8		
-	Uminor	-39.2	-24.0	-14.6	-9.0	-5.2	-4.8	-1.2	8.3	14.3	7.1	23.6		
30-Jun-2010	Speed	0.2	1.3	3.5	9.2	15.4	16.2	22.1	31.6	45.3	9.2	55.6	8736	8736
01-Jul-2010	Umajor	-20.7	-11.3	2.5	15.5	20.7	19.3	25.3	30.7	33.3	9.0	37.8		
-	Uminor	-19.3	-17.0	-13.8	-9.1	-5.7	-5.6	-2.2	2.9	7.1	5.1	14.0		
28-Jul-2010	Speed	1.1	8.0	11.6	18.2	22.0	21.8	25.8	31.1	33.8	5.8	37.8	2612	2612

The current speeds are further illustrated through compass plots (Figure 3-21), which show the speed and direction joint frequency distribution. The color of each segment denotes its speed interval. The radial length of each segment denotes the proportion of measurements within the illustrated speed and direction interval. The mean and maximum are illustrated through the second radial scale as the green and red lines respectively.

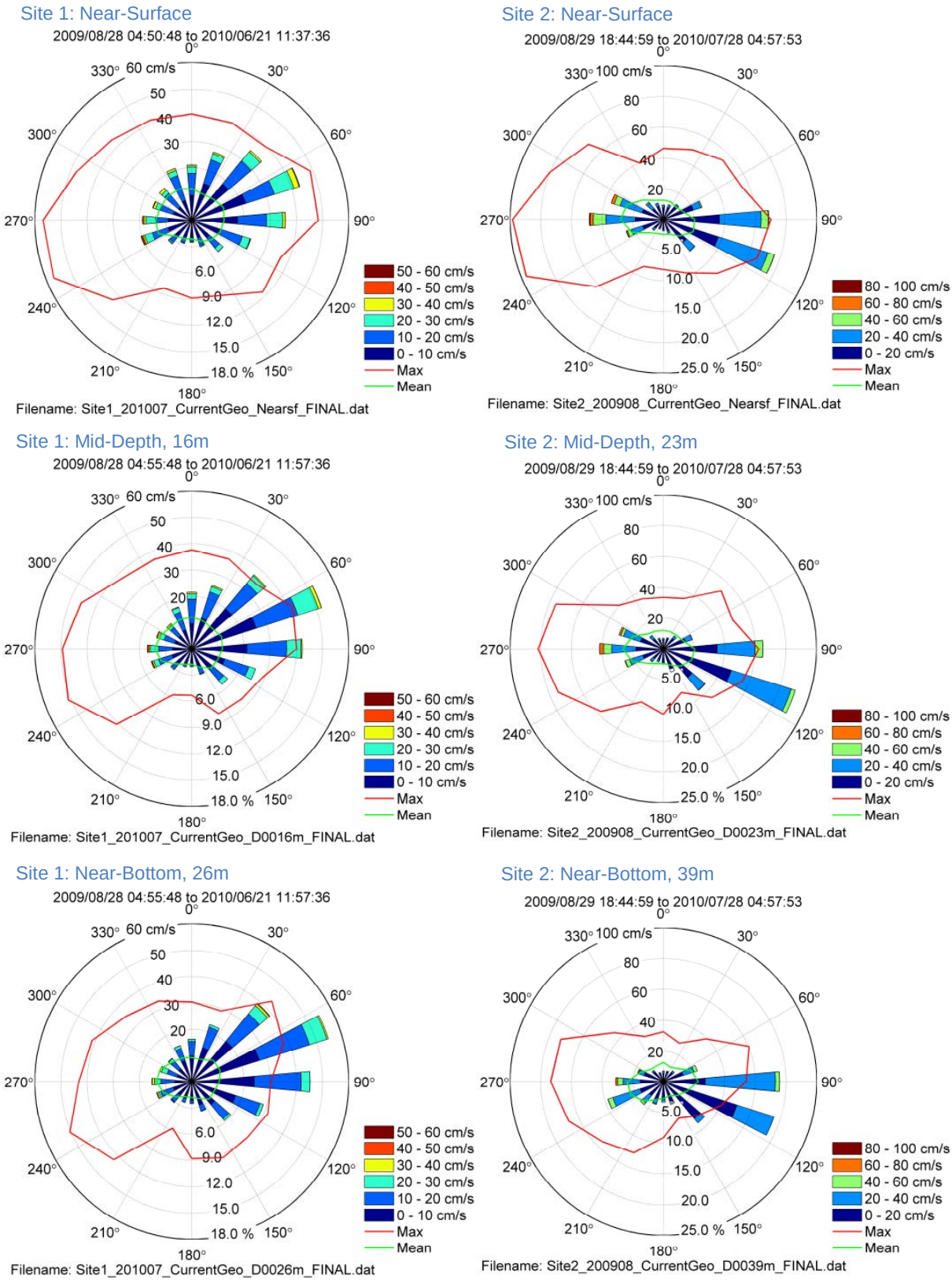

Figure 3-21. Compass plots of the directional distribution at the near-surface, mid-depth, and near-bottom at Site1 and Site 2 for the entire deployment period.

3.4.3 SUMMARY OF OCEAN CURRENTS

Continuous measurements of ocean current profiles were obtained at Site 1 for approximately 10 months, from August 28, 2009 to June 21, 2010. The instrument stopped recording data before its recovery on July 26, 2010 due to a power pin which was pitted by corrosion. There were about 11 months of data collected at Site 2, where the instrument functioned properly for the entire deployment. At both sites, the quality of the data recorded was reasonably high with a small number of gaps where the instrument rejected data due to low backscatter amplitudes or inconsistencies between the beams.

The ocean currents were characterized by occasional events of large currents, particularly on January 29, 2010, where the speed was about 57.1 cm/s near the surface at Site 1, and 88.1 cm/s at Site 2. This event corresponds to wind speeds close to 8 m/s at Wainwright, Alaska. The maximum recorded current speed was 98.4 cm/s at the near-surface and occurred on May 12, 2010 at Site 2. This event corresponds to wind speeds of about 6.4 m/s at Wainwright. Another instance of high current speeds was on October 22, 2009 where Site 1 peaked at 56.9 cm/s and Site 2 at 84.8 cm/s. The wind at this time was around 8.6 m/s.

The average and maximum currents are somewhat larger at near-surface levels than at mid-depth and near-bottom levels. The average current speeds (and maximum speeds) at Site 1 were 11.8 (57.1) cm/s at the near-surface, 11.3 (51.1) cm/s at mid-depths (16 m) and 10.3 (50.4) cm/s at near-bottom (26 m) depths. At Site 2 the average (and maximum) current speeds are larger at 19.5 (98.4) cm/s at the near-surface, 18.5 (81.7) cm/s at mid-depths (23 m) and 17.7 (73.5) cm/s at near-bottom (39 m) depths.

3.5 BOTTOM TEMPERATURES, SALINITY AND DENSITY

The ADCP instruments were equipped with temperature sensors from which time series measurements of near bottom temperatures are available. SBE37 CT instrument is attached to the IPS-5 mooring cage at both Sites 1 and 2. This instrument provides bottom temperature and conductivity data which could be used to derive a salinity and density time series. The ADCP and CT data sets require truncation of data values immediately after the instruments were deployed and on recovery to limit the time series to the in-water part of the deployment where the sensors were in thermal equilibrium with the ambient water.

Temperature records at both sites show similar seasonal trends (Figure 3-22) with Site 2 exhibiting more variability at sub-seasonal time periods. By early November the near-bottom waters are approximately 2 ˚C, with ongoing cooling until the freezing point temperature is reached at both sites. The cooling of the near bottom waters at Site 1 happened more gradually over a month from mid-October to mid-November 2009. Small temperature variations continued until end of December 2009 and stayed at freezing until about the first week in June. The near-bottom waters at Site 2 reached at freezing temperature more suddenly around mid-November. After an initial period of small temperature variations between mid-November and early December 2009 it stayed at freezing temperature consistently until mid-May. 2010.

The salinity and density measurements at Site 1 (Figure 3-23) reveal increasing salinities from early November to early April which is likely associated with the formation of sea ice which extrudes salt into the water column. In the remainder of the winter and in spring, salinity varies between 30.9 PSU and 34.1 PSU which as different water masses advected through the measurement area. Salinity variations are not as regular at Site 2 as they are at Site 1. The most consistent increase in salinity -and density- occurred from early December 2009 to late March 2010. High level of salinity variability observed in the remainder of the year indicates that Site 2 is located in a more dynamic region. Site 2 salinities varied between 30.8 PSU and 34.6 PSU over the measurement period, presenting a slightly larger range than the Site 1 salinities.

Table 3-23. Record-length statistics computed for the near-bottom temperature data at Sites 1 and 2.

Site	Instrument	Instrument Depth (m)	Water Depth (m)	Sample Interval (min)	Mean (°C)	Standard Deviation (°C)	Min (°C)	Max (°C)
Site 1	ADCP #12706	32	36	5	-0.73	1.79	-1.93	4.23
	CT Sensor: SBE37 #6271	31	38	15	-0.76	1.73	-1.86	4.41
Site 2	ADCP #6593	43	47	5	-1.00	1.28	-1.78	5.20
	CT Sensor: SBE37 #6868	39	46	15	-1.04	1.29	-1.81	5.12

Table 3-24. Temperature, salinity and density statistics computed for the near bottom (31 m) at Site 1.

CPAI Site 1 CT											
28-Aug-2009 04:30:01 to 25-Jul-2010 02:15:01											
Channel	min	1%	5%	25%	50%	mean	75%	95%	99%	std	max
Temperature:	-1.86	-1.851	-1.834	-1.778	-1.712	-0.739	-0.576	2.795	3.649	1.737	4.413
Salinity (psu):	30.922	31.188	31.352	31.735	32.269	32.398	32.95	33.758	34.076	0.777	34.125
Density (kg/m^3):	1024.77	1025.05	1025.19	1025.61	1026.11	1026.167	1026.66	1027.32	1027.58	0.677	1027.62

Table 3-25. Temperature, salinity and density statistics computed for the near bottom (39 m) at Site 2.

CPAI Site 2 CT											
29-Aug-2009 18:45:01 to 25-Jul-2010 02:45:01											
Channel	min	1%	5%	25%	50%	mean	75%	95%	99%	std	max
Temperature:	-1.807	-1.793	-1.78	-1.753	-1.666	-1.037	-1.051	2.157	4.323	1.29	5.119
Salinity (psu):	30.763	31.433	31.549	31.913	32.282	32.382	32.695	33.554	33.751	0.627	34.637
Density (kg/m^3):	1024.92	1025.22	1025.45	1025.83	1026.14	1026.209	1026.49	1027.19	1027.35	0.529	1027.98

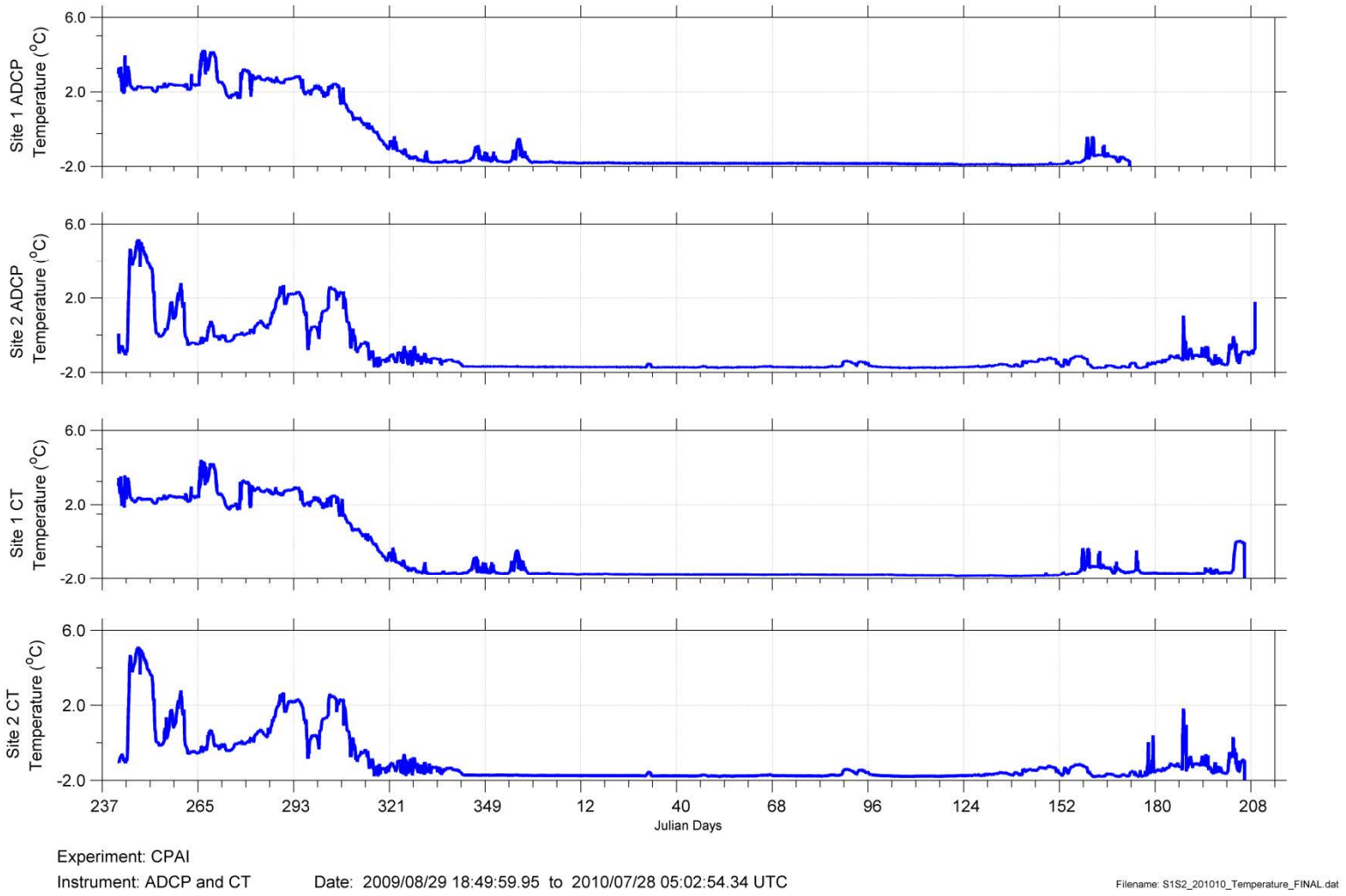

Figure 3-22. Near-bottom temperature data measured by ADCP and CT sensors at Sites 1 and 2.

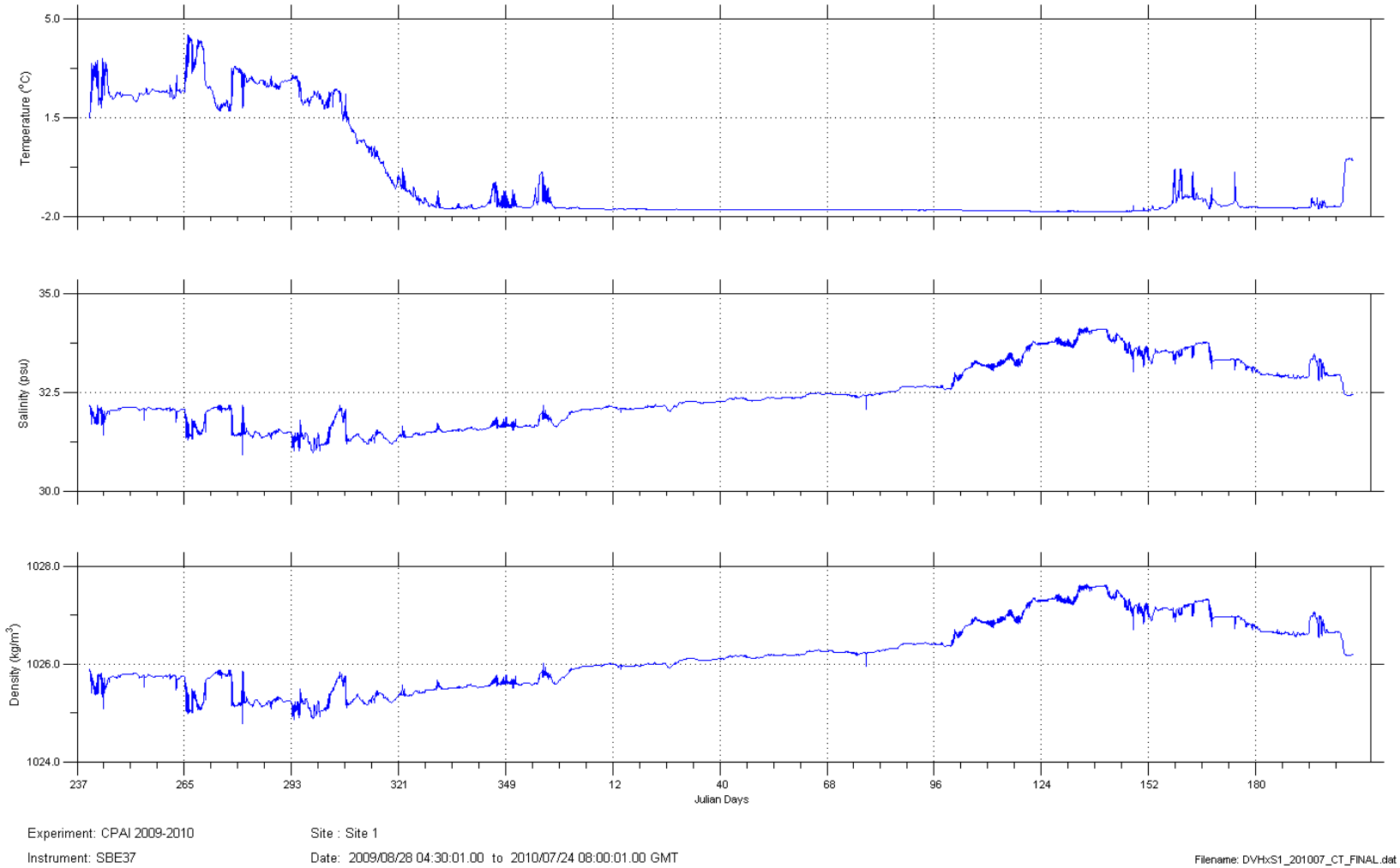

Figure 3-23: Near-bottom temperature, salinity, and density data measured by the SBE37 at Site 1.

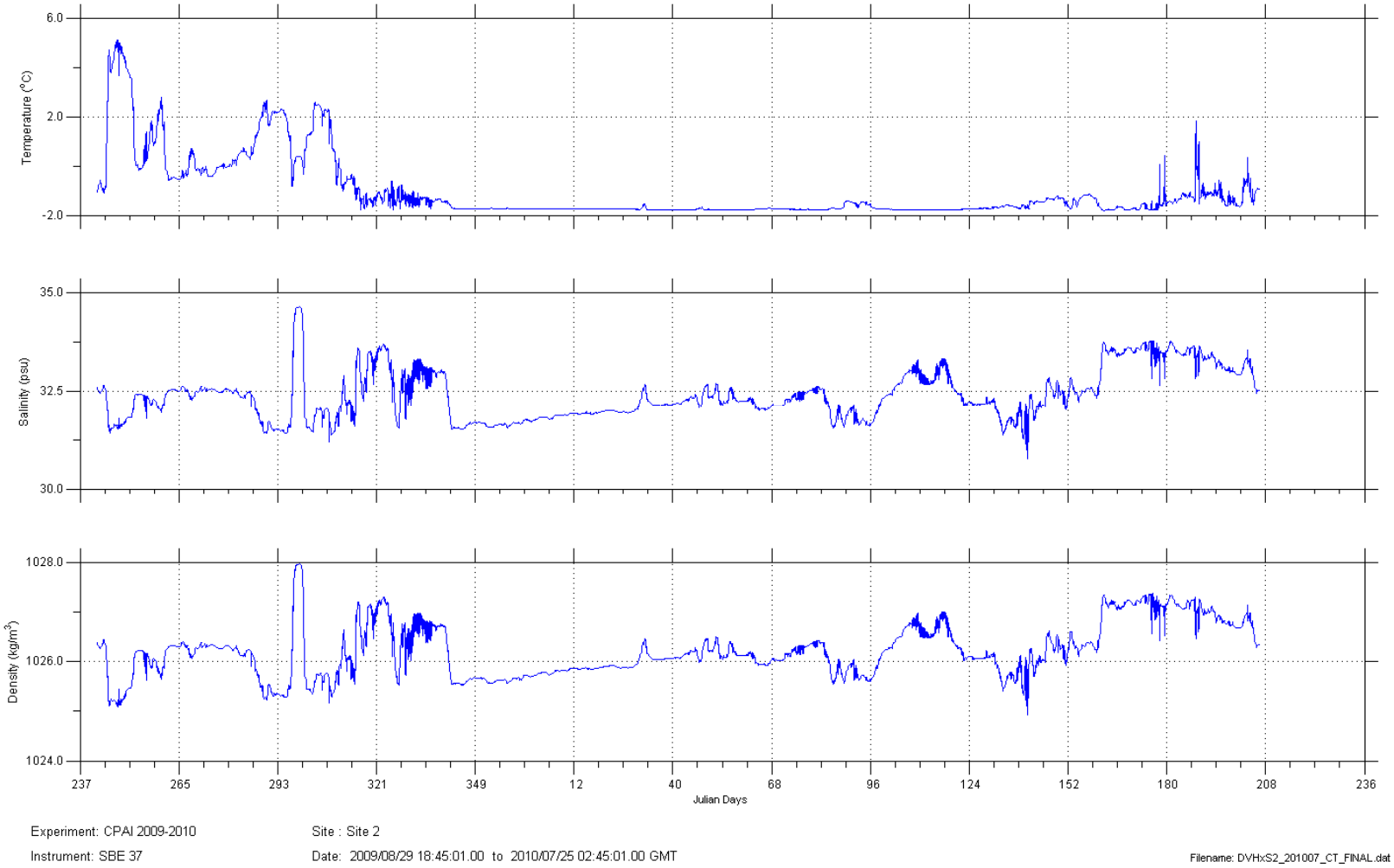

Figure 3-24. Near-bottom temperature, salinity, and density data measured by the SBE37 at Site 2.

3.6 METEOROLOGICAL DATA

Meteorological station measurements were obtained from Point Lay, and Wainwright, Alaska.

All of the measurements were obtained from the Weather Underground online weather service (*http://www.wunderground.com*). The wind data represents the standard 10 m anemometer height and represents mean wind values (1 minute or longer sampling duration) reported at hourly intervals.

The data from this site contained hourly- time series measurements of:

- atmospheric pressure (dbar)
- air temperature (°C)
- wind direction (°)
- wind speed ($m \cdot s^{-1}$)

The daily observations of wind speed and air temperature are shown in Figure 3-25. The meteorological observations were used to assist in interpreting and classifying ice keel features at the measurement site. The sea level pressure measurements (not illustrated) were also required to provide quantitative values for the purposes of computing ice drafts (equation 1 in section 3.1.2.1) for processing the ice profiling sonar data. Note that the wind data measurements are missing for Point Lay from day 303 (2009) to day 36 (2010).

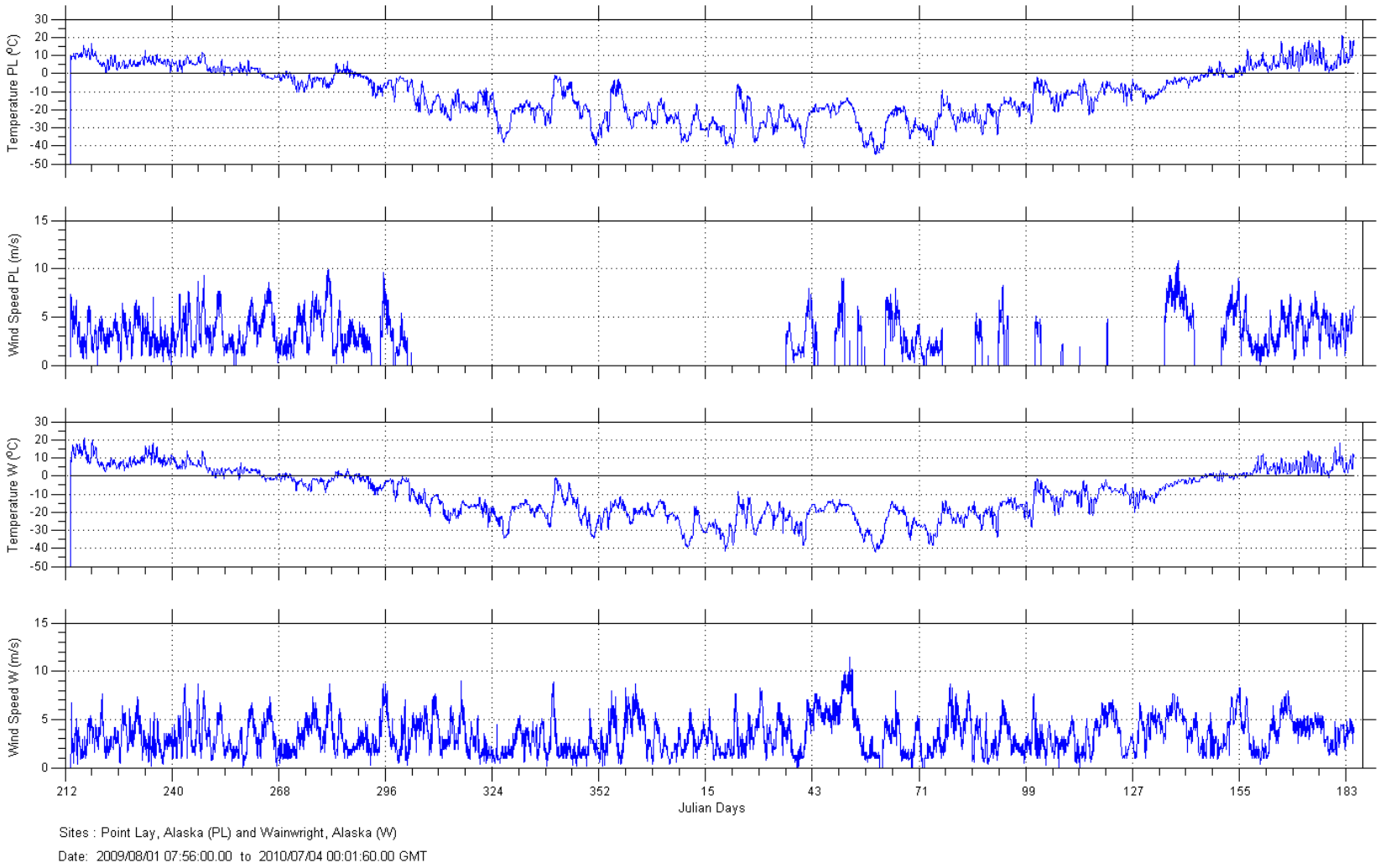

Figure 3-25. Daily air temperature and wind speed as observed at Point Lay and Wainwright weather stations from August 2009 to July 2010.

3.7 OTHER ICE DATA SETS

In addition to the underwater profiling measurements of ice keels collected at the measurement sites over the October 2008 to October 2009 period, other ice data were also obtained:

1. Weekly ice charts prepared by the U.S. National Ice Service (http://www.natice.noaa.gov/) from the week of July 31, 2009 to the week of July 29, 2010.
2. Daily SSM/I passive microwave ice concentration data provided by NOAA (http://polar.ncep.noaa.gov/seaice/Analyses.html) from July 27, 2009 to July 31, 2010.

These ice data sets were used to assist in interpretation of the ice profiling sonar data set; in particular, for determining if very thin ice or open water was present to assist in making corrections for variations to the ice drafts due to changing sound speeds in the ocean.

A source book was created using all the above data types, as well as the weather measurements. It was circulated among ASL's in-house scientific analysts to aid in interpretation and verification of ice movements in the region and, specifically, at the monitoring sites.

3.8 DATA ARCHIVE

All data sets collected directly as part of the present study are provided on an FTP site or via DVD (upon request). The organization of the data, plots and other documentation is as shown in Figure 3-26.

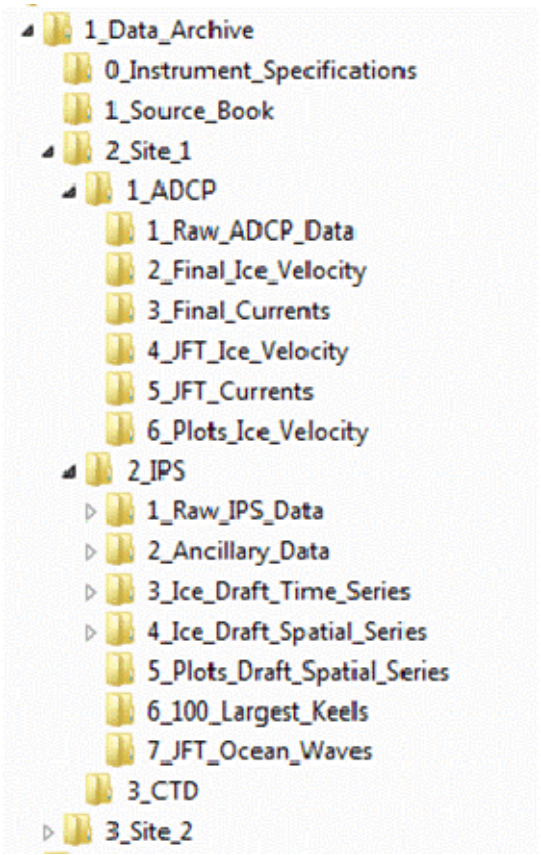

Figure 3-26. Directory tree of the Data Archive provided on ASL FTP site. Site 2 subdirectory branches are not shown as they are the same as Site 1 subdirectories.

Data are provided in ASL Standard Format: one data file, and header file pair for each dataset. The header file has the file extension '.hdr' and is a text file contains metadata for the data in the data file. The data file has the file extension '.dat' and is a text file that contains columns of data.

4 ANALYSIS RESULTS

4.1 OVERVIEW OF SEA ICE CONDITIONS IN 2009-2010

For the fourth year in a row, the fall season in Arctic Ocean was characterized by a major retreat north of the edge of the pack ice (Figure 4-1). The Arctic Ocean ice extent was at a historic low in 2007, with the second, third and fourth lowest values occurring in 2008, 2010 and 2009, respectively. The retreat of the minimal sea ice extent was particularly pronounced in the western Arctic Ocean in all four years.

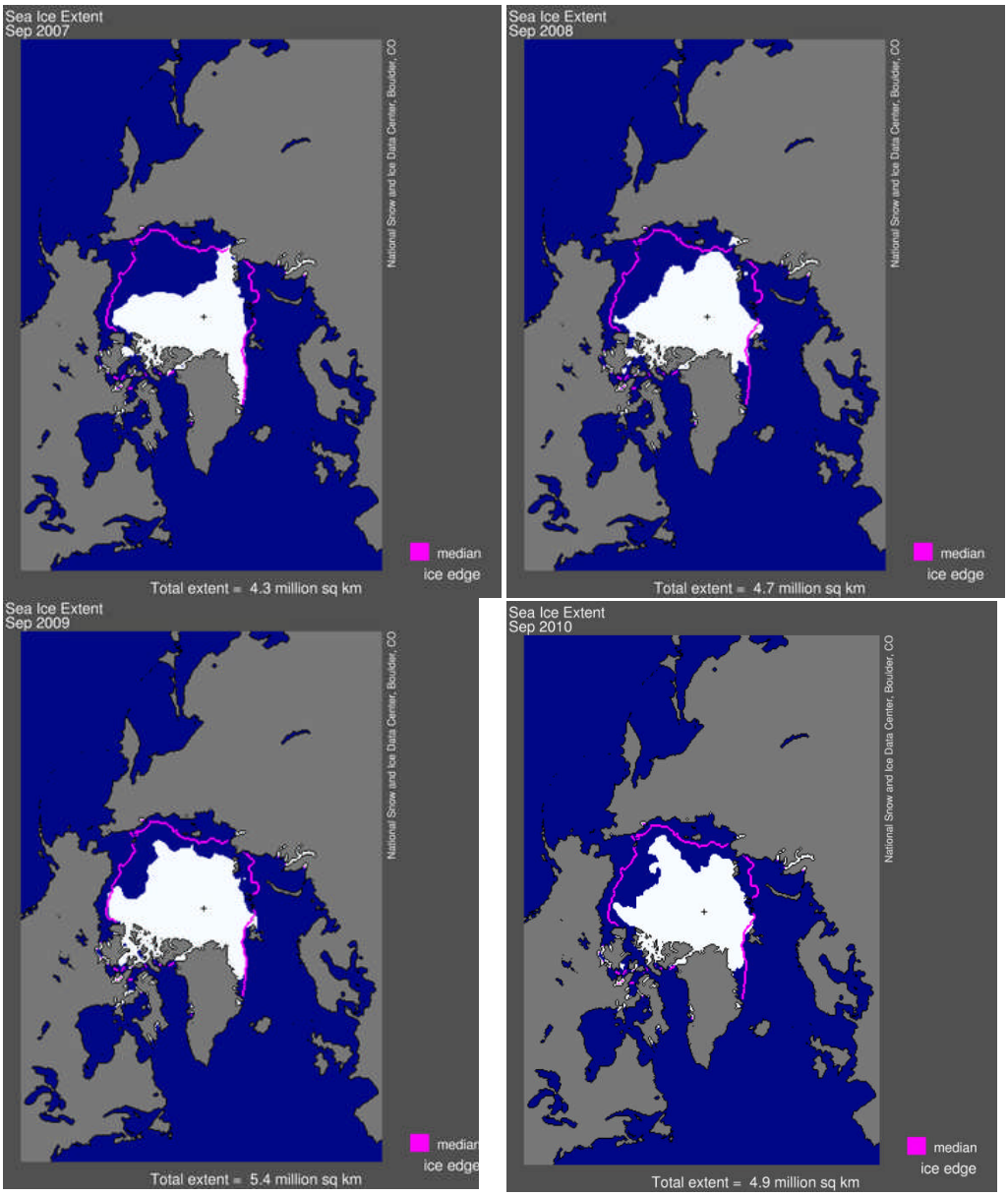

Figure 4-1. September sea ice extent concentrations for 2007 to 2010. (http://nsidc.org/).

4.1.1 FREEZE-UP PATTERNS: OF FALL 2009

In the fall of 2009, pack ice was for the most part located well offshore in the northern Chukchi Sea with the ice edge extending well beyond the continental shelf and slope waters to northerly latitudes, rivalling late summer 2007. However, the open water did not extend as far west off East Siberia as experienced in the last three years (Figure 4-1).

Ice formation began along the coast in mid October 2009 following the usual seasonal pattern (Figure 4-2 and Figure 4-3). Although some new ice, at concentrations of 4 to 6 tenths, is shown in the vicinity of Site 1 in the RADARSAT image of November 8-9, it was not until the week of November 16 that the ice concentrations attained values of 9+ tenths for Site 1, and 1 to 3 tenths at Site 2. High concentrations of new ice (9-10 tenths) were recorded by November 23 in the vicinity of Site 2. By this time, the ice charts indicate that the ice is made up of mainly young ice with ice free waters remaining in close proximity to Site 2. The last few days of November 2009 represented the transitional time when there were no more ice-free regions in the Chukchi Sea.

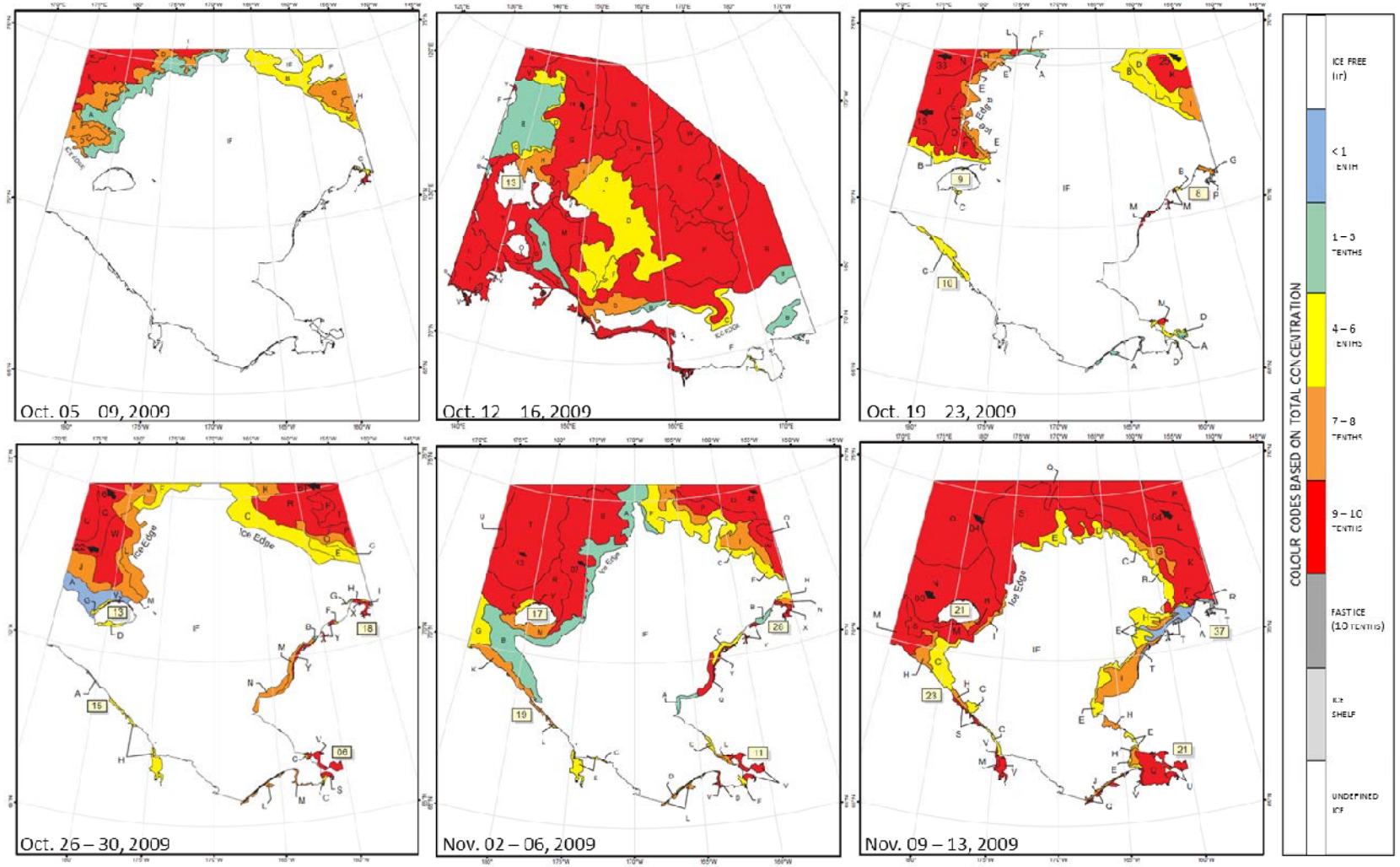

Figure 4-2. Fall 2009 freeze-up patterns. Ice charts are presented for the period of October 5-9 to November 9-13 in the Chukchi Sea. Site 1 is located at 71 ˚N, 165 ˚W and Site 2 is located at 71 ˚N, 161 ˚W.

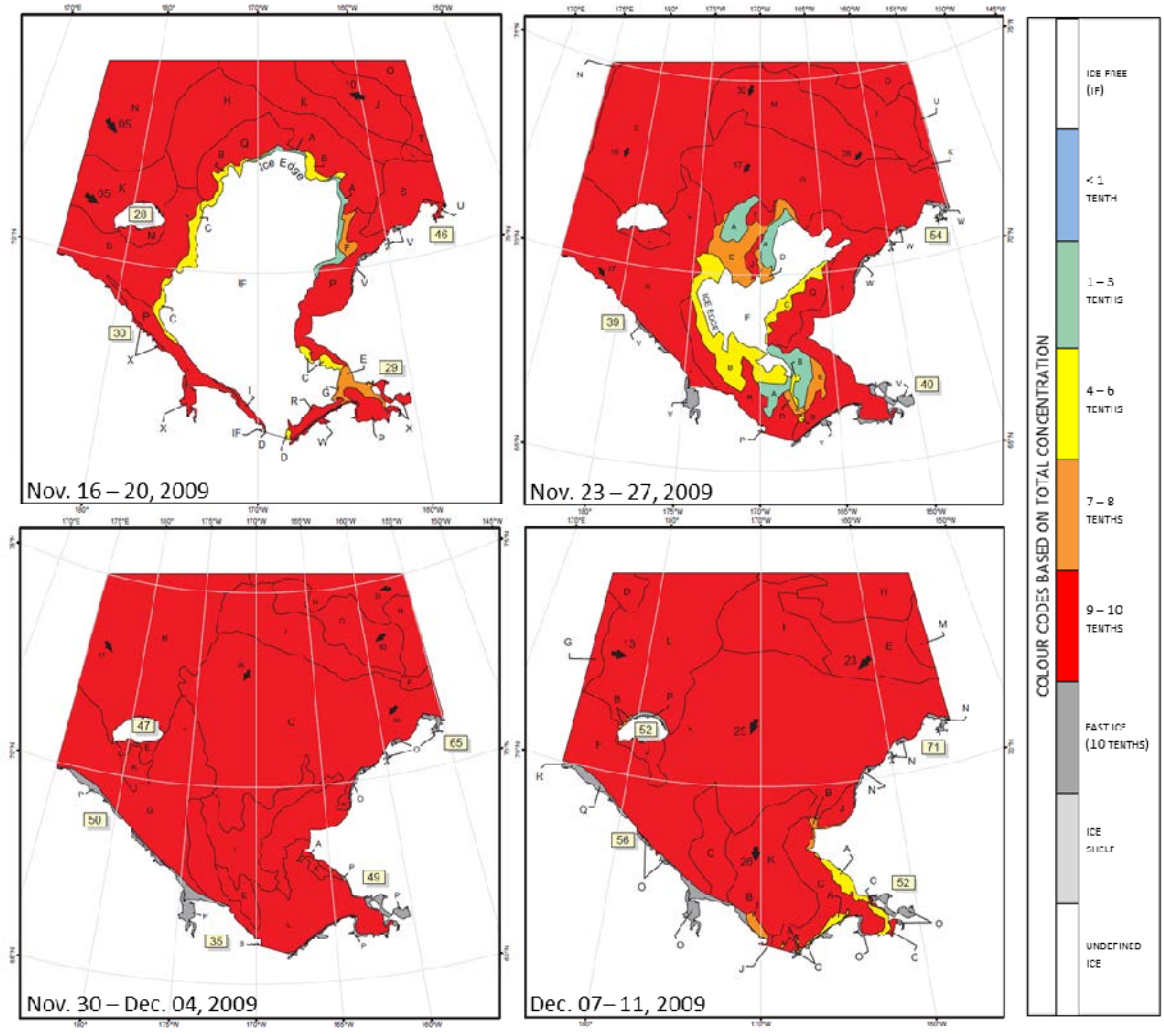

Figure 4-3. Fall 2009 freeze-up patterns. Ice charts are presented for the period of November 16-20 to December 7-11 in the Chukchi Sea. Site 1 is located at 71 ˚N, 165 ˚W and Site 2 is located at 71 ˚N, 161 ˚W.

4.1.2 BREAK-UP PATTERNS: SUMMER 2010

In the summer of 2010 (Figure 4-4 through Figure 4-6), ice began to clear along the Alaskan coastline in the first week of May with an extensive flaw lead present from south of Nome to Pt. Barrow. By this time the ice concentrations were reduced to 4 to 6 tenths at Site 2. This area of low ice concentrations persisted throughout May, reaching the Site 1 location in the third week of May and progressively expanding to the more offshore areas of Site 1. Site 1 is shown to be ice free by the week of June 10 for the first time in 2010, while low concentrations of coastal sea ice remained in the vicinity of Site 2 until the third week of June.

Occasional ice floes originating to the north from the pack ice edge (just north of 72°N) continued to pass the measurement sites until well into July. The clearing of the sea ice in the eastern Chukchi Sea was approximately 3 to 5 weeks earlier in 2010 than in the year 2009. However, the ice conditions in the northern and western Chukchi Sea were comparable, or had more ice in 2010, than in 2009 through to the end of July.

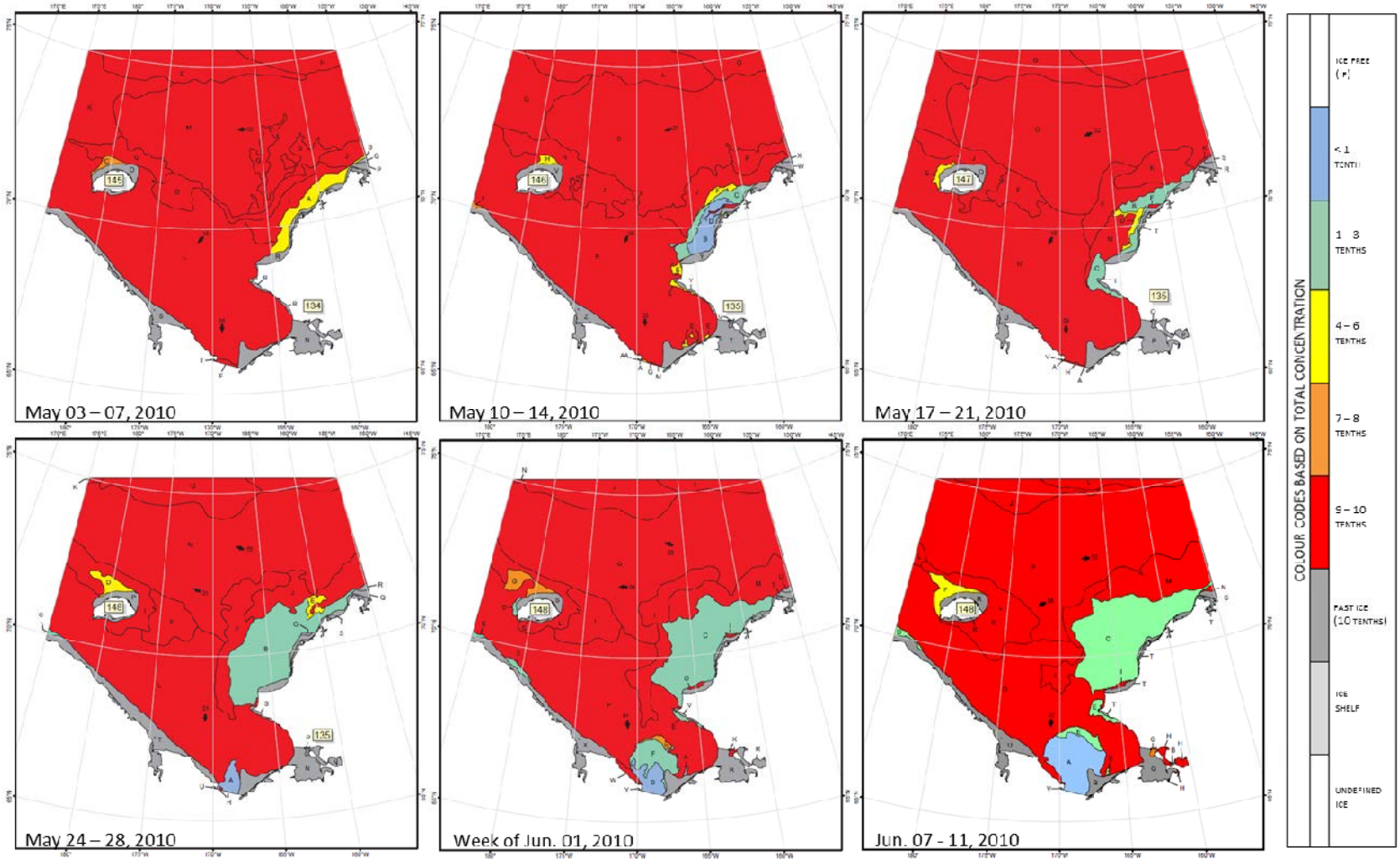

Figure 4-4. Summer 2010 break-up patterns. Ice charts are presented for the period of May 3-7 to June 7-11 in the Chukchi Sea. Site 1 is located at 71 ˚N, 165 ˚W and Site 2 is located at 71 ˚N, 161 ˚W.

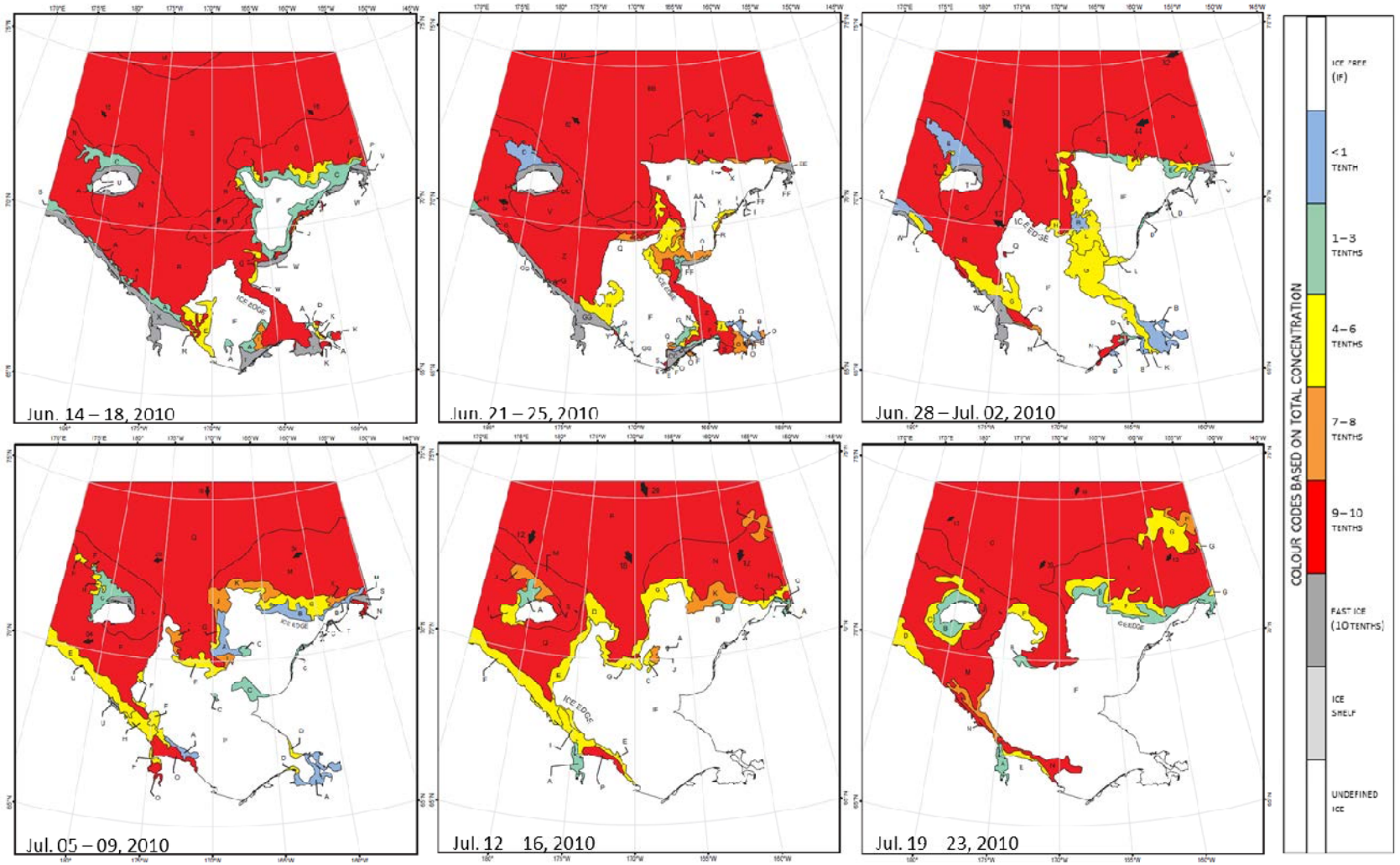

Figure 4-5. Summer 2010 break-up patterns. Ice charts are presented for the period of June 14-18 to July 19-23 in the Chukchi Sea. Site 1 is located at 71 ˚N, 165 ˚W and Site 2 is located at 71 ˚N, 161 ˚W.

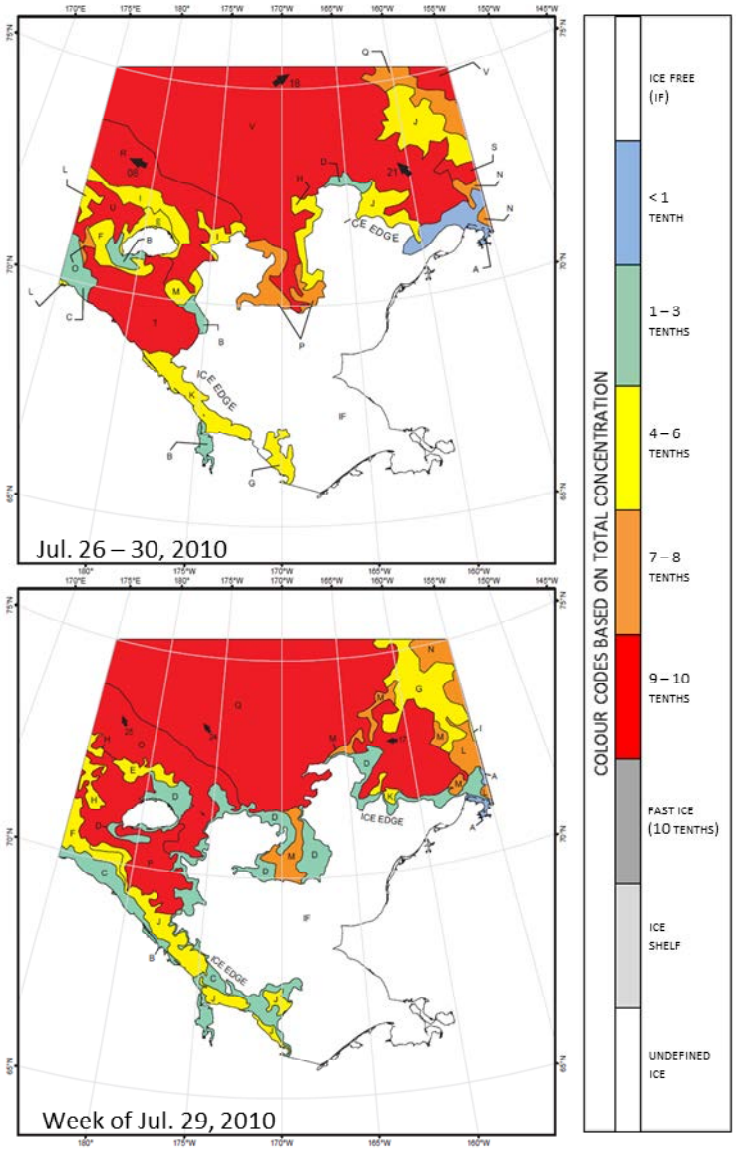

Figure 4-6. Summer 2010 break-up patterns. Ice charts are presented for the period of July 16-30 to July 29-August 2 in the Chukchi Sea. Site 1 is located at 71 ˚N, 165 ˚W and Site 2 is located at 71 ˚N, 161 ˚W.

4.2 ICE KEEL STATISTICS

4.2.1 METHODOLOGY FOR IDENTIFYING ICE KEELS

Ice keels that exceeded 5, 8, and 11 m were identified using either a Rayleigh criterion (α = 0.5), or a lower threshold of 2 m to end a feature. The keel detection algorithm was based on "Criterion A" as described in Vaudrey (1987). The algorithm found the start and end of individual ice features using three thresholds, as shown in Figure 4-7. For illustrative purposes, a 13 m starting threshold was used. A keel started, shown as "Start Point" in the figure, once the draft exceeded the "Start Threshold". The keel ended if it crossed the "End Threshold" at 2m, or if it reversed slope at a point less than a threshold given by (1 - α)*Maximum Draft, where α = 0.5 is the Rayleigh criterion.

The beginning of the keel is then found by scanning backwards from the previously designated "Start Point". The earlier keel start was found at a point that crossed the "End Threshold," or reversed slope, at a point less than the threshold given by (1 - α)*Maximum Draft.

Unlike the forward search to find the keel endpoint, the maximum draft was not updated; instead the value found for the forward search was used.

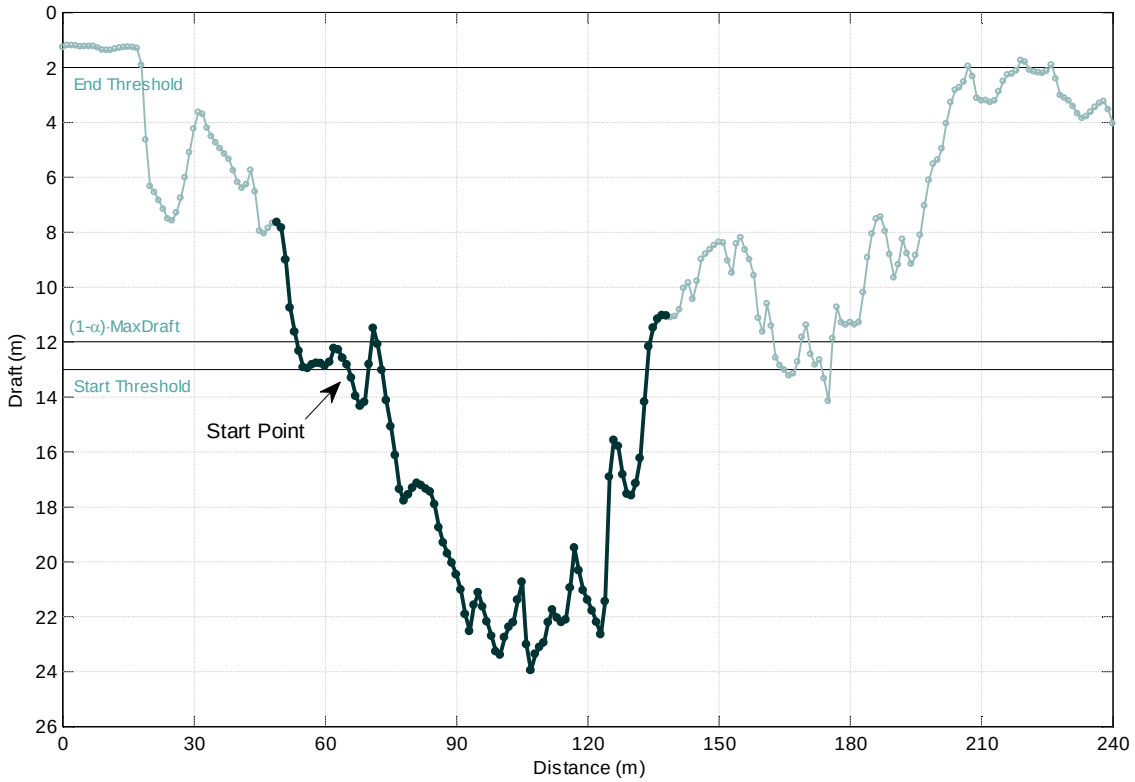

Figure 4-7. An example of the thresholds used by the keel identification algorithm. The keel was found using a 13 m start threshold, 2 m end threshold, and α equal to 0.5

4.2.2 OVERLAPPING FEATURES

The backwards search technique used to find the start of a keel can result in overlapping keel features when a keel with a larger maximum draft was followed by one with a lower maximum draft. In the backwards search on the second lower draft keel, the beginning of the keel can extend past the beginning of the first keel since the lower draft means a lower α threshold. It is also possible that the second keel can overlap with more than one previous feature. After the preliminary keels were selected, they were re-processed and the overlapping features were combined into a single event by using the start of the first keel in the overlap and the end of the last keel in the overlap.

An example of this type of overlap and the resulting combined feature is shown in Figure 4-8. For illustrative purposes, a 13 m starting threshold was used and applied to the ice keel shown in Figure 4-7. Figure 4-8 shows an overlap with the feature in Figure 4-7, and the effect of combining the two features.

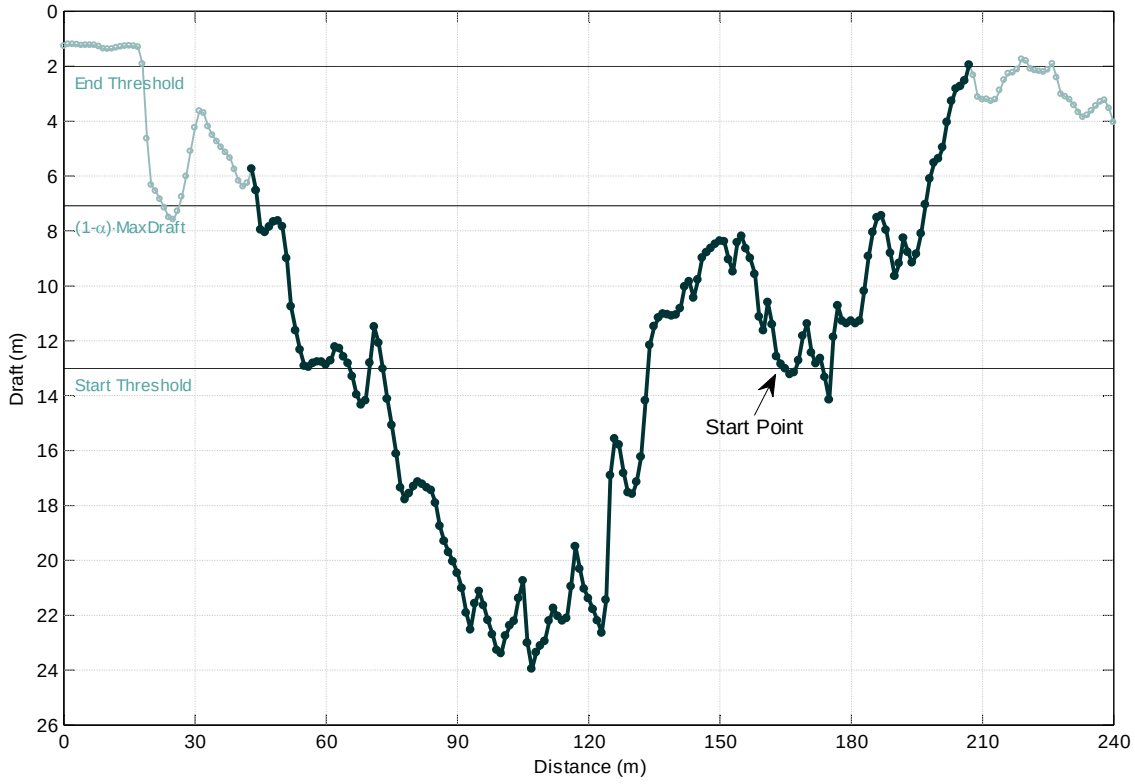

Figure 4-8. An example of a keel feature extending from the “Start Point” beyond the feature shown in Figure 4-7.

4.2.3 DESCRIPTION OF THE DATABASE OF KEEL FEATURES

A database of keel features was constructed using starting thresholds of 5, 8, and 11 m, an end threshold of 2 m and a Rayleigh criterion (α = 0.5). For each site and starting threshold, a data file was created containing the start time, end time, start distance, end distance, width, mean draft, maximum draft, minimum draft and the standard deviation of the draft for each keel feature. A description of each of the fields is provided in Table 4-1.

Statistical results are given over monthly and ice season time periods. For each starting threshold, a data file was created containing the start time of the statistic segment, the end time of the statistic segment, the minimum, mean, maximum and standard deviation of the maximum draft, the mean and standard deviation of the mean draft, the minimum, mean, maximum and standard deviation of the width, the total ice distance (sum of all ice distances for the time period), the total waves in ice and open water distance (sum of all waves in ice + open water distances for the time period), the total distance (sum of all ice + waves in ice + open water + data flagged as bad distances for this time period), the sum of all keel widths for this time period, the sum of all keel areas (sum of the product of each keel segment width and mean draft) and the number of keels in this time period. If a keel feature occurred on the boundary of consecutive monthly time segments, the keel was considered to be in the month where it had the greatest width. A description of each of the fields is provided in Table 4-2.

In the ice keel statistical results, the average keel width is typically over 30 m. The widest keels may represent an amalgamation of individual keels or a rubbled ice field.

Table 4-1. A description of each field in the keel feature data file.

Name	Description
Start Time	The start time of the segment
End Time	The end time of the segment
Start Distance	The keel start distance (km)
End Distance	The keel end distance (km).
Width	The width of the keel feature (m).
Mean Draft	The mean draft value of the keel feature (m).
Maximum Draft	The maximum draft value of the keel feature (m).
Minimum Draft	The minimum draft value of the keel feature (m).
Std Dev of Draft	The standard deviation of the draft of the keel feature (m).

Table 4-2. A description of each field in the keel statistics (monthly and ice season) data file.

Name	Description
Start Time	The start time of the statistic segment.
End Time	The end time of the statistic segment.
Min of Max Draft	The minimum of all the maximum keel segment drafts in the time period (m).
Mean of Max Draft	The mean of all the maximum keel segment drafts in the time period (m).
Max of Max Draft	The maximum of all the maximum keel segment drafts in the time period (m).
Std of Max Draft	The standard deviation of all the maximum keel segment drafts in the time period (m).
Mean of Mean Draft	The mean of all the mean keel segment drafts in the time period (m).
Std of Mean Draft	The standard deviation of all the mean keel segment drafts in the time period (m).
Min Width	The minimum of all the keel segment widths in the time period (m).
Mean Width	The mean of all the keel segment widths in the time period (m).
Max Width	The maximum of all the keel segment widths in the time period (m).
Std of Width	The standard deviation of all the keel segment widths in the time period (m).
Total Ice Distance	The total distance of ice covered for the time period (km). This total distance includes all non-flagged data (ice).
Total O/W + Waves in Ice Dist	The total distance of waves in ice and open water covered for the time period (km). This total distance includes data flagged as open water (-200) and data flagged as waves in ice (-500).
Total Distance	The total distance covered for the time period (km). This total distance includes ice, data flagged as open water (-200), data flagged as waves in ice (-500) and data flagged as bad (-9999).
Sum of Keel Widths	The sum of the keel widths for the time period (km).
Sum of Keel Areas	The sum of the keel areas for the time period ($x10^3$ m^2). The area is calculated from the sum of the product of the mean draft and the width of each segment.
Number of Keels	The number of keel features in the time period.

Some statistical results from the ice keel feature database are presented as plots, including:

- the **daily** statistics of the number of keels and the total keel area for the 5, 8 and 11 m thresholds are shown in Figure 4-9 and Figure 4-10. Note that the large episodic variations in the number of ice keels and daily ice keel area are very strongly related to the episodic nature of daily ice movement distance. Site 2, located nearer the landfast ice edge. has more keels in both total number and by total ice keel area than Site 1
- **monthly** histograms of maximum ice drafts using the 5m threshold are shown in Figure 4-11 and Figure 4-12.
- histograms of maximum ice drafts for the full ice **season** using the 5m threshold are shown in Figure 4-13 and Figure 4-14.
- Statistics for keels detected with the 5, 8 and 11 m thresholds are presented in Table 4-3 through Table 4-10.

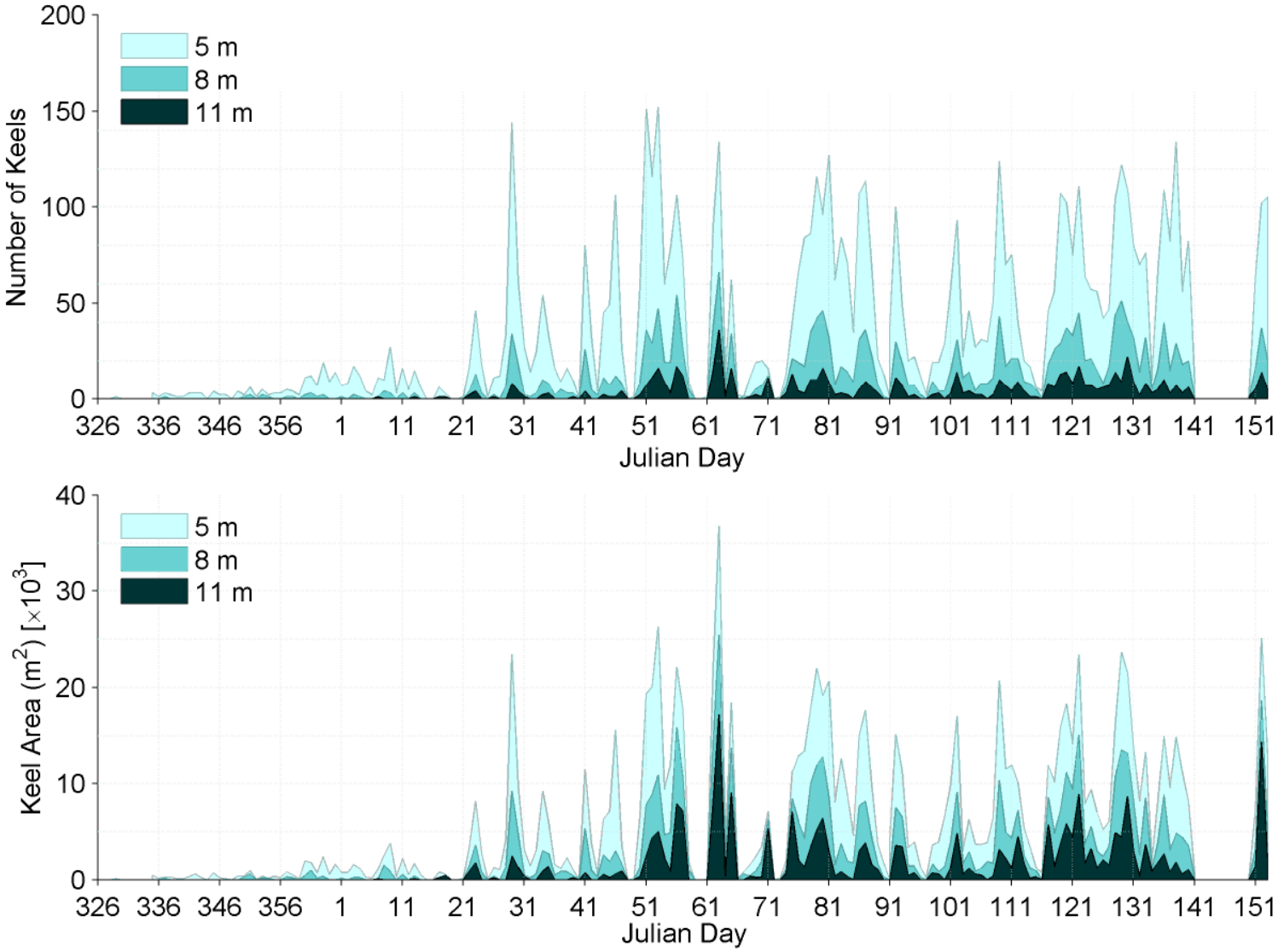

Figure 4-9. Daily numbers of keel features (top) and daily keel area (bottom) found using the 5m, 8m, and 11m thresholds at Site 1.

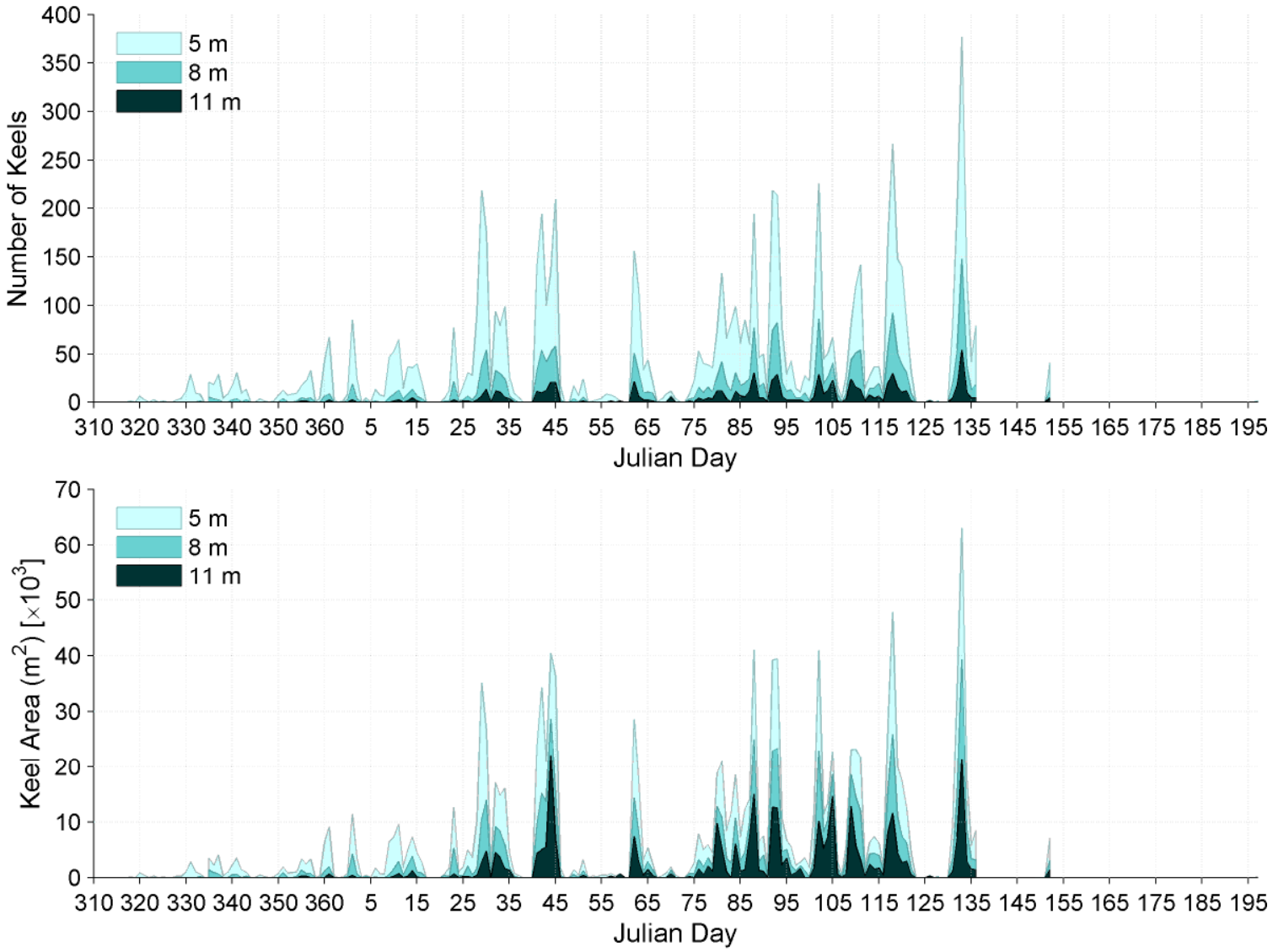

Figure 4-10. Daily numbers of keel features (top) and daily keel area (bottom) found using the 5m, 8m, and 11m thresholds at Site 2.

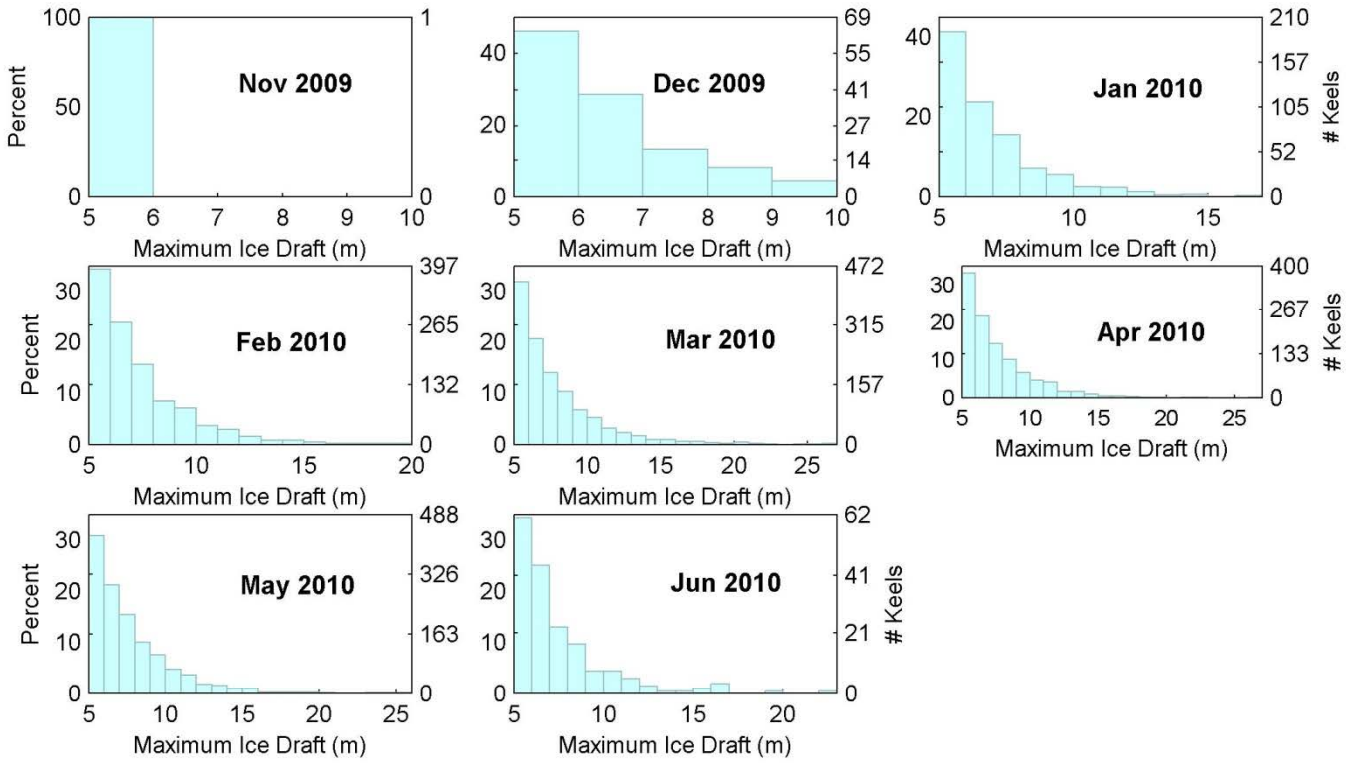

Figure 4-11. Monthly histograms of maximum ice draft for keels found using the 5 m threshold at Site 1.

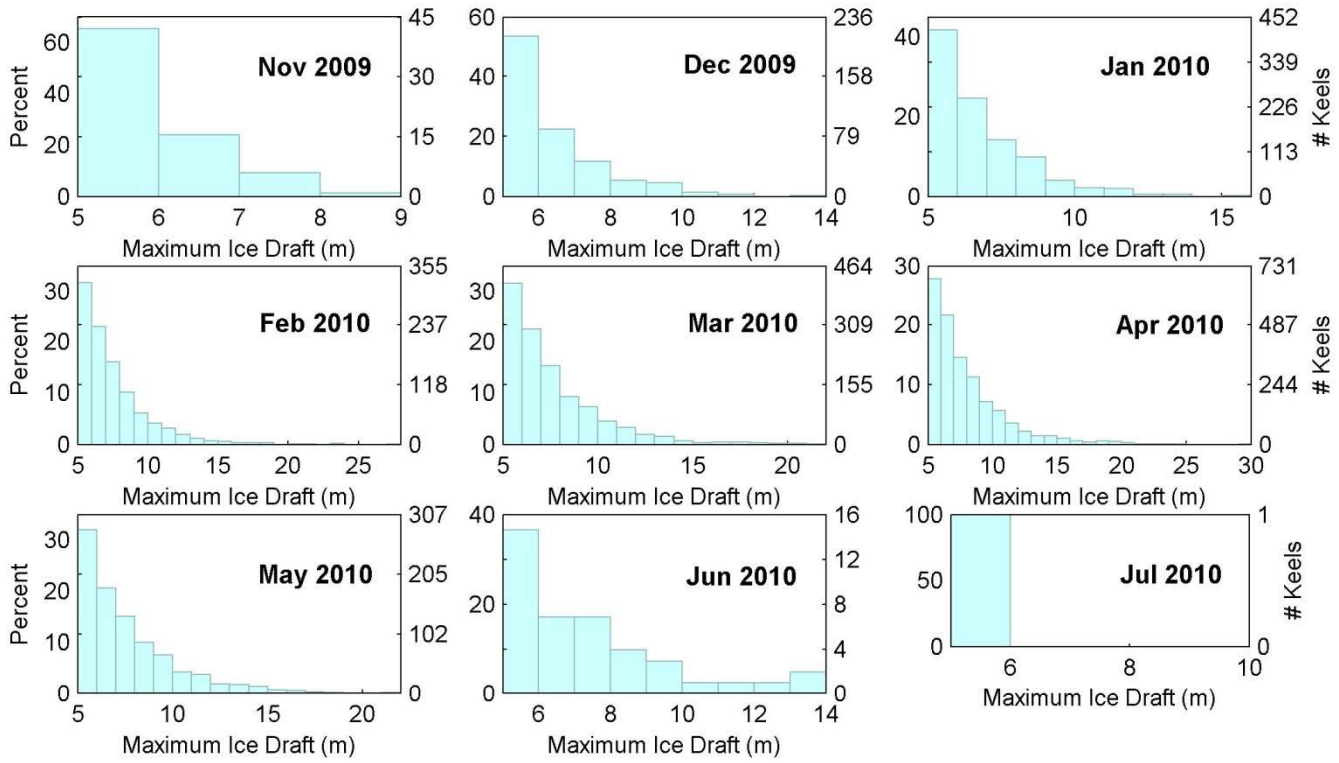

Figure 4-12. Monthly histograms of maximum ice draft for keels found using the 5 m threshold at Site 2.

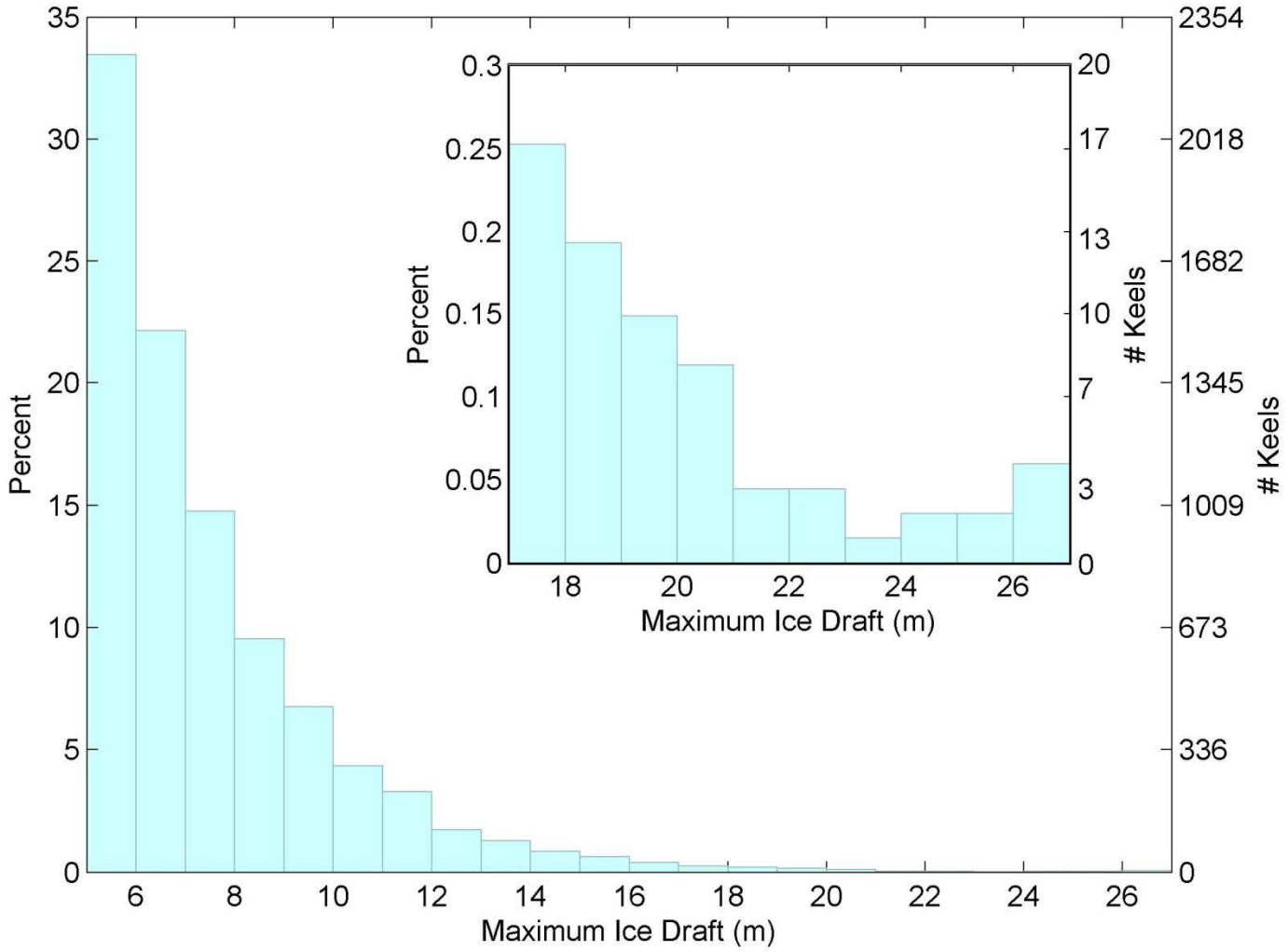

Figure 4-13. Full ice season histogram of the maximum ice draft for keels found using the 5 m threshold at Site 1.

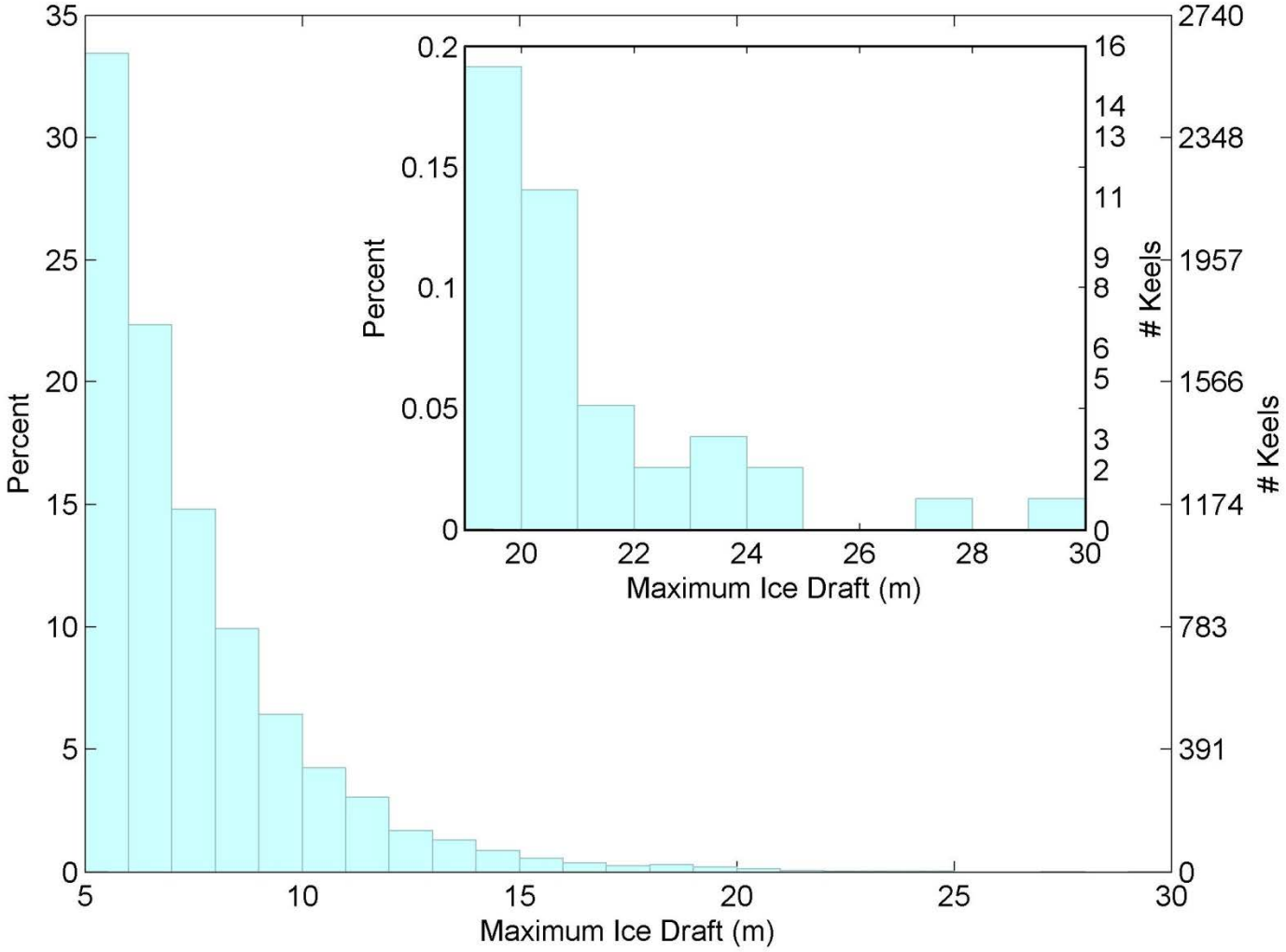

Figure 4-14. Full ice season histogram of the maximum ice draft for keels found using the 5 m threshold at Site 2.

Table 4-3. Site 1 monthly statistics of keel features for the 5m threshold level.

Site 1, 2009-2010: 5 m Threshold																
Month	Maximum Draft				Mean Draft		Width				Distance			Keels		
	Min (m)	Mean (m)	Max (m)	StdDev (m)	Mean (m)	StdDev (m)	Min (m)	Mean (m)	Max (m)	StdDev (m)	Total Ice (km)	Total O/W + WI (km)	Total Ice + O/W (km)	Sum of Width (km)	Sum of Area ($\times 10^3$ m^2)	Number
November	5.37	5.37	5.37	0.00	3.65	0.00	25.00	25.00	25.00	0.00	208.94	1.06	210.00	0.03	0.09	1
December	5.03	6.35	9.58	1.18	4.41	0.83	4.00	25.77	99.00	15.34	561.53	9.64	571.21	3.53	16.61	137
January	5.00	6.86	16.24	1.84	4.65	1.11	3.00	28.45	112.00	16.56	396.38	0.00	396.38	14.91	75.94	524
February	5.01	7.29	19.81	2.20	4.95	1.36	2.00	28.58	167.00	20.21	267.99	0.00	267.99	37.84	209.41	1324
March	5.00	7.77	26.67	2.95	5.21	1.86	2.00	31.72	260.00	25.39	267.57	0.00	267.59	49.90	297.19	1570
April	5.00	7.53	26.25	2.51	5.02	1.50	2.00	30.54	218.00	24.98	221.31	0.00	221.35	40.71	228.35	1333
May	5.00	7.64	25.18	2.58	5.15	1.58	2.00	25.44	376.00	23.11	186.58	25.21	211.90	41.42	246.30	1627
June	5.02	7.47	22.51	2.74	5.04	1.64	2.00	27.08	490.00	44.86	39.75	5.65	45.41	5.61	37.74	207

Table 4-4. Site 2 monthly statistics of keel features for the 5m threshold level.

Site 2, 2009-2010: 5 m Threshold																
Month	Maximum Draft				Mean Draft		Width				Distance			Keels		
	Min (m)	Mean (m)	Max (m)	StdDev (m)	Mean (m)	StdDev (m)	Min (m)	Mean (m)	Max (m)	StdDev (m)	Total Ice (km)	Total O/W + WI (km)	Total Ice + O/W (km)	Sum of Width (km)	Sum of Area ($\times 10^3$ m^2)	Number
November	5.01	5.90	8.21	0.77	4.05	0.51	7.00	23.84	58.00	11.23	294.07	66.92	360.99	1.79	7.57	75
December	5.00	6.39	13.13	1.37	4.41	0.90	7.00	27.19	115.00	16.54	626.42	0.00	626.45	10.71	50.60	394
January	5.01	6.77	15.96	1.65	4.60	1.05	4.00	28.73	159.00	19.00	373.66	24.69	398.35	32.43	162.74	1129
February	5.00	7.49	27.29	2.52	5.03	1.47	2.00	31.47	328.00	26.14	529.04	9.07	538.10	37.26	218.92	1184
March	5.00	7.54	21.91	2.51	5.07	1.55	2.00	27.82	242.00	23.45	404.51	0.00	404.51	42.99	254.31	1545
April	5.00	7.93	29.96	2.93	5.31	1.78	2.00	28.43	203.00	23.00	343.32	0.00	343.34	69.24	433.34	2435
May	5.00	7.58	21.28	2.43	5.07	1.49	3.00	26.00	255.00	22.11	282.70	227.14	509.84	26.63	155.63	1024
June	5.00	7.36	13.90	2.33	5.26	1.66	7.00	29.98	217.00	34.49	6.99	19.11	26.11	1.23	7.12	41
July	5.44	5.44	5.44	0.00	3.55	0.00	3.00	3.00	3.00	0.00	0.61	18.62	19.22	0.00	0.01	1

Table 4-5. Site 1 monthly statistics of keel features for the 8m threshold level.

Site 1, 2009-2010: 8 m Threshold																
Month	Maximum Draft				Mean Draft		Width				Distance			Keels		
	Min (m)	Mean (m)	Max (m)	StdDev (m)	Mean (m)	StdDev (m)	Min (m)	Mean (m)	Max (m)	StdDev (m)	Total Ice (km)	Total O/W + WI (km)	Total Ice + O/W (km)	Sum of Width (km)	Sum of Area ($\times 10^3$ m^2)	Number
November	-	-	-	-	-	-	-	-	-	-	208.94	1.06	210.00	0.00	0.00	0
December	8.05	8.71	9.58	0.54	5.93	0.68	8.00	35.35	99.00	20.03	561.53	9.64	571.21	0.60	3.62	17
January	8.02	9.92	16.24	1.69	6.69	1.18	11.00	37.43	90.00	17.05	396.38	0.00	396.38	3.86	26.84	103
February	8.01	10.26	19.81	2.13	7.13	1.49	4.00	34.25	143.00	20.01	267.99	0.00	267.99	11.99	90.98	350
March	8.00	10.90	26.67	3.12	7.49	2.23	2.00	36.56	150.00	24.60	267.57	0.00	267.59	19.49	159.32	530
April	8.00	10.46	26.25	2.42	7.20	1.67	2.00	33.04	192.00	24.36	221.31	0.00	221.35	13.91	107.91	421
May	8.00	10.55	25.18	2.52	7.30	1.66	3.00	31.43	212.00	22.62	186.58	25.21	211.90	16.75	132.15	532
June	8.01	10.88	22.51	3.10	7.48	2.02	4.00	42.60	398.00	69.95	39.75	5.65	45.41	2.43	23.27	57

Table 4-6. Site 2 monthly statistics of keel features for the 8m threshold level.

Site 2, 2009-2010: 8 m Threshold																
Month	Maximum Draft				Mean Draft		Width				Distance			Keels		
	Min (m)	Mean (m)	Max (m)	StdDev (m)	Mean (m)	StdDev (m)	Min (m)	Mean (m)	Max (m)	StdDev (m)	Total Ice (km)	Total O/W + WI (km)	Total Ice + O/W (km)	Sum of Width (km)	Sum of Area ($\times 10^3$ m^2)	Number
November	8.21	8.21	8.21	0.00	5.36	0.00	25.00	25.00	25.00	0.00	294.07	66.92	360.99	0.02	0.14	1
December	8.16	9.34	13.13	1.07	6.44	0.88	12.00	34.94	115.00	19.79	626.42	0.00	626.45	1.68	11.35	48
January	8.01	9.51	15.96	1.48	6.52	1.10	6.00	36.29	111.00	20.38	373.66	24.69	398.35	7.91	53.76	218
February	8.02	10.49	27.29	2.70	7.24	1.75	7.00	39.48	328.00	31.52	529.04	9.07	538.10	13.70	110.61	347
March	8.01	10.53	21.91	2.47	7.22	1.67	3.00	34.03	242.00	27.05	404.51	0.00	404.51	16.13	131.20	474
April	8.00	10.88	29.96	2.97	7.45	1.94	2.00	34.74	177.00	24.98	343.32	0.00	343.34	30.74	255.09	885
May	8.00	10.42	21.28	2.21	7.16	1.58	3.00	31.35	221.00	23.77	282.70	227.14	509.84	10.44	81.27	333
June	8.11	10.28	13.90	2.07	7.52	1.70	8.00	32.92	118.00	30.96	6.99	19.11	26.11	0.39	3.10	12
July	-	-	-	-	-	-	-	-	-	-	0.61	18.62	19.22	0.00	0.00	0

Table 4-7. Site 1 monthly statistics of keel features for the 11m threshold level.

Site 1, 2009-2010: 11 m Threshold																
Month	Maximum Draft				Mean Draft		Width				Distance			Keels		
	Min (m)	Mean (m)	Max (m)	StdDev (m)	Mean (m)	StdDev (m)	Min (m)	Mean (m)	Max (m)	StdDev (m)	Total Ice (km)	Total O/W + WI (km)	Total Ice + O/W (km)	Sum of Width (km)	Sum of Area ($\times 10^3$ m^2)	Number
November	-	-	-	-	-	-	-	-	-	-	208.94	1.06	210.00	0.00	0.00	0
December	-	-	-	-	-	-	-	-	-	-	561.53	9.64	571.21	0.00	0.00	0
January	11.00	12.44	16.24	1.44	8.34	1.37	14.00	37.04	72.00	17.76	396.38	0.00	396.38	0.89	7.80	24
February	11.08	13.08	19.81	2.01	9.14	1.58	4.00	38.58	114.00	20.92	267.99	0.00	267.99	3.67	35.63	95
March	11.00	14.20	26.67	3.31	10.02	2.74	2.00	42.77	128.00	25.22	267.57	0.00	267.59	7.74	80.49	178
April	11.01	13.20	26.25	2.48	9.25	1.86	3.00	37.22	138.00	25.99	221.31	0.00	221.35	4.95	48.40	133
May	11.01	13.50	25.18	2.55	9.50	1.92	4.00	36.07	124.00	24.79	186.58	25.21	211.90	5.92	58.80	163
June	11.18	14.33	22.51	3.08	10.03	1.97	9.00	72.16	394.00	100.84	39.75	5.65	45.41	1.37	16.05	19

Table 4-8. Site 2 monthly statistics of keel features for the 11m threshold level.

Site 2, 2009-2010: 11 m Threshold																
Month	Maximum Draft				Mean Draft		Width				Distance			Keels		
	Min (m)	Mean (m)	Max (m)	StdDev (m)	Mean (m)	StdDev (m)	Min (m)	Mean (m)	Max (m)	StdDev (m)	Total Ice (km)	Total O/W + WI (km)	Total Ice + O/W (km)	Sum of Width (km)	Sum of Area ($\times 10^3$ m^2)	Number
November	-	-	-	-	-	-	-	-	-	-	294.07	66.92	360.99	0.00	0.00	0
December	11.38	11.90	13.13	0.83	8.11	0.46	31.00	33.75	39.00	3.77	626.42	0.00	626.45	0.14	1.12	4
January	11.11	12.18	15.96	1.20	8.42	1.13	9.00	37.39	88.00	19.50	373.66	24.69	398.35	1.35	11.69	36
February	11.03	13.63	27.29	2.95	9.38	1.91	11.00	51.76	328.00	43.89	529.04	9.07	538.10	5.38	56.22	104
March	11.02	13.47	21.91	2.40	9.53	1.85	5.00	44.18	233.00	33.63	404.51	0.00	404.51	6.54	67.56	148
April	11.00	14.15	29.96	2.98	9.90	2.10	8.00	41.29	168.00	26.86	343.32	0.00	343.34	12.31	130.41	298
May	11.00	13.07	21.28	1.84	9.12	1.37	8.00	38.97	207.00	30.27	282.70	227.14	509.84	4.17	39.63	107
June	11.67	12.85	13.90	1.10	9.61	1.07	19.00	34.25	70.00	23.96	6.99	19.11	26.11	0.14	1.34	4
July	-	-	-	-	-	-	-	-	-	-	0.61	18.62	19.22	0.00	0.00	0

Table 4-9. Site 1 ice season statistics of keel features for the three thresholds (5, 8 and 11 m).

Site 1, 2009-2010																
Threshold	Maximum Draft				Mean Draft		Width				Distance			Keels		
	Min (m)	Mean (m)	Max (m)	StdDev (m)	Mean (m)	StdDev (m)	Min (m)	Mean (m)	Max (m)	StdDev (m)	Total Ice (km)	Total O/W + WI (km)	Total Ice + O/W (km)	Sum of Width (km)	Sum of Area ($\times 10^3$ m^2)	Number
5	5.00	7.49	26.67	2.54	5.04	1.56	2.00	28.83	490.00	23.77	2150.05	41.57	2191.82	193.93	1111.63	6723
8	8.00	10.54		2.60	7.26	1.80	2.00	34.27	398.00	24.37				69.03	544.11	2010
11	11.00	13.56		2.73	9.51	2.15	2.00	39.82	394.00	27.07				24.53	247.16	612

Table 4-10. Site 2 ice season statistics of keel features for the three thresholds (5, 8 and 11 m).

Site 2, 2009-2010																
Threshold	Maximum Draft				Mean Draft		Width				Distance			Keels		
	Min (m)	Mean (m)	Max (m)	StdDev (m)	Mean (m)	StdDev (m)	Min (m)	Mean (m)	Max (m)	StdDev (m)	Total Ice (km)	Total O/W + WI (km)	Total Ice + O/W (km)	Sum of Width (km)	Sum of Area ($\times 10^3$ m^2)	Number
5	5.00	7.47	29.96	2.48	5.03	1.51	2.00	28.40	328.00	22.65	2861.32	365.54	3226.90	222.28	1290.25	7828
8	8.00	10.52		2.59	7.22	1.73	2.00	34.95	328.00	25.93				81.02	646.52	2318
11	11.00	13.64		2.63	9.54	1.88	5.00	42.82	328.00	31.35				30.01	307.97	701

4.3 ESTIMATION OF EXTREME KEELS DRAFTS

4.3.1 EXTREME ICE KEELS

The 10 largest keels observed at Site 1 and Site 2 are listed in Table 4-11 and Table 4-12. At Site 1, the maximum depths of the listed exceptional keels ranged from 21.51 to 26.67 m. At Site 2, the maximum keel depths ranged from 21.91 to 29.96 m. Overall, 19 keels at Site 1 and 24 keels at Site 2 were observed with depths in excess of 20 m.

Table 4-11. List of keels with the ten largest drafts observed at Site 1. The draft values are provided as the maximum and mean (average) draft computed for each of the 10 largest individual ice keels.

Site 1		
Date/ Time	**Max Draft (m)**	**Mean Draft (m)**
12-Mar-2010 02:14:03	26.67	15.18
22-Apr-2010 13:22:10	26.25	18.89
10-May-2010 10:32:38	25.18	16.62
06-Mar-2010 17:26:44	24.06	17.11
05-May-2010 15:33:32	23.70	18.22
01-Jun-2010 08:41:06	22.51	12.09
22-Apr-2010 14:03:46	22.47	15.04
06-Mar-2010 09:17:23	22.17	14.79
16-Mar-2010 22:26:55	21.67	13.66
29-Apr-2010 04:06:55	21.51	15.25

Table 4-12. List of keels with the ten largest drafts observed at Site 2. The draft values are provided as the maximum and mean (average) draft computed for each of the 10 largest individual ice keels.

Site 2		
Date/ Time	**Max Draft (m)**	**Mean Draft (m)**
13-Apr-2010 00:26:03	29.96	16.90
13-Feb-2010 07:57:46	27.29	18.79
15-Apr-2010 03:54:18	24.71	17.93
15-Apr-2010 04:11:34	24.07	15.98
13-Feb-2010 08:19:53	23.93	14.12
19-Apr-2010 05:50:55	23.77	18.16
13-Feb-2010 15:30:19	23.11	15.59
19-Apr-2010 01:52:14	22.98	14.02
12-Apr-2010 13:28:47	22.28	13.96
21-Mar-2010 17:56:52	21.91	14.90

4.3.2 METHODOLOGY FOR EXTREMAL ANALYSIS

Probability estimation for extreme keel depth occurrences is limited due to both the short duration of our measurement program (2008-2010 at Site 1 and 2009-2010 at Site 2) and the limitations on maximum measurable draft imposed by the depth of IPS-5 transducer. The parameter most relevant to such estimates is the 100-year return draft value, D_{100}, which is representative of the largest keel depth likely to be encountered in 100 years at a given site. Previously, 100-year return values were derived by fitting the high draft end of the empirical keel probabilities to a three-parameter Weibull probability distribution. However, as a result of the limitations noted above, the return values calculated are not deemed statistically reliable, and hence, not presented here. As data collection spans more years, these results will become more statistically robust.

4.3.3 SELECTION OF FEATURES OF EXTREME DRAFT

The selection of ice keels for inclusion in our analyses of extreme draft probabilities followed a two-step process (ASL, 2000):

1. The largest individual ice keels were selected for each site from the final version of the 1 m smoothed spatial data set, by selecting individual big keel segments having a maximum ice draft above a chosen threshold level. The threshold was set to eventually allow selection of roughly 100 or more extreme keel values as representatives of the largest ice keel drafts observed at a given site.

2. Each of the ice keel data segments, as selected (as per item 1) were plotted and manually reviewed. In a few cases, two or more individual keels were combined into a single keel of greater horizontal extent. The final set of the largest ice keels by site are presented as individual plots of ice draft spatial series in the Data Archive which can be downloaded from ASL's FTP site.

In terms of data collected during 2009-2010 and based on the 13 m keel depth threshold, there were approximately 50 more deep keels detected at Site 2 (326 keels) than at Site 1 (272 keels).

4.3.4 STATISTICAL ANALYSIS

The distributions of maximum keel draft values in 2009-2010 for keels with maximum drafts above the 13 m threshold are presented in Table 4-13 for Site 1 and Site 2.

Table 4-13. Ice draft distributions in 2009-2010 for ice keels exceeding 13.0 m maximum draft.

Number of Keels		
Draft (m)	**Site 1**	**Site 2**
13.0 - 13.5	51	50
13.5 - 14.0	36	53
14.0 - 14.5	37	38
14.5 - 15.0	21	31
15.0 - 15.5	26	19
15.5 - 16.0	16	24
16.0 - 16.5	17	14
16.5 - 17.0	9	15
17.0 - 17.5	9	13
17.5 - 18.0	8	7
18.0 - 18.5	5	13
18.5 - 19.0	8	10
19.0 - 19.5	4	9
19.5 - 20.0	6	6
20.0 - 20.5	4	8
20.5 - 21.0	4	3
21.0 - 21.5	1	2
21.5 - 22.0	2	2
22.0 - 22.5	2	1
22.5 - 23.0	1	1
23.0 - 23.5	0	1
23.5 - 24.0	1	2
24.0 – 24.5	1	1
24.5 – 25.0	0	1
25.0 – 25.5	1	0
25.5 – 26.0	0	0
26.0 – 26.5	1	0
26.5 – 27.0	1	0
27.0 – 27.5	0	1
27.5 – 28.0	0	0
28.0 – 28.5	0	0
28.5 – 29.0	0	0
29.0 – 29.5	0	0
29.5 – 30.0	0	1

To provide an appreciation of the character of the largest ice keels, plots of spatial profiles are provided in Figure 4-15 and Figure 4-16 for the widest and deepest keels encountered at each site. Arguably, the widest keels in the entire data sets could be considered to be part of rubble ice fields. Note, however, that the detected keels in the ice keel database are defined according to the quantitative criteria specified above in section 4.2.1 for large ice keels. More advanced analysis methods to distinguish between different ice deformation processes such as singular large keels and rubbled and/or hummocky ice are recommended for further investigation of these very extensive Ice Profiler data sets.

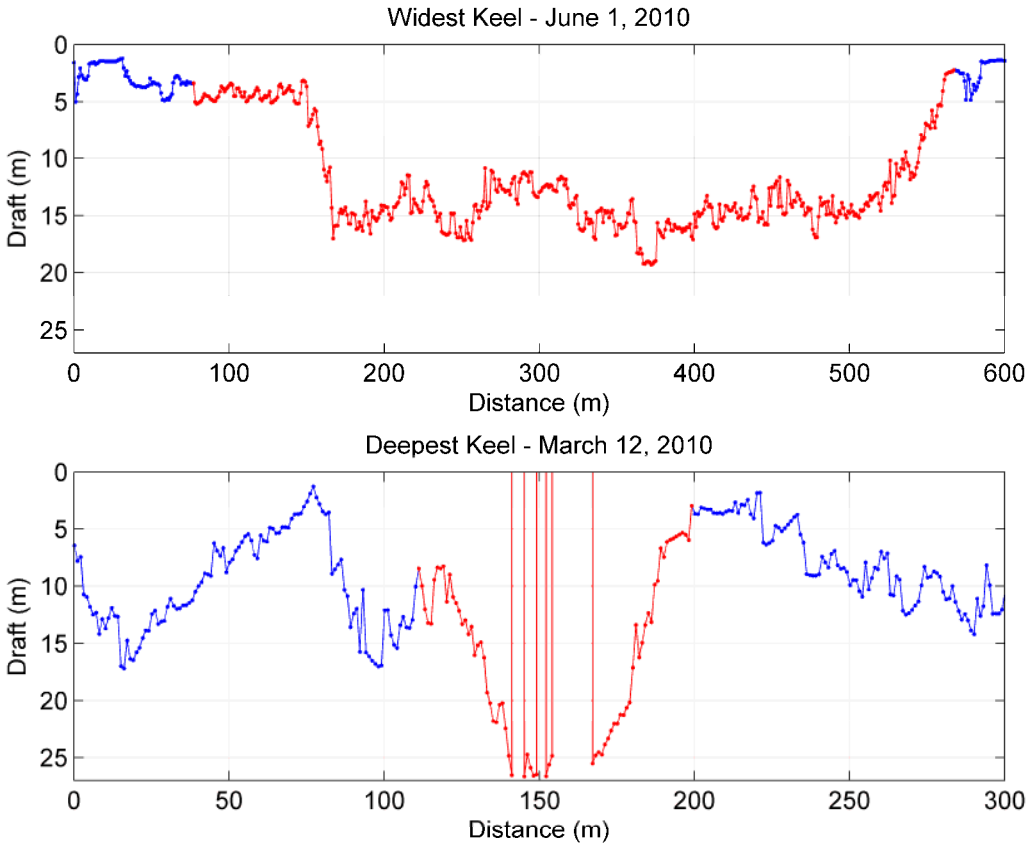

Figure 4-15. The widest keel (490 m, *top*) observed at Site 1 occurred on June 1, 2010. The deepest keel (26.67 m, *bottom*) occurred on March 12, 2010. The vertical lines indicate where there are no measurements of draft due to the insufficient distance between the keel and the IPS-5.

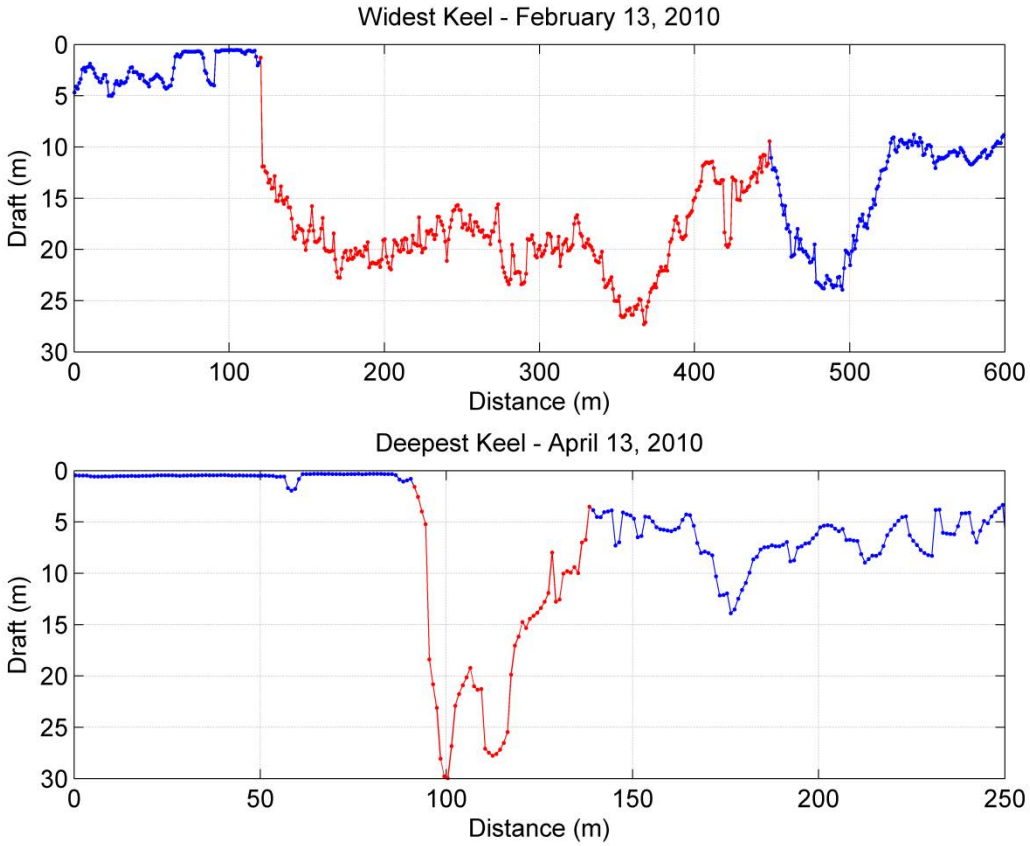

Figure 4-16. The widest keel (328 m, top) observed at Site 2 occurred on February 13, 2010. The deepest keel (29.96 m, bottom) occurred on April 13, 2010.

4.4 ICE MOTION: EPISODES OF LARGE MOVEMENT AND NO MOVEMENT

The ice velocity measurements (Section 3.3) and the resulting distances of ice movement measured were subjected to further analyses to identify the episodes of alternately large and then negligible ice movements for the winter and spring of 2009-2010 at Sites 1 and 2 where ice velocity measurements were made.

Each episode of large ice movement was identified using a criterion of having an average speed exceeding 19 cm/s over a minimum duration of 12 hours. The episodes of large ice movement are presented in Table 4-14 and Table 4-15 for Site 1 and Site 2 respectively. Information on the winds (direction from and maximum wind speed) is also presented for each episode of large ice movement. The maximum ice speed both at Site 1 and Site 2 was recorded over the same observation period in late January when strong winds from the East were prevalent in the area with average speeds of 8.3 m/s.

As presented earlier in Table 3-10, the percentage of no-motion observations at Site 2 is, on average, larger than that of at Site 1, which is consistent with Site 2 being closer to the land fast ice zone. The maximum of no-motion episodes occurred in February with a value of 16.8 % at Site 2 and 8.1 % at Site 1. However, the mean (and maximum) ice speed calculated for the entire 2009-2010 measurement period were higher for Site 2 with a value of 19.8 cm/s (114.8 cm/s) than that of Site 1 with a value of 13.8 cm/s (75.8 cm/s). This result indicates that Site 2 is located in a more dynamic region and when ice concentrations are not very close to 100% to allow for ice movement, ice floes travel at higher speeds at Site 2.

By December, Site 2 started exhibiting significant (5.5 %) periods of no-motion, while Site 1 which is further offshore and where high concentrations of new sea ice occur later in the year did not show no-motion ice episodes until January 2010. Overall, the no-motion episodes were registered at Site 2 from December 2009 to April 2010 and only from January 2010 to April 2010 for Site 1.

At both sites the episodes of large ice movements occur at approximately the same times as do the episodes of little or no ice movement. One exception to this was observed in May at Site 2 when the 99th percentile of ice speeds were the second highest on record for the whole 2009-2010 measurement period with a value of 91.8 cm/s (Table 3-12). The importance of the underlying wind forcing in causing the large ice movements is clearly evident in these statistical results.

Table 4-14. Large ice motion events at Site 1.

Start Date/Time	Stop Date/Time	Duration (days)	Distance Travelled (km)	Average Speed (cm/s)	Maximum Speed (cm/s)	Net Ice Dir (degT)	Maximum Wind Speed (m/s)	Wind Direction from (deg)
24-Nov-2009 03:41	28-Nov-2009 11:56	4.34	139.02	37.0	56.5	227	5.4	E
29-Nov-2009 01:26	29-Nov-2009 22:11	0.86	18.51	24.8	28.9	155	4.2	W
30-Nov-2009 06:56	01-Dec-2009 01:56	0.79	17.23	25.2	34.4	224	4.8	E
01-Dec-2009 14:41	03-Dec-2009 12:11	1.90	44.26	27.0	31.8	197	5.1	W
05-Dec-2009 12:41	06-Dec-2009 09:56	0.89	30.28	39.6	58.1	263	8.9	E
06-Dec-2009 13:11	07-Dec-2009 09:56	0.86	20.28	27.1	38.2	64	5.1	W
09-Dec-2009 05:26	10-Dec-2009 05:41	1.01	21.12	24.2	31.9	80	2.6	E
13-Dec-2009 15:41	14-Dec-2009 09:11	0.73	15.68	24.9	30.2	147	2.3	W
15-Dec-2009 09:56	16-Dec-2009 02:11	0.68	17.07	29.2	33.6	209	6.1	E
21-Dec-2009 10:56	22-Dec-2009 14:56	1.17	26.49	26.3	32.7	296	7.4	E
24-Dec-2009 20:26	25-Dec-2009 11:56	0.65	15.97	28.6	33.7	298	8.3	E
25-Dec-2009 12:56	29-Dec-2009 15:56	4.13	148.50	41.7	72.3	264	8.6	E
10-Jan-2010 13:56	11-Jan-2010 08:26	0.77	22.90	34.4	45.8	304	6.1	E
22-Jan-2010 13:41	24-Jan-2010 12:11	1.94	57.09	34.1	51.3	26	7.7	E
26-Jan-2010 09:26	26-Jan-2010 23:41	0.59	12.15	23.7	28.3	103	5.4	W
27-Jan-2010 19:26	30-Jan-2010 15:26	2.83	115.40	47.1	75.9	244	8.3	E
10-Feb-2010 08:41	11-Feb-2010 14:56	1.26	32.68	30.0	44.6	257	7.0	E
19-Feb-2010 23:11	22-Feb-2010 19:41	2.85	62.34	25.3	33.2	285	11.5	E
03-Mar-2010 09:56	04-Mar-2010 05:41	0.82	17.86	25.1	29.8	222	5.1	E
17-Mar-2010 19:57	18-Mar-2010 08:42	0.53	11.57	25.2	29.7	42	2.6	E
21-Mar-2010 22:42	23-Mar-2010 04:27	1.24	26.26	24.5	27.7	298	6.7	E
24-Mar-2010 02:57	25-Mar-2010 11:57	1.38	38.16	32.1	42.2	258	8.0	E
26-Mar-2010 22:27	29-Mar-2010 03:42	2.22	51.94	27.1	34.4	222	5.4	E
11-Apr-2010 20:42	12-Apr-2010 09:27	0.53	12.01	26.2	32.1	48	3.5	E
17-May-2010 23:27	19-May-2010 08:42	1.39	26.50	22.1	26.0	303	7.4	E
31-May-2010 02:42	02-Jun-2010 11:42	2.38	69.46	33.9	53.4	208	7.4	E
	Total of Events	38.74	1070.73					

Table 4-15. Large ice motion events at Site 2.

Start Date/Time	Stop Date/Time	Duration (days)	Distance Travelled (km)	Average Speed (cm/s)	Maximum Speed (cm/s)	Net Ice Dir (degT)	Maximum Wind Speed (m/s)	Wind Direction from (deg)
06-Nov-2009 19:55	07-Nov-2009 17:10	0.89	48.76	63.7	81.5	282	3.2	E
13-Nov-2009 08:39	15-Nov-2009 17:39	2.38	78.98	38.5	57.3	260	4.8	E
24-Nov-2009 19:24	28-Nov-2009 09:53	3.60	100.94	32.4	45.6	244	5.4	E
01-Dec-2009 12:38	02-Dec-2009 03:53	0.64	14.45	26.3	33.0	245	4.5	E
02-Dec-2009 12:53	03-Dec-2009 20:23	1.31	33.18	29.3	34.1	243	5.1	W
06-Dec-2009 09:38	10-Dec-2009 16:07	4.27	152.82	41.4	71.9	90	6.1	E
19-Dec-2009 19:22	20-Dec-2009 10:22	0.63	12.82	23.7	27.7	83	3.5	E
21-Dec-2009 10:22	22-Dec-2009 18:22	1.33	29.49	25.6	31.9	303	7.4	E
22-Dec-2009 23:22	24-Dec-2009 13:07	1.57	39.54	29.1	33.6	100	4.2	E
25-Dec-2009 17:21	29-Dec-2009 23:36	4.26	188.15	51.1	96.7	260	8.6	E
01-Jan-2010 10:36	02-Jan-2010 07:36	0.88	19.24	25.4	29.5	130	5.7	W
09-Jan-2010 15:05	11-Jan-2010 12:35	1.90	40.67	24.8	28.8	271	6.1	E
22-Jan-2010 23:05	24-Jan-2010 05:04	1.25	26.41	24.5	32.0	53	7.7	E
28-Jan-2010 03:19	31-Jan-2010 00:19	2.88	172.85	69.6	114.8	261	8.3	E
02-Feb-2010 15:19	03-Feb-2010 12:19	0.88	18.50	24.5	27.0	122	6.7	W
10-Feb-2010 10:33	11-Feb-2010 23:03	1.52	56.08	42.7	65.1	262	7.0	E
13-Feb-2010 08:18	16-Feb-2010 07:48	2.98	94.57	36.7	67.8	257	7.4	E
19-Feb-2010 19:03	26-Feb-2010 13:17	6.76	278.31	47.7	100.1	263	11.5	E
03-Mar-2010 05:47	05-Mar-2010 00:17	1.77	58.07	38.0	51.7	251	5.1	E
21-Mar-2010 22:01	22-Mar-2010 19:16	0.89	17.55	22.9	26.0	269	6.7	E
23-Mar-2010 21:45	26-Mar-2010 07:45	2.42	96.76	46.3	77.7	254	8.0	E
26-Mar-2010 08:30	30-Mar-2010 05:00	3.85	122.58	36.8	63.8	244	5.7	E
02-Apr-2010 01:15	04-Apr-2010 19:30	2.76	78.97	33.1	45.9	240	7.0	E
11-Apr-2010 11:44	12-Apr-2010 20:14	1.35	34.60	29.6	38.6	81	5.7	E
27-Apr-2010 10:58	29-Apr-2010 13:58	2.13	67.83	37.0	51.3	256	6.7	E
30-Apr-2010 19:13	03-May-2010 23:43	3.19	127.19	46.2	89.6	265	7.0	E
10-May-2010 03:12	15-May-2010 15:42	5.52	262.08	54.9	108.7	259	6.4	E
15-May-2010 21:27	16-May-2010 17:42	0.84	27.17	37.27	44.53	282.9	6.4	E
30-May-2010 03:56	31-May-2010 02:26	0.94	30.27	37.37	49.39	227.4	3.5	E
31-May-2010 18:11	01-Jun-2010 19:41	1.06	32.63	35.54	40.07	185.8	6.5	W
	Total of Events	66.65	2361.46					

4.5 OCEAN WAVE RESULTS

The time series of significant wave height (H_s) and peak period (T_p) for Sites 1 and 2 are presented in Figure 4-17 and 4-23, respectively.

At Site 1, H_{max} (maximum wave height) was also computed. There was one storm with H_s exceeding 5 m at Site 1, two events at Site 1 and one at Site 2 with H_s greater than 4 m and nine events with H_s greater than 3 m at Site 1 and four at Site 2. The largest storm, which occurred between 2009/10/21 18:00 and 2009/10/24 12:00, had H_s over 5 m and T_p up to 10 s (and H_{max} > 10m) at Site 1 and H_s over 4 m at 8 seconds at Site 2. At this time, wind speeds at Prudhoe Bay and Barter Island were from the east at 30-40 knots and winds at Wainwright and Barrow were from the east at 15-20 knots. This event is shown in detail in Figure 4-19.

Statistics and joint frequency tables of significant wave height (H_s) and peak period (T_p) for Sites 1 and 2 are presented in Table 4-16 to Table 4-19. Most of the peak period data corresponding to wave heights below 0.1 m was flagged due to the autospectra's uncertainty in identifying the correct period. The joint frequency tables show that most of the waves have a period in the 4-7 second range and were 0.5-1.5 m.

The percent exceedances of H_s are presented in Table 4-20 and Figure 4-20 for both sites. For both data sets, more than 50% of the data had H_s greater than 0.75 m. Site 1 had 18% of the data above 2 m and Site 2 had 10%. Site 1 had 4.9% of the data above 3 m and Site 2 had 1.5%.

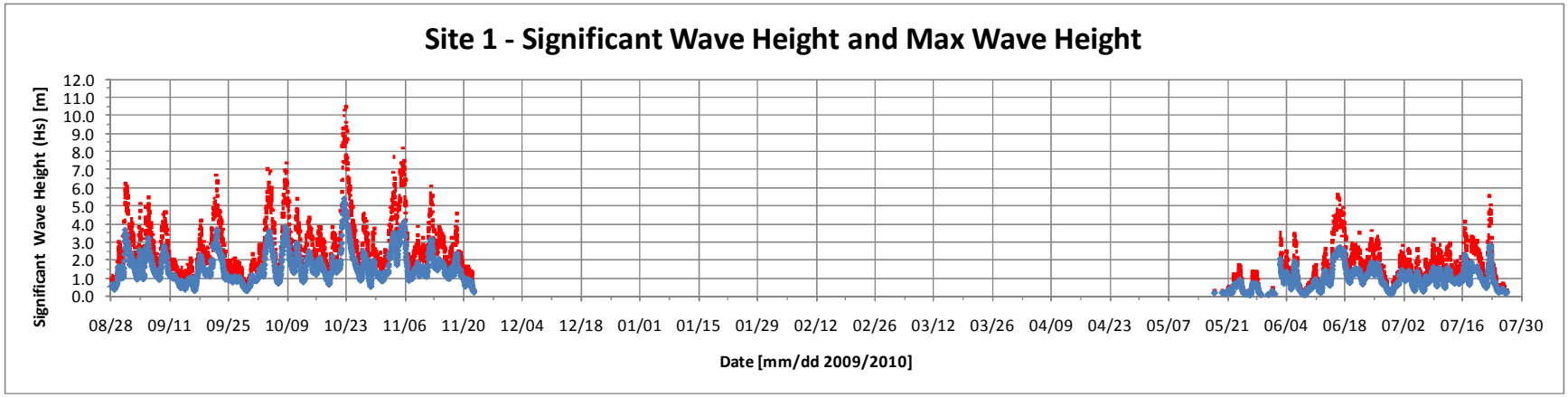

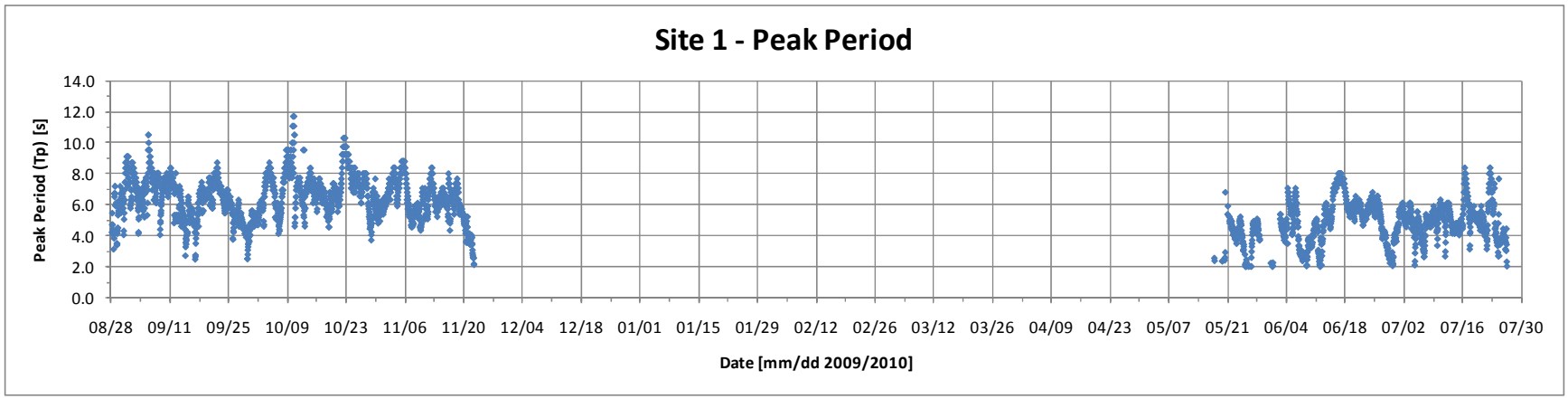

Figure 4-17. Significant wave height (H_s), maximum wave height (H_{max}) and peak period (T_p) at Site 1 for 2009/2010.

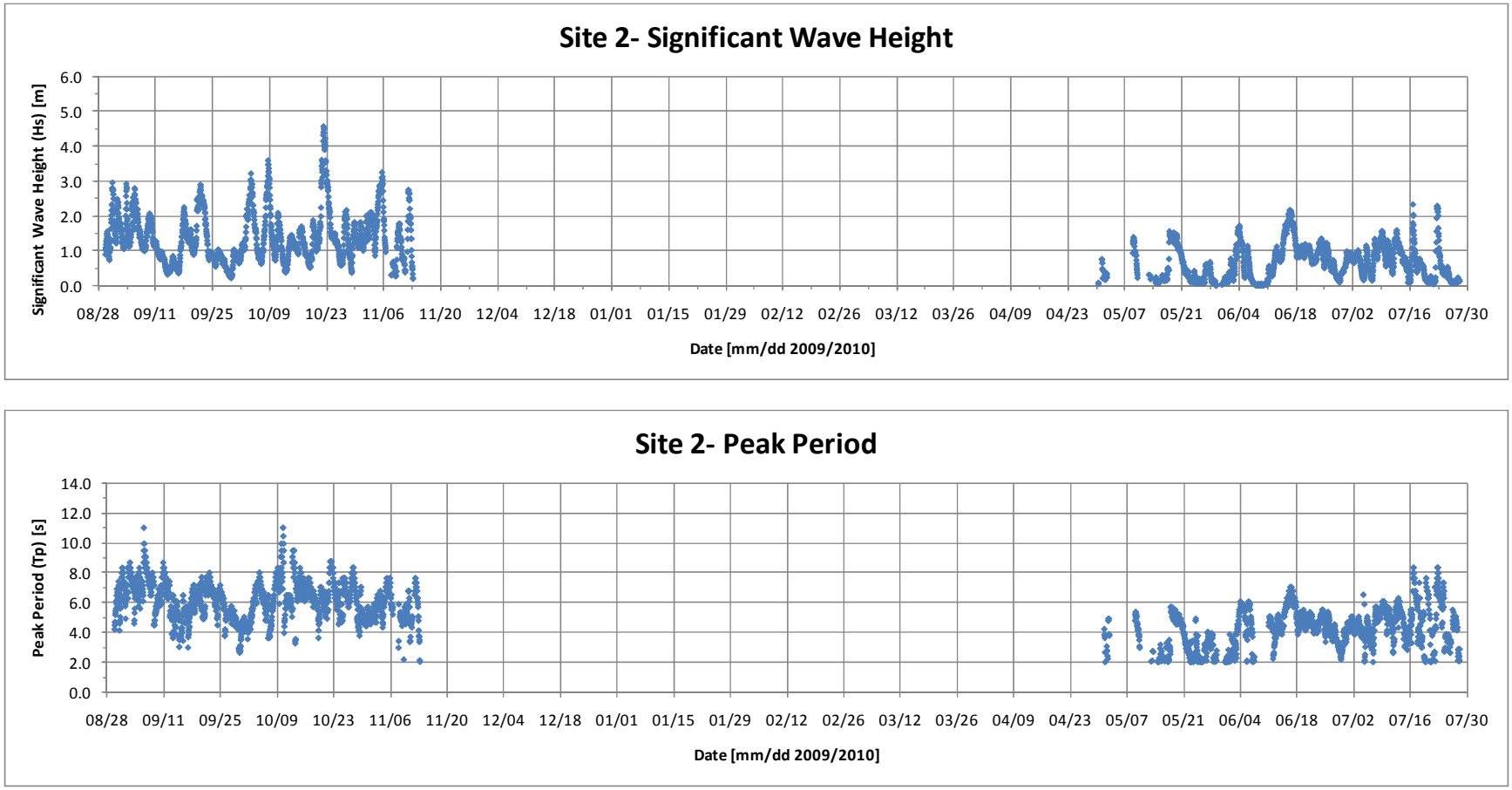

Figure 4-18. Significant wave height (H_s) and peak period (T_p) at Site 2 for 2009/2010.

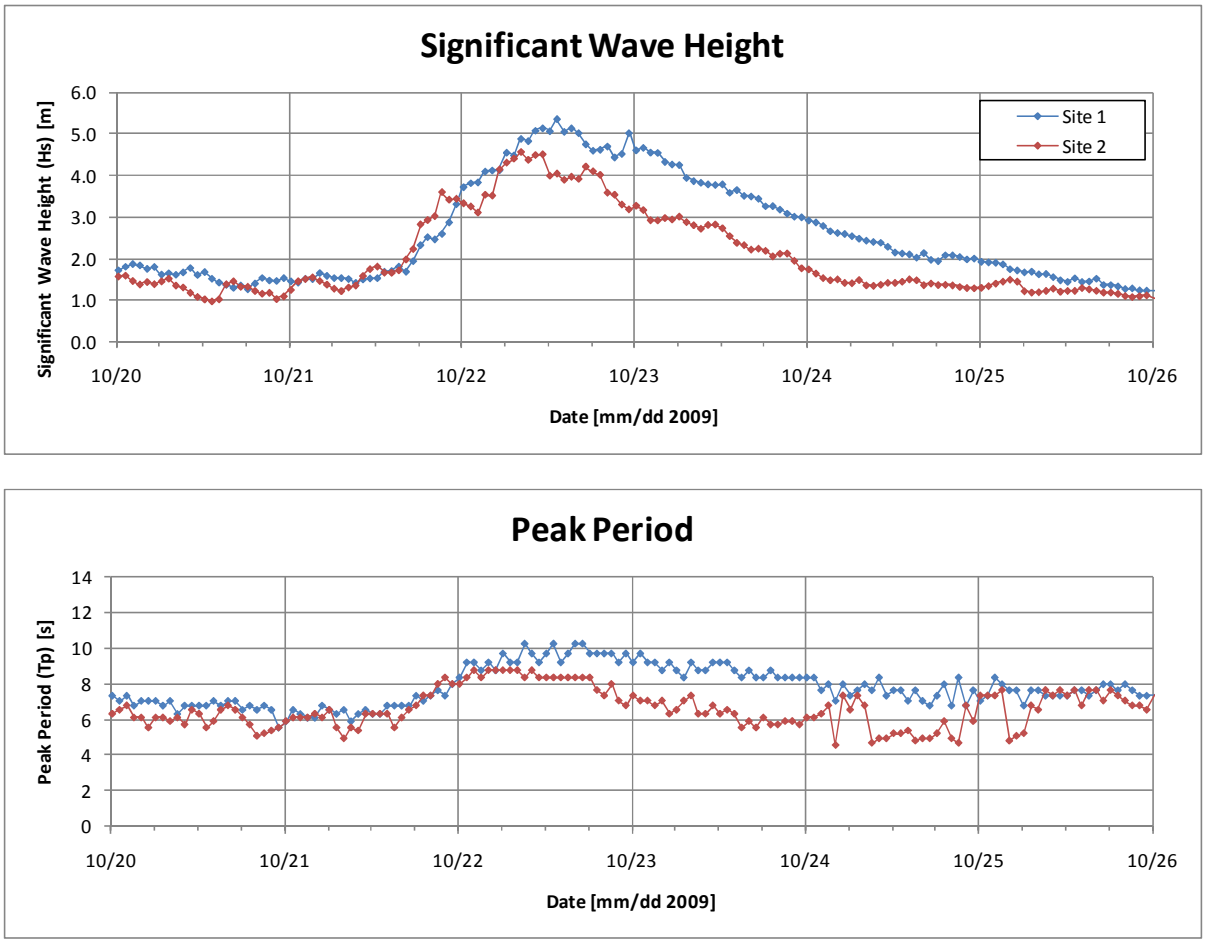

Figure 4-19. Significant wave height (H_s) and peak period (T_p) for both sites from October 20 – 26, 2009.

Table 4-16. Monthly statistics of significant wave height (H_s) and peak period (T_p) at Site 1.

Date		25%	50%	mean	75%	95%	99%	max	# valid	total #
28-Aug-2009 to 31-Aug-2009	Hs (m) :	0.56	1.18	1.43	1.60	3.34	3.43	3.63	92	92
	Tp (s) :	4.7	6.1	6.1	6.7	8.7	9.1	9.1	92	92
September 2009	Hs (m) :	0.88	1.11	1.34	1.89	2.67	3.17	3.65	720	721
	Tp (s) :	5.2	6.5	6.3	7.2	8.3	9.1	10.5	720	721
October 2009	Hs (m) :	1.18	1.60	1.84	2.19	3.74	5.03	5.35	743	743
	Tp (s) :	5.9	6.8	6.9	7.7	9.2	10.3	11.7	743	743
November 2009	Hs (m) :	1.12	1.44	1.68	2.07	3.46	3.85	4.09	516	719
	Tp (s) :	5.5	6.3	6.2	7.1	8.4	8.8	8.8	516	719
December 2009	Hs (m) :								0	744
	Tp (s) :								0	744
January 2010	Hs (m) :								0	744
	Tp (s) :								0	744
February 2010	Hs (m) :								0	672
	Tp (s) :								0	672
March 2010	Hs (m) :								0	744
	Tp (s) :								0	744
April 2010	Hs (m) :								0	720
	Tp (s) :								0	720
May 2010	Hs (m) :	0.13	0.30	0.36	0.59	0.77	0.83	0.88	189	744
	Tp (s) :	3.6	4.2	4.0	4.7	5.1	5.4	6.8	159	744
June 2010	Hs (m) :	0.52	0.91	1.00	1.37	2.41	2.55	2.66	685	720
	Tp (s) :	4.1	5.2	5.1	5.9	7.3	8.0	8.0	653	720
01-Jul-2010 to 26-Jul-2010	Hs (m) :	0.67	0.93	0.97	1.28	1.73	2.65	2.79	614	614
	Tp (s) :	4.3	4.9	5.0	5.5	7.3	8.0	8.4	614	614

Table 4-17. Joint Frequency Table of H_s vs. T_p at Site 1.

Location: Site 1
Instrument: IPS5-060
For period: 2009/08/28 04:59:59 to 2010/07/26 13:17:00

		Hs (m)												
		0.00 to 0.50	0.50 to 1.00	1.00 to 1.50	1.50 to 2.00	2.00 to 2.50	2.50 to 3.00	3.00 to 3.50	3.50 to 4.00	4.00 to 4.50	4.50 to 5.00	5.00 to 5.50	5.50 to 6.00	Row Total (%)
Tp (s)														
0.00	1.00													0.00
1.00	2.00													0.00
2.00	3.00	3.49	0.03											3.52
3.00	4.00	4.49	2.97											7.46
4.00	5.00	2.92	13.04	2.80	0.06									18.82
5.00	6.00	0.51	9.12	13.13	3.12	0.09								25.97
6.00	7.00	0.31	2.20	9.06	6.21	2.43	0.31	0.03						20.56
7.00	8.00	0.09	0.86	2.46	3.00	5.29	3.40	0.97	0.17					16.24
8.00	9.00		0.06	0.40	0.83	0.74	0.74	1.49	1.00	0.14				5.40
9.00	10.00		0.06	0.11	0.11	0.17	0.26	0.14	0.23	0.11	0.29	0.17		1.66
10.00	11.00			0.06			0.03	0.03			0.06	0.06		0.23
11.00	12.00			0.11	0.03									0.14
12.00	13.00													0.00
13.00	14.00													0.00
Column Total (%)		11.81	28.34	28.14	13.35	8.72	4.75	2.66	1.40	0.26	0.34	0.23	0.00	

Filename: Site1_HsTp.dat
Max Hs: 5.35 m
Mean Hs: 1.34 m
non-flagged Hs records: 3559
non-flagged Tp records: 3497

Table 4-18. Monthly statistics of significant wave height (H_s) and peak period (T_p) at Site 2.

Date		25%	50%	mean	75%	95%	99%	max	# valid	total #
29-Aug-2009 to 31-Aug-2009	Hs (m) :	1.05	1.36	1.60	2.14	2.76	2.79	2.95	53	53
	Tp (s) :	5.5	6.1	6.3	7.2	8.0	8.3	8.3	53	53
September 2009	Hs (m) :	0.79	1.13	1.25	1.69	2.44	2.76	2.92	720	720
	Tp (s) :	5.2	6.3	6.1	7.2	8.0	9.1	11.0	720	720
October 2009	Hs (m) :	0.94	1.29	1.47	1.73	3.10	4.14	4.56	744	744
	Tp (s) :	5.5	6.3	6.3	7.2	8.4	9.5	11.0	744	744
November 2009	Hs (m) :	1.00	1.47	1.53	1.97	2.75	3.09	3.24	246	719
	Tp (s) :	4.9	5.5	5.6	6.3	7.3	7.7	7.7	245	719
December 2009	Hs (m) :	0.06	0.07	0.07	0.09	0.09	0.09	0.09	2	720
	Tp (s) :								0	744
January 2010	Hs (m) :								0	744
	Tp (s) :								0	744
February 2010	Hs (m) :								0	672
	Tp (s) :								0	672
March 2010	Hs (m) :								0	744
	Tp (s) :								0	744
April 2010	Hs (m) :								0	720
	Tp (s) :								0	720
May 2010	Hs (m) :	0.15	0.30	0.48	0.69	1.38	1.48	1.56	415	744
	Tp (s) :	2.2	3.2	3.4	4.4	5.2	5.5	5.7	370	744
June 2010	Hs (m) :	0.34	0.74	0.76	1.06	1.72	2.08	2.16	713	720
	Tp (s) :	3.9	4.6	4.5	5.2	6.1	6.8	7.1	626	720
01-Jul-2010 to 28-Jul-2010	Hs (m) :	0.30	0.62	0.68	0.95	1.48	2.20	2.33	648	652
	Tp (s) :	3.8	4.6	4.7	5.4	7.3	8.0	8.4	625	652

Table 4-19. Joint Frequency Table of H_s vs. T_p at Site 2.

Location: Site 2
Instrument: IPS5-092
For period: 2009/08/29 19:00:00 to 2010/07/28 03:22:45

		Hs (m)												
Tp (s)		0.00 to 0.50	0.50 to 1.00	1.00 to 1.50	1.50 to 2.00	2.00 to 2.50	2.50 to 3.00	3.00 to 3.50	3.50 to 4.00	4.00 to 4.50	4.50 to 5.00	5.00 to 5.50	5.50 to 6.00	Row Total (%)
0.00	1.00													0.00
1.00	2.00													0.00
2.00	3.00	9.07	0.18											9.25
3.00	4.00	5.70	5.94											11.65
4.00	5.00	3.81	12.56	6.36	0.24									22.97
5.00	6.00	1.48	7.39	9.73	4.23	0.44								23.26
6.00	7.00	0.56	4.11	5.05	4.32	2.96	0.83	0.06						17.88
7.00	8.00	0.38	0.77	3.46	2.19	1.30	2.01	0.50	0.09	0.03				10.73
8.00	9.00	0.15	0.18	0.92	0.62	0.59	0.24	0.24	0.21	0.27	0.03			3.43
9.00	10.00	0.15	0.12	0.15	0.03	0.21	0.06							0.71
10.00	11.00		0.03											0.03
11.00	12.00		0.06				0.03							0.09
12.00	13.00													0.00
13.00	14.00													0.00
Column Total (%)		21.31	31.33	25.66	11.62	5.50	3.16	0.80	0.30	0.30	0.03	0.00	0.00	

Filename: Site2_HsTp.dat
Max Hs: 4.56 m
Mean Hs: 1.07 m
non-flagged Hs records: 3541
non-flagged Tp records: 3383

Table 4-20. Percent exceedance tables of significant wave height (H_s) for Sites 1 and 2.

Site 1			Site 2		
Instrument: IPS5-060			Instrument: IPS5-092		
2009/08/28 04:59:59 to 2010/07/26 13:17:00			2009/08/29 19:00:00 to 2010/07/28 03:22:45		
# non-flagged Hs records: 3559			# non-flagged Hs records: 3541		
# non-flagged Tp records: 3497			# non-flagged Tp records: 3383		
Hs (m)	**# Exceeding**	**% Exceedance**	**Hs (m)**	**# Exceeding**	**% Exceedance**
0.00	3559	100.00	0.00	3541	100.00
0.25	3344	93.96	0.25	3061	86.44
0.50	3084	86.65	0.50	2662	75.18
0.75	2691	75.61	0.75	2168	61.23
1.00	2093	58.81	1.00	1602	45.24
1.25	1579	44.37	1.25	1114	31.46
1.50	1109	31.16	1.50	734	20.73
1.75	831	23.35	1.75	508	14.35
2.00	642	18.04	2.00	341	9.63
2.25	470	13.21	2.25	219	6.18
2.50	337	9.47	2.50	155	4.38
2.75	240	6.74	2.75	94	2.65
3.00	171	4.80	3.00	48	1.36
3.25	119	3.34	3.25	31	0.88
3.50	78	2.19	3.50	21	0.59
3.75	46	1.29	3.75	15	0.42
4.00	29	0.81	4.00	11	0.31
4.25	25	0.70	4.25	6	0.17
4.50	20	0.56	4.50	1	0.03
4.75	11	0.31	4.75	0	0.00
5.00	8	0.22	5.00	0	0.00
5.25	1	0.03	5.25	0	0.00
5.50	0	0.00	5.50	0	0.00
5.75	0	0.00	5.75	0	0.00
6.00	0	0.00	6.00	0	0.00

Figure 4-20. Percent exceedance plot of significant wave height (H_s) for both sites.

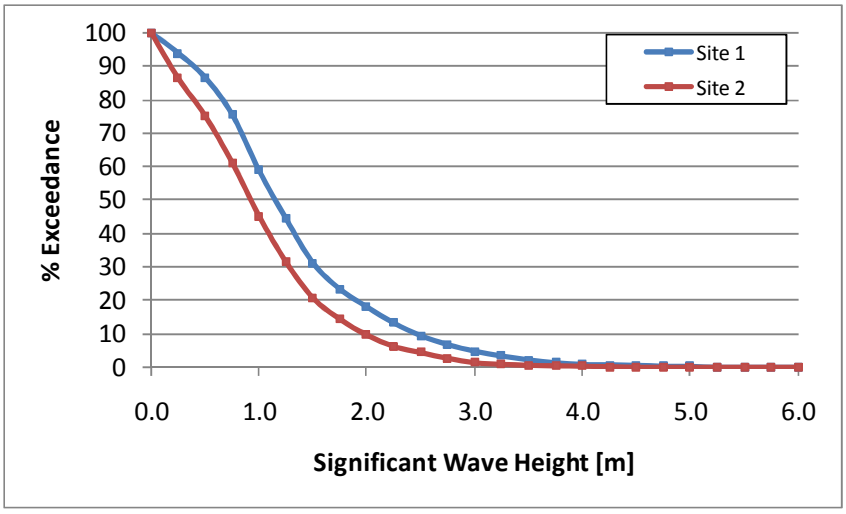

5 SUMMARY AND CONCLUSIONS

A program of ice keel depth and ice velocity measurements was carried out off northwestern Alaska in support of oil and gas exploration by ConocoPhillips Alaska Inc. (CPAI) in the Chukchi Sea from August 2009 to July 2010. The data collection program involved the deployment and operation of two underwater, internally recording instruments at two sites (Site 1 and Site 2) in 37-46 m depth for nearly a year.

At each measurement site, an Ice Profiling Sonar (IPS-5) instrument was operated to provide ice draft measurements at one- or two- second intervals. The IPS-5 also provided non-directional wave measurements at 2 Hz sampling rates. Ice velocity measurements, at 5 minute sampling intervals, were obtained from Acoustic Doppler Current Profilers (ADCP), which also provided ocean current profile data.

5.1 OVERVIEW OF THE 2009-2010 ICE SEASON

Ice conditions in the region were reduced or lighter than normal with the September 2009 ice edge well north of its median position. The region has a very dynamic ice regime with ice movement occurring 98% to 95% of the time at Sites 1 and 2 respectively from August 2009 to July 2010. Ice features having large vertical drafts, of up to 68% and 64% the total water depth, were observed from December until May at Site 1 and Site 2, respectively. Thousands of Ice keels with horizontal dimensions of typically 25-50 m, up to a few hundred meters, were observed. The great majority of these ice keels are individual ice keel features of which a few of the very widest keels representing massively deformed features. As was seen in the 2008-2009 data sets, the ice proved to be quite mobile, with only the months of January through April for Site 1 and December through April for Site 2 having more than 1% no-motion events. The greatest percentage of no-motion events in the 2009-2010 measurement period was observed in February at both sites, with 8% at Site 1 and 17% at Site 2.

The results from this measurement period were obtained during the two years with the historically third and fourth smallest summer ice retreat. Extensive open water conditions existed in the study area until late November 2009 and ice clearing began in late May, but some ice remained in the vicinity of Site 2 until late July.

5.2 DEEPEST ICE KEELS

Very deep ice keels were observed at both Site 1 and Site 2 with 19 keels at Site 1 and 24 keels at Site 2 measuring over 20 m ice draft. The deepest keels at Site 1 and Site 2 were 26.7 m and 30.0 m respectively.

Keels exceeding 11 m ice draft were measured in all months from January to June 2010 at both sites and in December 2009 at Site 2. From the distance of ice passage (derived for ice velocity measurements in the November to late July period), the total distances of sea ice

passing by Site 1 and Site 2 were 2150 and 2861 km. Ice keels having threshold drafts of 5, 8 and 11 m were individually identified and statistics on these were compiled. The total number of ice keels greater than 5, 8 and 11 m were 6723, 2010 and 612 respectively for Site 1 and 7828, 2318 and 701 for Site 2. The average widths of the individual ice 5, 8 and 11 m keels were 28.8, 34.3 and 39.8 m for Site 1 and 28.4, 35.0 and 42.8 m for Site 2.

By comparison to the first year of measurements, 2008-2009, there was a notable reduction at Site 1 for the total number of keels and the total distance of ice measured. Note that no ice draft data were obtained at Site 2 during the 2008-2009 measurement program. For Site 1, the number of keels > 5 m ice draft was 14,484, the total ice distance was 2990 km and the maximum keel ice draft was 26.4 m in 2008-2009.

5.3 WIDEST ICE KEELS

There were occurrences of ice keels with very large horizontal dimensions of up to a few hundred meters and large maximum keel depths. Detection of keels and their beginning and ending positions are determined by objective criteria as outlined in Section 4.2.1. The widest keels, using a threshold of 5 m, were 490 m for Site 1 and 328 m for Site 2. Arguably, the widest keels in the entire data sets could be considered to be part of rubble ice fields, in particular the widest keel at Site 2. More advanced analysis methods to distinguish between different ice deformation processes such as singular large keels and rubbled and/or hummocky ice are recommended for further investigation of these very extensive Ice Profiler data sets. Nevertheless, some wide ice keels (e.g. June 1 at Site 1, Figure 4-15) feature continuous ice drafts exceeding 10 m over distances of up to 400 m.

5.4 ICE VELOCITY

Over ten occurrences of large ice velocities were measured throughout the year with peak ice velocities of 76 cm/s at Site 1 and 115 cm/s at Site 2. This is considerably less than the 2008-2009 peak ice speeds exceeding 112 cm/s at Site 1 and 124 cm/s at Site 2. The episodes of large ice velocities were associated with strong wind events having peak speeds of 6.4 to 11.5 m/s. At both sites, the median ice drift was highest in June with a value of 28.7 cm/s and 37.5 cm/s for Sites 1 and 2, respectively. The second and third largest ice drifts occurred around this time at Site 2 with a value of 34.1 cm/s in May and 28.6 cm/s in July, while the median ice drift was high in November (27.3 cm/s) and December (18.6 cm/s) at Site 1. The median ice speeds were lower (between 5 and 20 cm/s) from November to April for Site 2 and from December to May at Site 1. The highest median speeds of the 2008-2009 data were generally larger (at 30-50 cm/s) than those observed in the 2009-2010 measurement program.

5.5 OCEAN CURRENTS

The ocean currents at Site 1 were weaker than those observed at Site 2 with events rarely exceeding 30 cm/s near the surface. The maximum current speed near the surface was

98.4 cm/s at Site 2 and 57.1 cm/s at Site 1. From September to late December, current speeds were typically large and associated with strong wind events that were at times greater than 8 m/s as measured at Wainwright. During January the currents were typically lower except for a large event late in the month. Currents then generally stayed weak for the rest of the ice season, except for about ten high speed events. As was seen in the ice velocities, the currents during the 2008-2009 measurement period were generally larger at both Site 1 and Site 2.

The surface currents at Site 1 were variable but predominantly directed to the ENE, whereas the surface current direction at Site 2 aligned along an E-W axis. Mid-depth and near-bottom current directions were less variable than the surface currents and were predominately towards the ENE and ESE for Site 1 and Site 2, respectively. Strongest currents, on the other hand, were generally directed to the West at both sites. The same directionality was observed with the 2008-2009 data sets. These current directions are likely influenced by the local topography, the inflows from the Pacific Ocean and by offshore winds. The current directions at Site 1 and Site 2 are similar to the mean flows observed by Weingartner et al. (2009) where the main water flow coming in from the Pacific bifurcates and flows around the west and southern parts of Hanna Shoal. Site 2 is located in a deep and narrow channel between the Hanna Shoal and the coast, where the ocean currents are accelerated due to local topography.

Inertial oscillations are present in the ocean current data during the times of reduced or zero ice concentrations. These twice-daily ocean current variations produced a peak to trough current variation of up to 25 cm/s, and they appeared to be more prevalent at Site 1 than at Site 2.

5.6 OCEAN WAVES

The acoustic range data from the ASL Ice Profiler was used to derive information on ocean waves when sea ice was not present. From late August to early November, there were six storms when the significant wave heights approached or exceeded 4 m. The largest wave heights occurred between 2009/10/21 and 2009/10/25, where the wave heights at Site 1 reached a maximum significant wave height value of 5.4 m (10.6 m maximum individual wave height) with a corresponding peak period of 10s. At Site 2, the maximum significant wave height was measured at 4.6 m. During this event, wind speeds at Point Lay exceeded 19 knots for several hours. For all non-ice measurement times, the average wave heights were 1.3 m at Site 1 and 1.1 m at Site 2.

5.7 RECOMMENDATIONS

Further analyses of this one year data set may be useful to extract further information on the properties of the sea ice regime in the Eastern Alaskan Beaufort Sea lease areas. Possibilities for further analysis are provided below:

(1) **Additional wave analysis using a combined analysis of winds** (NCEP-2 Reanalysis winds along with the Point Lay and Wainwright weather stations) and the measured non-directional wave parameters and wave spectra to estimate wave directions and to examine the fetch and duration scales applicable to the generation of the measured waves.

(2) **Compute the frequency and properties of Rubbled and Hummocky Ice from the ice distance series.** Rubbled and hummocky ice can pose operational threats that are comparable to those presented by large ice ridges and keels. The statistics of rubbled and hummocky ice will be derived using existing software developed for this purpose.

(3) **Prepare Joint-Bivariate Distributions of ice keel drafts (e.g. > 5m, > 8 m, > 11 m) and ice speeds, for each site.**
An important factor is statistics on ice drift direction persistence and the rates of change in ice drift direction (i.e.: the radius of curvature), for example, for tanker loading and supply vessel offloading considerations. This can be readily done for the full record, and by individual months using software that already available. It is also proposed to investigate whether the occurrence of deep-draft features is statistically independent of drift speed. From a statistical test of the null hypothesis that deep-draft features are not dependent on ice drift speed, using the data compiled for this task, the hypothesis will be tested.

(4) **Compute the radius of curvature of ice drift from the x- and y-displacement values derived from the vector velocity time series.**
From these x- and y-displacement values, the radius of curvature can be computed as a function of time. Occurrences of events for the radius of curvature values, ranging from being comparable to the vessel length to an order of magnitude greater than the hull length, will be identified and statistics on the frequency of occurrence and persistence of such events will be prepared by radius categories. An analysis of joint-bivariate distributions of radius of curvature and drift speed will also be prepared; it will be useful to examine if they have a negative correlation, and make the offloading operations manageable**.**

6 LITERATURE CITED

ASL Environmental Sciences Inc., 2000. Analyses of Ice Keel and Ice Velocity Data Sets (1996 to 1999) from Offshore Sakhalin Island, D.B. Fissel, ed. Report for Sakhalin Energy Investment Company Ltd., by ASL Environmental Sciences Inc., Sidney, B.C. Canada. ix +124p.

Barrett, S.A., and W.J. Stringer. 1978. Growth Mechanisms of "Katie's Floeberg". *Arctic and Alpine Research*, 10(4): 775-783.

Belliveau, D.J., G.L. Bugden, B.M. Eid and C.J. Calnan, 1990. Sea ice velocity measurements by upward-looking Doppler current profilers. *J. Atmos. Oceanic Technol.*, 7(4): 596-602.

Borg, K., J. Lawrence, T. Mudge, and D. Fissel. 2010. Recovery and Redeployment of IPS and ADCP Moorings in the Chukchi Sea July 2010. Cruise Report prepared for Conoco Phillips Alaska Inc. 24 p.

Fissel, D.B., J.R. Marko and H. Melling, 2008. Advances in Upward Looking Sonar Technology for Studying the Processes of Change in Arctic Ocean Ice Climate. Paper to be published in the Journal of Operational Oceanography and presented at the Oceanology International Conference, London UK, 12 March 2008.

Garrison G.R., R.E. Francois and T. Wen. 1991. Acoustic reflections from Arctic ice at 15-300 kHz. *J. Acoust. Soc. Amer.* 90(2): 973-984.

Huntington, H.P., Brower, H., Jr., and Norton, D.W. 2001. The Barrow Symposium on Sea Ice, 2000: Evaluation of one means of exchanging information between subsistence whalers and scientists. Arctic 54(2):201–204.

Kovacs, A., and M. Mellor. 1974. Sea ice morphology and ice as geological agent in the southern Beaufort Sea. In: *The Coast and Shelf of the Beaufort Sea,* 113-161. Proceedings of a Symposium on Beaufort Sea and Shelf *Research*. J.C. Reed and J.A. Sater, Ed. The Arctic Institute of North America: Virginia.

Mahoney, A., H. Eicken, L. Shapiro, and T. C. Grenfell 2004. Ice motion and driving forces during a spring ice shove on the Alaskan Chukchi coast, Journal of Glaciology, 50(169), 195-207.

Melling, H., P.H. Johnston and D.A. Riedel, 1995. Measurements of the underside topography of sea ice by moored subsea sonar. *J. Atmospheric and Oceanic Technology,* 13(3): 589-602.

Norton, D.W. and G.A. Gaylord, 2004. Drift Velocities of Ice Floes in Alaska's Northern Chukchi Sea Flaw Zone: Determinants of Success by Spring Subsistence Whalers in 2000 and 2001. *Arctic,* 57 (4), 347-362.

Urick, R.J., 1983. *Principles of Underwater Sound,* Third Edition. New York: McGraw-Hill, Inc. 423 p.

Vaudrey, K., 1987. 1985-86 Ice Motion measurements in Camden Bay, AOGA Project 328, Vaudrey & Associates, Inc. San Luis Obispo, CA.

Weingartner, T., K. Aagaard, D. Cavalieri, S. Danielson, M. Kulakov, V. Pavlov, A. Roach, Y. Sasaki, K. Shimada, T. Whitledge, and R. Woodgate, 2009. Chukchi Sea Circulation. *http://www.ims.uaf.edu/chukchi/*